No. 339
January 1999

Slow Motion Dynamics of Mooring Systems in Deep Water with Buoy Supported Catenary Lines

L.O. Garza Rios
M.M. Bernitsas

Department of Naval Architecture
and Marine Engineering

No. 339
January 1999

SLOW MOTION DYNAMICS OF MOORING SYSTEMS IN DEEP WATER WITH BUOY SUPPORTED CATENARY LINES

by

L. O. Garza-Rios

M. M. Bernitsas

Prepared for the University of Michigan/Industry Consortium in Offshore Engineering

Department of Naval Architecture
and Marine Engineering
College of Engineering
The University of Michigan
Ann Arbor, Michigan 48109-2145

ABSTRACT

The mathematical model for the horizontal plane slow motion dynamics of mooring systems with catenary chains supported by buoys is developed. Buoys are attached to a mooring line to help support part of the chain weight, thus avoiding excessive vertical forces exerted on the line and on the moored vessel. Each mooring line consists of two or more segments with a buoy attached to each connection point. The first segment is anchored to the sea bed, and part of it, of variable length, is in contact with the sea bed modeling touchdown effects. The ensuing system results in a model for mooring in deep and ultra-deep waters. The mathematical model consists of three equations of motion in the horizontal plane - surge, sway, and yaw - for the slow motion dynamics of the vessel, and three equations of motion in surge, sway and heave for each of the buoys in the system. External excitation consists of time independent current, steady wind, and second order mean drift forces.

ACKNOWLEDGMENTS

This report is a product of research sponsored by the University of Michigan/Industry Consortium in Offshore Engineering. Industry participants include Amoco, Inc.; Chevron, Inc.; Conoco, Inc.; Exxon Production Research; Mobil Research and Development; Shell Companies Foundation; and Petrobrás, Rio de Janeiro, Brazil.

TABLE OF CONTENTS

LIST OF FIGURES

LIST OF TABLES

LIST OF APPENDIXES

NOMENCLATURE

This nomenclature corresponds to mooring systems with one buoy per mooring line. To simplify notation, the subscripts that identify a mooring line or a buoy are omitted. Most definitions in this nomenclature can be directly extended to definitions for multi-buoy mooring systems.

AC	anchored catenary
CG	center of gravity of moored vessel
d	horizontal distance of AC on the ground
F_{1D}	integrated drag force on catenary segment S1 concentrated at its upper point
F_{2AD}	integrated drag force on catenary segment S2A concentrated at its upper point
F_{2BD}	integrated drag force on catenary segment S2B concentrated at its upper point
F_{DB}	drag force acting on the buoy
h	water depth
h_1	vertical distance of the lower point of the buoy from the sea bed
h_{2A}	vertical distance from the lower point of SC to the lower point of the buoy
h_{2B}	vertical distance from the lower point of SC to the point of attachment to the floating vessel
ℓ_1	length of the horizontal projection of the suspended part of AC
ℓ_2	length of the horizontal projection of SC
ℓ_{2A}	length of the horizontal projection of segment S2A
ℓ_{2B}	length of the horizontal projection of segment S2B
ℓ_1'	length of the horizontal projection of AC
ℓ_{eff1}	length of the suspended part of AC
ℓ_{eff2A}	total length of segment S2A
ℓ_{eff2B}	total length of segment S2B
ℓ_{wT}	total length of the mooring line ($\ell_{wT} = \ell_{w1} + \ell_{w2}$)
ℓ_{w1}	total length of AC
ℓ_{w2}	total length of SC ($\ell_{w2} = \ell_{eff2A} + \ell_{eff2B}$)
m	mass of vessel
m_B	mass of buoy
MBSMS	multi-buoy spread mooring system

n	number of mooring lines
n_B	number of buoys
N_H	velocity dependent hydrodynamic moment on vessel in yaw
r	yaw angular velocity of the vessel
R_B	buoy radius
S1	anchored catenary segment
S2	suspended catenary segment
S2A	part of SC segment from the buoy to the lowest point of SC
S2B	part of SC segment from the lowest point of SC to the floating vessel
SC	suspended catenary
SMS	Spread Mooring System
SPM	Single Point Mooring
T_{o1}	horizontal tension components of AC
T_{o2}	horizontal tension components of SC
T_{oP}	horizontal pretension of the catenary
T_P	total pretension of the catenary
T_{v1}	vertical tension of AC
T_{v2A}	vertical tension of segment S2A of SC
T_{v2B}	vertical tension of segment S2A of SC
T_{vP}	vertical pretension of the catenary
u	forward velocity of vessel with respect to water
u_B	relative surge velocity of buoy in water
U_c	current speed
v	lateral velocity of vessel with respect to water
v_B	relative sway velocity of buoy in water
w_B	relative heave velocity of buoy in water
X_H	velocity dependent hydrodynamic force on vessel in surge
(x,y,z)	inertial reference frame / position of vessel CG with respect to the inertial frame
(x_B,y_B,z_B)	position of the center of gravity of buoy with respect to the inertial frame
(X,Y,Z)	reference coordinate frame fixed on the vessel
(X_B,Y_B,Z_B)	reference coordinate frame fixed on the buoy
(x_m,y_m,z_m)	coordinates of the mooring point at the sea floor
(x_p,y_p)	body fixed coordinates of the fairlead
Y_H	velocity dependent hydrodynamic force on vessel in sway

Greek Symbols

α	current angle with respect to the inertial frame
β	horizontal angle between the X- axis and the mooring line, measured counterclockwise
β_B	horizontal angle between two segments of the catenary, measured counterclockwise from the buoy
γ	horizontal angle between the x- axis and the mooring line, measured counterclockwise from the vessel
γ_B	horizontal angle between the x- axis and segment S1, measured counterclockwise from the buoy
λ_i	ith eigenvalue
ψ	drift angle

Special Symbols

$\overline{(\bullet)}$	equilibrium of $(\bullet)$

I. INTRODUCTION

Recent discovery of oil and gas in deep waters has lead to the development of mooring systems capable of operating in such environments. For water depths greater than 1500 ft, dynamic positioning [6, 28], rather than mooring, is preferred partly due to the high vertical loads that the mooring lines exert on the moored vessel and onto themselves, and partly because of limited understanding of mooring system dynamics in deep waters. A preliminary work on the dynamics of Turret Mooring Systems (TMS) [11] shows that a system stable in moderate water depths may lose its dynamic stability in deeper waters. These shortcomings presently make mooring operations unpredictable and therefore risky in deep water.

It is of particular interest to the offshore community to be able to utilize a combination of mooring and dynamic positioning to effectively position a vessel in deep waters. A thorough study of mooring systems in deep water is essential to understanding the dynamics that these combined systems exhibit. The weight of mooring lines is one of the challenges of deep water mooring and is studied in this report. Future research will add a dynamic positioning system to model the hybrid mooring problem.

For general mooring operations, several types of mooring lines are used [12, 26]. These include synthetic fiber ropes (nylon, polyester), catenary chains, and steel cables. Catenary chains are commonly used in most mooring and anchoring situations in shallow and intermediate water depths. A hybrid combination of different types of mooring lines is commonly used in order to reduce the overall weight of the lines, and the vertical forces that the lines exert on the moored vessel while achieving the desired strength. In addition, buoys may be placed along catenary lines to support their weight. The object of this report is to develop a model for deep water mooring using chains partially supported by buoys.

In this work, a mathematical model for quasistatic analysis of deep water mooring with anchoring chains is developed as part of the slow motion dynamics model for spread mooring systems. In this model, each chain is modeled as a sequence of a number of segments which are delineated by buoys, each of which achieves catenary deformation. Every mooring line consists of an anchored catenary [12] and one or more suspended catenaries [26].

The main focus of this work is to derive the quasistatic equations of motion for a catenary mooring line with one buoy and to incorporate these equations into the mathematical model of mooring systems. First, Single Point Mooring (SPM) is studied. Then, the single buoy line model is implemented in Spread Mooring Systems (SMS), where any number of mooring lines may be used to position the vessel. An introduction to mooring systems with two or more buoys per mooring line is provided as well.

The equations for the quasistatic catenary motions with one buoy are derived in Chapter II, and incorporated to the mathematical model for slow motion dynamics of SPM systems. The concept of SPM state space representation and SPM equilibria are discussed, and used to study the developed model. An introduction to nonlinear time simulations and SPM nonlinear stability analysis based on eigenvalue theory is presented as well. Chapter III presents the SMS mathematical model with one buoy per mooring line. In this chapter, the SMS state space representation and equilibrium equations are derived, and the geometry of SMS is studied. A numerical application of a SMS consisting of nonlinear time simulations and eigenvalue analysis is provided. In Chapter IV, chains supported by two buoys are modeled and incorporated into the SMS model. An introduction to multi-buoy, multi-line systems is also discussed in Chapter IV. Finally, in Appendixes 1 and 2 the relationships between various geometrical properties of the mooring line segments with respect to changes in the vertical position of the buoys are derived. These relationships are used to obtain mathematical properties needed to study the dynamics of the system based on eigenvalue analysis.

II. DEEP WATER CATENARY MODEL WITH ONE BUOY FOR SPM SYSTEMS

In mooring operations, the typical equations that model Suspended Catenaries (SC) [26] cannot be applied because they do not take into account touchdown effects. Anchored Catenaries (AC) [12], on the other hand, can be utilized for mooring in water depths of up to 500-600 m. In deeper water mooring, the weight exerted by an AC would apply very high vertical loads on the moored vessel and may even result in mooring line breakage. A combination of the two catenary models mentioned above, with two or more segments (one or more buoys) makes it feasible to operate in deeper waters using chains as mooring lines. Buoys are used to support the weight of the catenary, thus avoiding excessive vertical forces exerted on the moored vessel and on the catenary itself.

Presently, the dynamics of these types of systems in deep water is not well understood for two reasons: First, practical experience is limited to using buoys on mooring systems mostly in shallow and intermediate waters. Second, solution methods are mainly limited to nonlinear time simulations which cannot reveal the complete picture of the system dynamics.

In this chapter, the mathematical model of slow motion dynamics of Single Point Mooring (SPM) systems with one buoy is developed. First, its equations of motion and kinematic relations are derived. Next, the SPM state space representation is developed and equilibria are derived. Simulation and stability analysis of the SPM model are introduced to better understand the dynamics of these types of systems. In the following chapters, the equations of motion of the SPM with one buoy are extended to Spread Mooring Systems (SMS). Finally, in Chapter IV, SMS models with more than one buoy per line are discussed.

2.1. Catenary Model with One Buoy

Figure 2.1 shows the geometry of a catenary mooring line consisting of two line segments connected via a buoy. Segment 1 (S1) is an Anchored Catenary (AC) [12] which is moored to the sea bed with its upper end connected to the buoy. Segment 2 (S2) is a Suspended Catenary (SC) [26] with its lower end connected to the buoy and its upper end connected to the moored vessel (usually a ship). Segment S2 is further divided into two parts: Segment S2A, which

extends from the point where SC is connected to the buoy to the lowest point of S2, and segment S2B which runs from the lowest point of S2 to the point of attachment of SC on the moored vessel.

In Figure 2.1, (x,z) is the inertial reference frame of the catenary, located at the point where the mooring line is anchored to the sea bed; (x_m,z_m) are the coordinates of the anchoring point $(x_m=0,\ z_m=0)$; U_c is the current speed acting in the $-x$ direction; ℓ_1' is the length of the horizontal projection of AC; ℓ_1 is the length of the horizontal projection of the suspended part of AC; d is the horizontal length of AC in the ground; ℓ_2 is the length of the horizontal projection of SC; ℓ_{2A} is the length of the horizontal projection of segment S2A; ℓ_{2B} is the length of the horizontal projection of segment S2B. These are related as follows:

$$\ell_1' = \ell_1 + d \ , \tag{2.1}$$

$$\ell_2 = \ell_{2A} + \ell_{2B} \ . \tag{2.2}$$

In addition, h is the water depth; h_1 is the vertical distance from the lower point of the buoy to the sea bed; h_{2A} is the vertical distance from the lower point of SC to the lower point of the buoy; h_{2B} is the vertical distance from the lower point of SC to the point of attachment to the moored vessel. The total water depth is constant, and is related to the various vertical distances of Figure 2.1 as follows:

$$h = h_1 - h_{2A} + h_{2B} \ , \tag{2.3}$$

where [12]

$$h_1 = \frac{T_{o1}}{P}\left[\cosh\left(\frac{P\ell_1}{T_{o1}}\right)-1\right], \tag{2.4}$$

$$h_{2A} = \frac{T_{o2}}{P}\left[\cosh\left(\frac{P\ell_{2A}}{T_{o1}}\right)-1\right], \tag{2.5}$$

$$h_{2B} = \frac{T_{o2}}{P}\left[\cosh\left(\frac{P\ell_{2B}}{T_{o1}}\right)-1\right]. \tag{2.6}$$

In equations (2.4) and (2.5)-(2.6), T_{o1} and T_{o2} are the horizontal tension components of AC and SC respectively, and P is the weight of the catenary per unit length.

The external forces acting on the catenary in Figure 2.1 are: F_{DB} is the drag force acting on the buoy due to current; F_{1D} is the integrated drag force on catenary segment S1 concentrated at its upper most point; F_{2AD} and F_{2BD} are the integrated drag components on segments S2A and S2B, concentrated at the upper point of the respective segment; and F_{EXT} is the external horizontal force imposed by the moored vessel acting at the top of the catenary (an end-point condition).

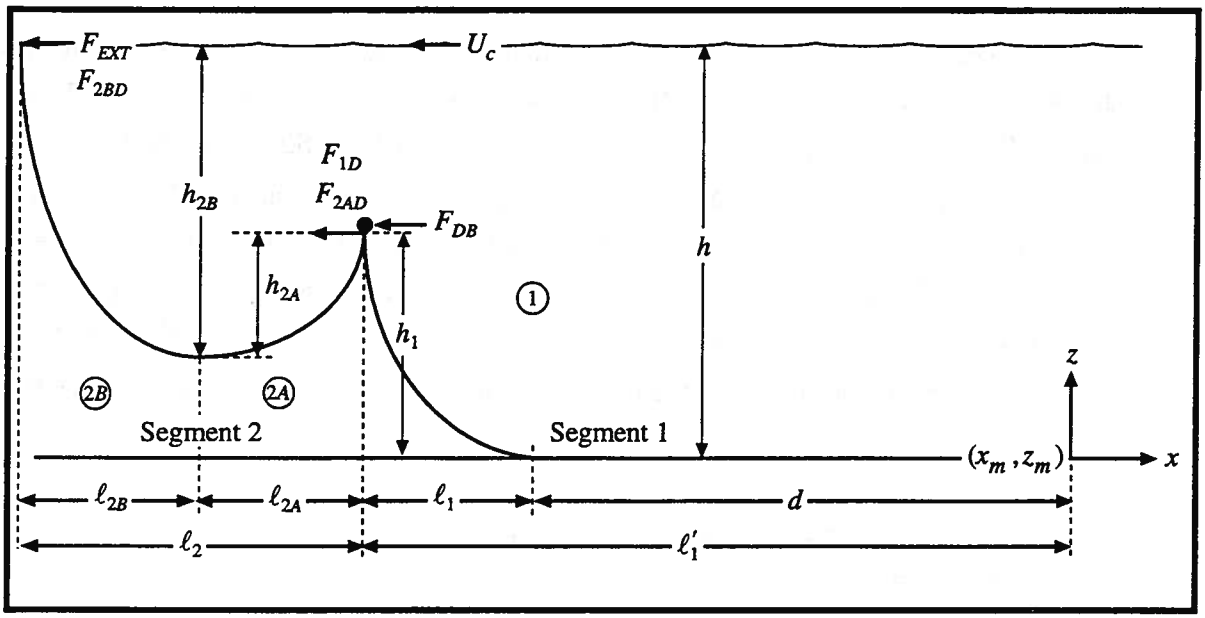

Figure 2.1. Geometry of deep water catenary with one buoy

The total length of the mooring line (ℓ_{wT}) is given by the sum of its components ℓ_{w1} and ℓ_{w2}:

$$\ell_{wT} = \ell_{w1} + \ell_{w2} \ , \tag{2.7}$$

where

$$\ell_{w1} = \ell_{eff1} + d \ , \tag{2.8}$$
$$\ell_{w2} = \ell_{eff2} = \ell_{eff2A} + \ell_{eff2B} \ , \tag{2.9}$$

are constant lengths of S1 and S2, respectively; and ℓ_{eff1}, ℓ_{eff2A} and ℓ_{eff2B} are the effective lengths of each of the three segments. Effective is defined as the suspended length of each segment of the line. These can be calculated as follows [12]:

$$\ell_{eff1} = \frac{T_{o1}}{P}\sinh\left(\frac{P\ell_1}{T_{o1}}\right) = \sqrt{h_1\left(h_1 + \frac{2T_{o1}}{P}\right)}\ , \tag{2.10}$$

$$\ell_{eff2A} = \frac{T_{o2}}{P}\sinh\left(\frac{P\ell_{2A}}{T_{o2}}\right) = \sqrt{h_{2A}\left(h_{2A} + \frac{2T_{o2}}{P}\right)}\ , \tag{2.11}$$

$$\ell_{eff2B} = \frac{T_{o2}}{P}\sinh\left(\frac{P\ell_{2B}}{T_{o2}}\right) = \sqrt{h_{2B}\left(h_{2B} + \frac{2T_{o2}}{P}\right)}\ . \tag{2.12}$$

The forces acting on the buoy are shown in Figure 2.2. F_B is the net buoyancy force (difference between buoyancy of the buoy and its weight); T_{v1} is the vertical tension of segment S1 at point A, T_{v2A} is the vertical tension of segment S2A at point A; and R_B is the radius of the spherical buoy. The origin of the system of coordinates of the buoy (X_B, Z_B) is located at the center of gravity of the buoy, with X_B pointing horizontally in the plane of deformation of S1 and Z_B pointing upwards. Note that the vertical component of the tension in segment S2B, which will be denoted as T_{v2B}, acts on the moored vessel rather than on the buoy. The equations of motion of the buoy in the horizontal (surge) and vertical (heave) planes are:

$$(m_B + A_{11})\ddot{x}_B = T_{o1} - T_{o2} - F_{DB} - F_{1D} - F_{2AD}\ , \tag{2.13}$$

$$(m_B + A_{33})\ddot{z}_B = F_B - T_{v1} - T_{v2A}\ , \tag{2.14}$$

where $\ddot{x}_B$ and $\ddot{z}_B$ are the surge and heave accelerations of the buoy with respect to the inertial reference frame (x,z); m_B is the mass of the buoy, and A_{11} and A_{33} are the added mass terms in surge and heave, respectively.

The vertical components of the mooring line tensions can be calculated as follows [12]:

$$T_{v1} = T_{o1}\sinh\left(\frac{P\ell_1}{T_{o1}}\right), \tag{2.15}$$

$$T_{v2A} = T_{o2}\sinh\left(\frac{P\ell_{2A}}{T_{o2}}\right), \tag{2.16}$$

$$T_{v2B} = T_{o2}\sinh\left(\frac{P\ell_{2B}}{T_{o2}}\right). \tag{2.17}$$

As shown in equations (2.15) - (2.17), the vertical tension components are functions of the horizontal tension components T_{o1} and T_{o2}. The solution to the catenary problem supported

by a single buoy, thus requires the knowledge of the two horizontal tension components (T_{o1} and T_{o2}) as well as the values for the depth of the buoy (h_1), and the horizontal components of the mooring line segments ℓ_1, ℓ_{2A}, and ℓ_{2B}. If these are known, the values for T_{o1} and T_{o2} can be found separately with a single equation for each using iterative processes as shown in [12] and [26] respectively. Once T_{o1} and T_{o2} are known, the other unknowns pertaining to the geometry of each segment can be readily found.

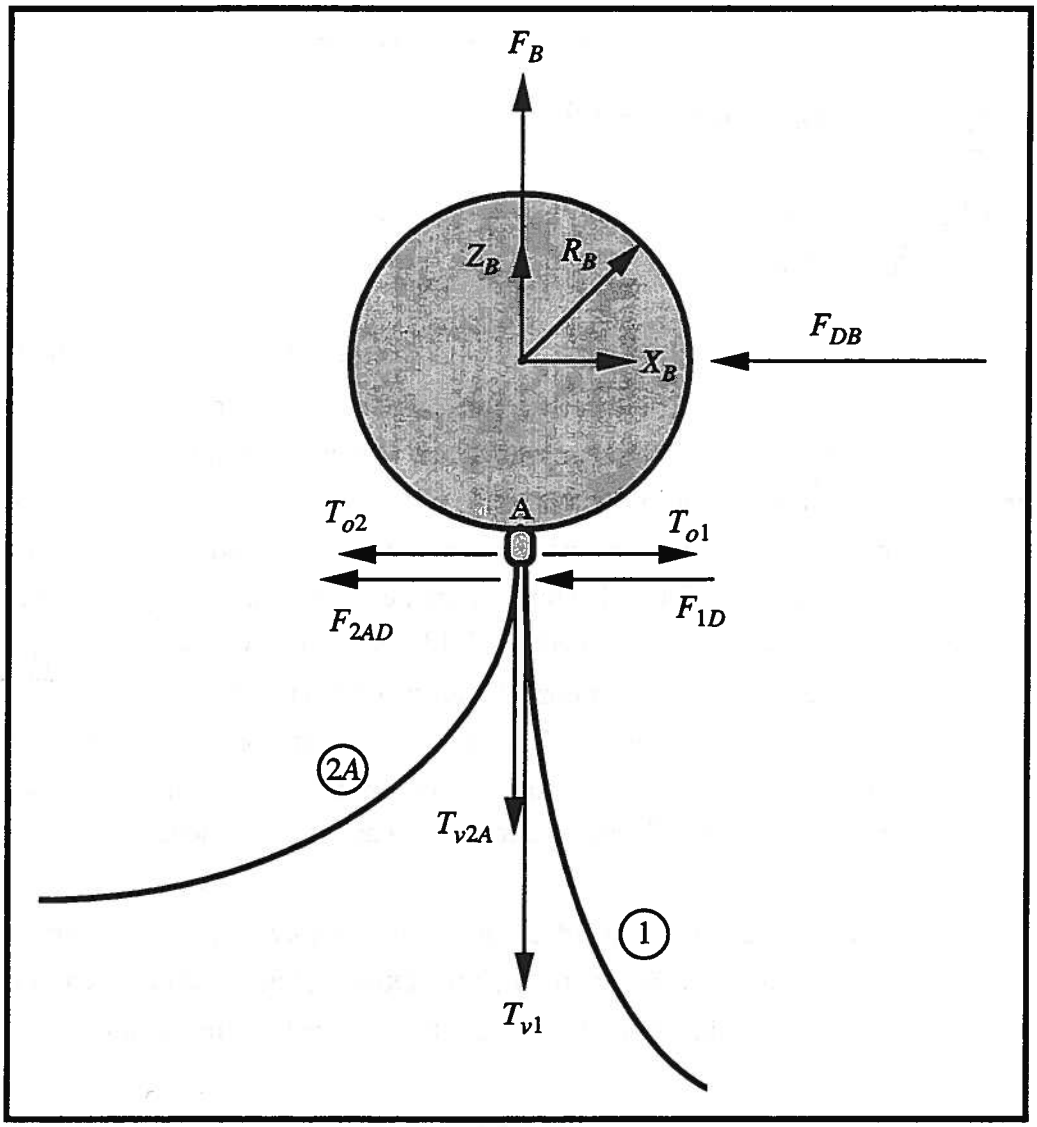

Figure 2.2. Forces acting on a buoy

The depth of the buoy, however, is not known a priori as it depends on the size of the buoy, its buoyancy, point of attachment along the mooring line, and the weight of each segment of the catenary. Calculation of the horizontal components of the mooring line tension in segments S1 and S2 requires an iterative process of more than two equations. The equilibrium solution

of the two-dimensional catenary model of Figures 2.1 and 2.2, can be found using six equations for the six unknowns mentioned above (T_{o1}, T_{o2}, ℓ_1, ℓ_{2A}, ℓ_{2B} and h_1), as follows:

$$\sinh\left(\frac{P\ell_1}{T_{o1}}\right)-\frac{P}{T_{o1}}\sqrt{h_1\left(h_1+\frac{2T_{o1}}{P}\right)}=0\ , \tag{2.18}$$

$$\sinh\left(\frac{P\ell_{2A}}{2T_{o2}}\right)\cosh\left(\frac{P\ell_{2B}}{2T_{o2}}\right)+\cosh\left(\frac{P\ell_{2A}}{2T_{o2}}\right)\sinh\left(\frac{P\ell_{2B}}{2T_{o2}}\right)$$
$$-\frac{P}{2T_{o2}}\sqrt{\ell_{w2}^2-(h-h_1)^2}=0\ , \tag{2.19}$$

$$T_{o1}-T_{o2}-F_{DB}-F_{1D}-F_{2AD}=0\ , \tag{2.20}$$

$$F_B-T_{v1}-T_{v2A}=0\ , \tag{2.21}$$

$$P\ell_{w2}-T_{v2A}-T_{v2B}=0\ , \tag{2.22}$$

$$T_{o2}-F_{EXT}-F_{2BD}=0\ . \tag{2.23}$$

Equations (2.18) and (2.19) are typically used to calculate T_{o1} and T_{o2} when the rest of the variables are known. Notice that calculation of the horizontal tension components in equations (2.18) and (2.19) does not require the value of d, the horizontal distance of AC in the ground, and thus this variable is not introduced as an unknown. The distance d will be introduced as an unknown when geometric properties, such as the exact location of the buoy and the moored vessel with respect to an inertial reference frame are required. Equations (2.20) and (2.21) correspond to the force balance equations (2.13) and (2.14), where $\ddot{x}_B$ and $\ddot{z}_B$ have been set to zero as is the case of static equilibrium. Equation (2.22) is the balance of vertical forces in SC which includes the total weight of SC and the vertical tension components of each end of SC. Equation (2.23) is the balance of horizontal forces on SC which includes the integrated external and drag forces exerted on SC and the horizontal tension component T_{o2}.

Equations (2.18) - (2.23) are coupled and thus must be solved simultaneously using a Newton-Rapson algorithm or any other method [29]. Other solution methods can be developed by selecting a different combination of equations to be solved for the unknowns.

Further, the drag force on the buoy is given by:

$$F_{DB}=\frac{1}{2}\rho C_D A_B|\dot{x}_{BR}|\dot{x}_{BR}\ , \tag{2.24}$$

where ρ is the water density, C_D is the drag coefficient on the buoy; and A_B is the projected area of the buoy in the direction of the relative buoy velocity $\dot{x}_{BR}$ with respect to the water.

The drag forces on each segment of the catenary (F_{1D}, F_{2AD}, F_{2BD}) can be calculated following [21] which treats the drag forces on the suspended part of AC. The forces on each segment of SC can be calculated by separating S2A and S2B and treating them as individual suspended ACs. These have the general form:

$$F_{*D} = \frac{1}{2}\rho C_{D*} D_{eff} h_* \gamma_{p*} |\dot{x}_*| \dot{x}_* \ , \tag{2.25}$$

where C_{D*} is the drag coefficient of catenary segment *; D_{eff} is the effective diameter of the catenary; h_* is the vertical distance of segment *; γ_{p*} is the energy dissipation function of segment *; and $\dot{x}_*$ is the relative velocity between the upper endpoint of segment * and the current [12, 21].

The drag forces as well as the external force imposed by the moored vessel (F_{EXT}) may introduce additional unknowns in equations (2.18) - (2.23), such as current speed, in which case new equations must be developed. Those equations assume that the external forces are functions of the six unknowns (T_{o1}, T_{o2}, h_1, ℓ_1, ℓ_{2A} and ℓ_{2B}) exclusively.

There exist a number of auxiliary equations (see [12] and [26]) that could be used to reduce the number of unknowns (and therefore the number of equations) to calculate T_{o1} and T_{o2}. For the set of six equations presented above, T_{o1} and T_{o2} depend on the values of h_1, ℓ_1, ℓ_{2A} and ℓ_{2B}, and thus, it is best to solve the six equations simultaneously.

2.2. Catenary Deformation with One Buoy

Due to the drag forces that act on the catenary segments and on the buoy, the deformation of the complete catenary is three-dimensional. Figure 2.3 shows the horizontal plane geometry of the configuration of a catenary with one buoy, with the origin of the inertial frame (x,y,z) located at the point where S1 is anchored to the sea bed. The buoy has a right hand coordinate system (X_B,Y_B,Z_B) with its origin at its center of gravity, with X_B pointing horizontally in the plane of S1 catenary and Z_B pointing upwards. The position of the buoy with respect to the inertial reference frame is given by the vector (x_B,y_B,z_B). The horizontal angle between the

projection of the two segments of the catenary in the $(x,\ y)$ plane is denoted as β_B, and is measured counterclockwise from X_B.

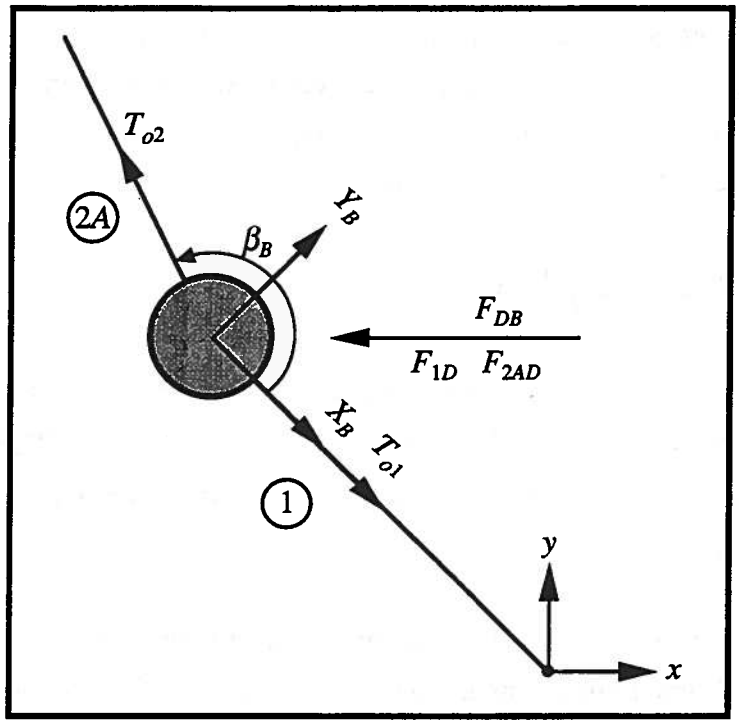

Figure 2.3. Three-dimensional catenary deformation with one buoy

Letting u_B be the velocity of the buoy in the X_B direction and v_B the velocity of the buoy in the Y_B direction, the horizontal plane equations of motion of the buoy in surge and sway are given by

$$(m_B + A_{11})\dot{u}_B = T_{o1} + T_{o2x} - F_{BDx} - F_{A1} - F_{A2Ax} - F_{L2Ax}\ , \tag{2.26}$$
$$(m_B + A_{22})\dot{v}_B = T_{o2y} - F_{BDy} - F_{L1} - F_{A2Ay} - F_{L2Ay}\ , \tag{2.27}$$

where A_{11} and A_{22} are the added mass terms in surge and sway, respectively; T_{o2x} is the projection of T_{o2} in the X_B direction; and T_{o2y} is the projection of T_{o2} in the Y_B direction. These are given by:

$$T_{o2x} = T_{o2}\cos\beta_B\ , \tag{2.28}$$
$$T_{o2y} = T_{o2}\sin\beta_B\ . \tag{2.29}$$

In equations (2.26) and (2.27), F_{DBx} and F_{DBy} are the buoy drag components in the X_B and Y_B directions respectively:

$$F_{DBx} = \frac{1}{2}\rho C_{Dx} A_B |u_B| u_B \ , \tag{2.30}$$

$$F_{DBy} = \frac{1}{2}\rho C_{Dy} A_B |v_B| v_B \ . \tag{2.31}$$

In equations (2.30) and (2.31), u_B and v_B are the relative velocities of the buoy with respect to water in the X_B and Y_B directions.

The drag forces acting on the catenary in equations (2.26) and (2.27) can be calculated following [12, 21] as follows:

Forces F_{A1} and F_{L1} are the drag forces on segment S1 in the X_B and Y_B directions respectively:

$$F_{A1} = \frac{1}{2}\rho C_{DX1} D_{eff} h_1 \gamma_{p1} |u_B| u_B \ , \tag{2.32}$$

$$F_{L1} = \frac{1}{4}\rho C_{DY1} D_{eff} h_1 \frac{\sin\theta_{\ell 1}}{1-\cos\theta_{\ell 1}} |v_B| v_B \ , \tag{2.33}$$

where C_{DX1} and C_{DY1} are the drag coefficients in the X_B and Y_B directions; $\theta_{\ell 1}$ is the angle between the tangent to S1 at its upper end and the Z_B axis [12].

Forces F_{A2Ax} and F_{L2Ax} are the parallel and perpendicular components of the mooring line drag forces on segment S2A acting in the X_B direction; and F_{A2Ay} and F_{L2Ay} are parallel and perpendicular components of the mooring line drag forces on segment S2A acting in the Y_B direction:

$$F_{A2Ax} = F_{A2A}\cos\beta_B \ , \tag{2.34}$$

$$F_{L2Ax} = -F_{L2A}\sin\beta_B \ , \tag{2.35}$$

$$F_{A2Ay} = F_{A2A}\sin\beta_B \ , \tag{2.36}$$

$$F_{L2Ay} = F_{L2A}\cos\beta_B \ , \tag{2.37}$$

where

$$F_{A2A} = \frac{1}{2}\rho C_{DX2A} D_{eff} h_{2A} \gamma_{p2A} |\dot{x}_{2A}| \dot{x}_{2A} \ , \tag{2.38}$$

$$F_{L2A} = \frac{1}{2}\rho C_{DY2A} D_{eff} h^*_{2A} \frac{\sin\theta_{\ell 2A}}{1-\cos\theta_{\ell 2A}} |\dot{y}_{2A}|\dot{y}_{2A} \ . \tag{2.39}$$

In equations (2.38) and (2.39), C_{DX2A} and C_{DY2A} are the drag coefficients of segment S2A, and $\dot{x}_{2A}$ and $\dot{y}_{2A}$ are the velocity components of the line in the directions parallel and perpendicular to the motion of S2A:

$$\dot{x}_{2A} = u_B \cos\beta_B + v_B \sin\beta_B \ , \tag{2.40}$$

$$\dot{y}_{2A} = -u_B \sin\beta_B + v_B \cos\beta_B \ . \tag{2.41}$$

Further, $\theta_{\ell 2A}$ is the angle between the tangent to S2A at its upper end and the Z_B axis; and h^*_{2A} is the effective height of S2A, taking into account the fact that the current velocity at the bottom of segment S2A is not zero. It is given by:

$$h^*_{2A} = \int_{h_1 - h_{2A}}^{h_1} \frac{h'}{h_1} dh' = \frac{1}{2} h_{2A} \left(\frac{2h_1 - h_{2A}}{h_1} \right) . \tag{2.42}$$

2.3. SPM Equations of Motion and Kinematic Relations

The equations of motion and kinematics of the moored vessel and buoy can be stated separately and then combined, resulting in the equations of motion and kinematic conditions of the mooring system, i.e. vessel and buoy.

The horizontal plane geometry of a Single Point Mooring (SPM) system connected to a deep water catenary is shown in Figure 2.4. In addition to the coordinate systems of Figure 2.3, the (X,Y,Z) coordinate system is introduced and is fixed to the vessel at its center of gravity (CG). In addition, γ is the horizontal angle between the x-axis and segment S2B, measured counterclockwise from the vessel; and γ_B is the horizontal angle between the x-axis and segment S1, measured counterclockwise from the buoy.

Note that the relationship between β_B, γ and γ_B is:

$$\beta_B = \gamma - \gamma_B + \pi \ . \tag{2.43}$$

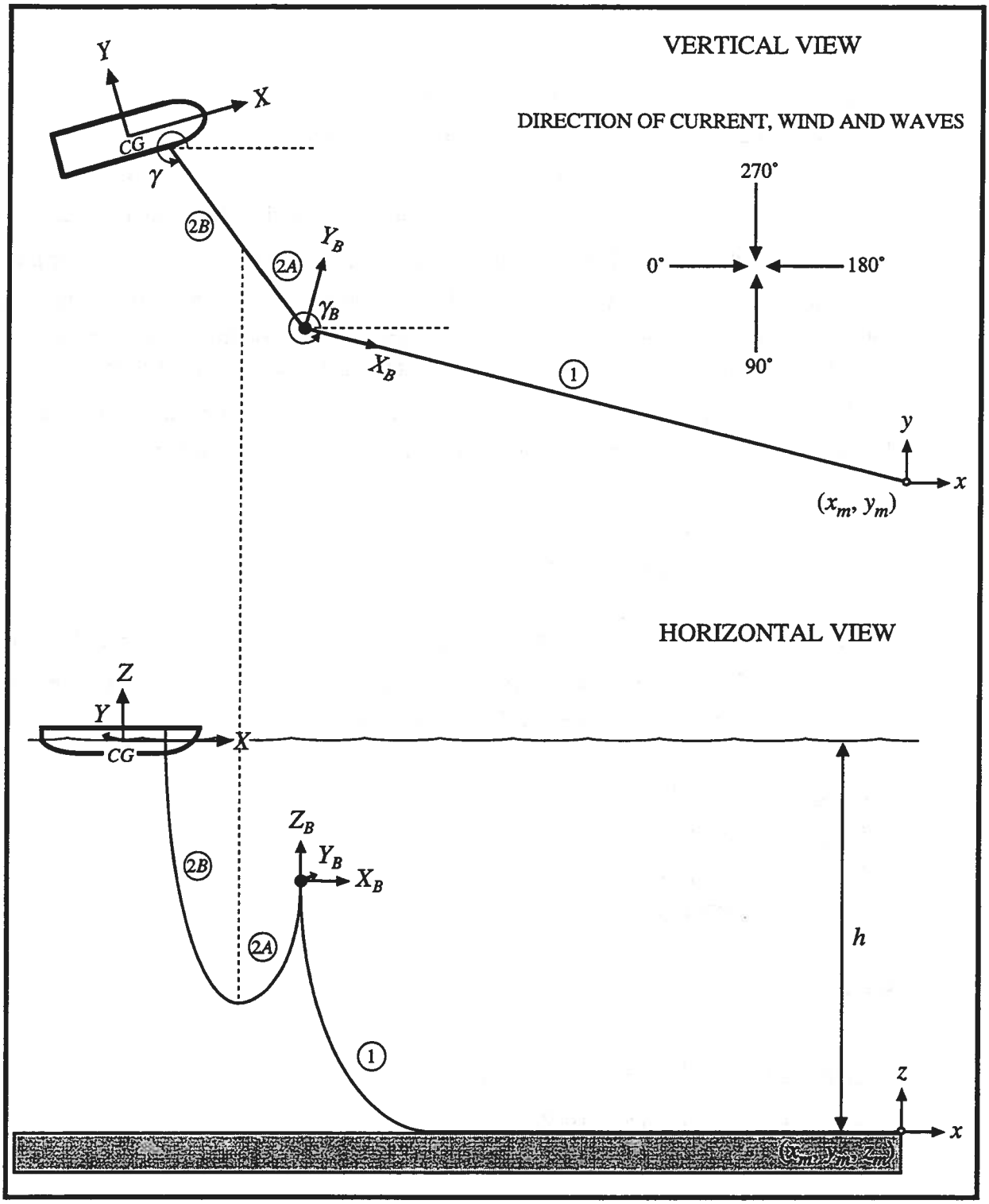

Figure 2.4. Geometry of Single Point Mooring system with one buoy

The horizontal plane equations of motion for the moored vessel - surge, sway and yaw - are given by [13, 27]:

$$(m+m_x)\dot{u}-(m+m_y)vr = X_H + T_{o2}\cos\beta - F_{2BDX} + F_{surge}\ , \tag{2.44}$$

$$(m+m_y)\dot{v}+(m+m_x)ru = Y_H + T_{o2}\sin\beta - F_{2BDY} + F_{sway}\ , \tag{2.45}$$

$$(I_{zz}+J_{zz})\dot{r} = N_H + x_p\left[T_{o2}\sin\beta - F_{2BDY}\right] - y_p\left[T_{o2}\cos\beta - F_{2BDX}\right] + N_{yaw}\ , \tag{2.46}$$

where m is the mass of the vessel; m_x and m_y are the added mass terms in surge and sway; I_{zz} is the second moment of inertia about the Z-axis; J_{zz} is the added moment of inertia; u, v, and $\dot{u}$, $\dot{v}$ are the relative velocities and accelerations in surge and sway with respect to water; r and $\dot{r}$ are the relative angular velocity and acceleration in yaw with respect to water; x_p and y_p are the body-fixed coordinates of the mooring line fairlead; β is the angle between the X-axis and the mooring line, measured counterclockwise from the vessel; F_{2BDX} and F_{2BDY} are the drag forces on segment 2B of SC in the X and Y directions, respectively:

$$F_{2BDX} = F_{A2BX} + F_{L2BX}\ , \tag{2.47}$$

$$F_{2BDY} = F_{A2BY} + F_{L2BY}\ , \tag{2.48}$$

where in equations (2.47) and (2.48), F_{A2BX}, F_{L2BX}, F_{A2BY}, F_{L2BY} are the drag forces on segment S2B of SC in the directions parallel and perpendicular to the mooring line motion in the X and Y directions, respectively. These are given by [12]

$$F_{A2BX} = F_{A2B}\cos\beta\ , \tag{2.49}$$

$$F_{L2BX} = -F_{L2B}\sin\beta\ , \tag{2.50}$$

$$F_{A2BY} = F_{A2B}\sin\beta\ , \tag{2.51}$$

$$F_{L2BY} = F_{L2B}\cos\beta\ , \tag{2.52}$$

where

$$F_{A2B} = \frac{1}{2}\rho C_{DX2B} D_{eff} h_{2B} \gamma_{p2B} |\dot{x}_{2B}|\dot{x}_{2B}\ , \tag{2.53}$$

$$F_{L2B} = \frac{1}{2}\rho C_{DY2B} D_{eff} h^*_{2B} \frac{\sin\theta_{\ell 2B}}{1-\cos\theta_{\ell 2B}} |\dot{y}_{2B}|\dot{y}_{2B}\ . \tag{2.54}$$

In equations (2.53) and (2.54), C_{DX2B} and C_{DY2B} are the drag coefficients of segment S2B, and $\dot{x}_{2B}$ and $\dot{y}_{2B}$ are the velocities parallel and perpendicular to the motion of S2B:

$$\dot{x}_{2B} = (u - y_p r)\cos\beta + (v + x_p r)\sin\beta \ , \tag{2.55}$$
$$\dot{y}_{2B} = -(u - y_p r)\sin\beta + (v + x_p r)\cos\beta \ . \tag{2.56}$$

In addition, $\theta_{\ell 2B}$ is the vertical angle of the upper point of segment S2B; and h^*_{2B} is the effective height of S2B

$$h^*_{2B} = \int_{h-h_1+h_{2A}}^{h} \frac{h'}{h} dh' = \frac{1}{2}(h_1 - h_{2A})\left[\frac{2h - h_1 + h_{2A}}{h}\right] . \tag{2.57}$$

Further, in equations (2.44) - (2.46), X_H, Y_H, N_H are the velocity dependent, horizontal plane, hull hydrodynamic forces and moment in surge, sway and yaw expressed in terms of the large drift, slow motion derivatives as [13, 31, 32]:

$$X_H = X_o + X_u u + \frac{1}{2}X_{uu}u^2 + \frac{1}{6}X_{uuu}u^3 + X_{vr}vr \ , \tag{2.58}$$
$$Y_H = Y_v v + Y_{vvv}v^3 + Y_{vvvvv}v^5 + Y_{ur}ur + Y_{ur|r|}ur|r| + Y_{v|r|}v|r| \ , \tag{2.59}$$
$$N_H = N_v v + N_{uv}uv + N_{vvv}v^3 + N_{uvvv}uv^3 + N_r r + N_{r|r|}r|r| + N_{uv|r|}uv|r| + N_{vvr}v^2 r \ . \tag{2.60}$$

Finally, F_{surge}, F_{sway} and N_{yaw} are the external forces and moment acting on the vessel due to steady wind and second order mean wave drift [2, 27].

The kinematics of the vessel are given by

$$\dot{x} = u\cos\psi - v\sin\psi + U_c\cos\alpha \ , \tag{2.61}$$
$$\dot{y} = u\sin\psi + v\cos\psi + U_c\sin\alpha \ , \tag{2.62}$$
$$\dot{\psi} = r \ , \tag{2.63}$$

where α is the current angle with direction of excitation as shown in Figure 2.4.

The equations of motion for the buoy in surge, sway and heave are:

$$(m_B + A_{11})\dot{u}_B = T_{o1} + T_{o2}\cos\beta_B - F_{BDx} - F_{A1} - F_{2ADX} \ , \tag{2.64}$$
$$(m_B + A_{22})\dot{v}_B = T_{o2}\sin\beta_B - F_{BDy} - F_{L1} - F_{2ADY} \ , \tag{2.65}$$

$$(m_B + A_{33})\dot{w}_B = F_B - T_{o1}\sinh\left(\frac{P\ell_1}{T_{o1}}\right) - T_{o2}\sinh\left(\frac{P\ell_{2A}}{T_{o2}}\right), \tag{2.66}$$

where $\dot{u}_B$, $\dot{v}_B$ and $\dot{w}_B$ are the relative acceleration components of the buoy in surge, sway and heave. Assuming a linear current profile, the buoy kinematics are given by

$$\dot{x}_B = u_B\cos\gamma_B - v_B\sin\gamma_B + U_c\frac{z_B}{h}\cos\alpha\ , \tag{2.67}$$

$$\dot{y}_B = u_B\sin\gamma_B + v_B\cos\gamma_B + U_c\frac{z_B}{h}\sin\alpha\ , \tag{2.68}$$

$$\dot{z}_B = w_B\ . \tag{2.69}$$

In equation (2.69), w_B is the heave velocity of the buoy and z_B is the vertical position of its center of gravity.

The equations of motion of the mooring system include the equations of motion of the vessel in the horizontal plane (2.44) - (2.46) and the equations of motion in surge, sway and heave of the buoy (2.64) - (2.66). These equations, along with the respective kinematics (2.61) - (2.63) and (2.67) - (2.69), define the basis of the mathematical model for the SPM system with one buoy. The mathematical model developed above is not limited to the Takashina hydrodynamic maneuvering model of equations (2.58) - (2.60). Different hydrodynamic models, such as those developed by Abkowitz [1], Leite et al. [19], Obokata [23, 24] and others [9], can be implemented instead.

2.4. State Space Representation and Equilibria of SPM Systems

The nonlinear model for the SPM system presented in the previous section consists of twelve equations that describe the behavior of the system as follows: vessel equations of motion in surge, sway and yaw (2.44) - (2.46); buoy equations of motion in surge, sway and heave (2.64) - (2.66); vessel kinematics (2.61) - (2.63); and buoy kinematics (2.67) - (2.69). These equations can be recast as a set of twelve first order nonlinear coupled differential equations of the form:

$$\dot{\boldsymbol{x}} = \boldsymbol{f}(\boldsymbol{x}), \qquad \boldsymbol{x} \in \Re^{12}\ . \tag{2.70}$$

It is convenient to represent the state space variables in terms of the position and velocity vectors of the moored vessel and the connecting buoy ("Ship Motions Flow") [5]. Then, the state space can be defined by the following twelve state space variables: $\boldsymbol{x}=[u,\ v,\ r,\ x,\ y,\ \psi,\ u_B,\ v_B,\ w_B,\ x_B,\ y_B,\ z_B]^{\mathrm{T}}$. The nonlinear model of the system can be written in Cauchy standard form as:

$$\dot{u}=\frac{X_H+(m+m_y)vr+T_{o2}\cos\beta-F_{2BDX}+F_{surge}}{(m+m_x)}\ , \tag{2.71}$$

$$\dot{v}=\frac{Y_H-(m+m_x)ru+T_{o2}\sin\beta-F_{2BDY}+F_{sway}}{(m+m_y)}\ , \tag{2.72}$$

$$\dot{r}=\frac{N_H+x_p[T_{o2}\sin\beta-F_{2BDY}]-y_p[T_{o2}\cos\beta-F_{2BDX}]+N_{yaw}}{(I_{zz}+J_{zz})}\ , \tag{2.73}$$

$$\dot{x}=u\cos\psi-v\sin\psi+U_c\cos\alpha\ , \tag{2.74}$$

$$\dot{y}=u\sin\psi+v\cos\psi+U_c\sin\alpha\ , \tag{2.75}$$

$$\dot{\psi}=r\ , \tag{2.76}$$

$$\dot{u}_B=\frac{T_{o1}+T_{o2}\cos\beta_B-F_{BDx}-F_{A1}-F_{2ADX}}{(m_B+A_{11})}\ , \tag{2.77}$$

$$\dot{v}_B=\frac{T_{o2}\sin\beta_B-F_{BDy}-F_{L1}-F_{2ADY}}{(m_B+A_{22})}\ , \tag{2.78}$$

$$\dot{w}_B=\frac{F_B-T_{o1}\sinh\left(\frac{P\ell_1}{T_{o1}}\right)-T_{o2}\sinh\left(\frac{P\ell_{2A}}{T_{o2}}\right)}{(m_B+A_{33})}\ , \tag{2.79}$$

$$\dot{x}_B=u_B\cos\gamma_B-v_B\sin\gamma_B+U_c\frac{z_B}{h}\cos\alpha\ , \tag{2.80}$$

$$\dot{y}_B=u_B\sin\gamma_B+v_B\cos\gamma_B+U_c\frac{z_B}{h}\sin\alpha\ , \tag{2.81}$$

$$\dot{z}_B=w_B\ . \tag{2.82}$$

The system equilibria can be found by setting the time derivative of the state variable vector equal to zero; i.e.

$$\bar{\boldsymbol{x}}\in\Re^{12}\ \text{ is an equilibrium of }\ \dot{\boldsymbol{x}}=\boldsymbol{f}(\boldsymbol{x})\quad\Leftrightarrow\quad\boldsymbol{f}(\bar{\boldsymbol{x}})=\boldsymbol{0}\ , \tag{2.83}$$

where the overbar on the state variable vector $\bar{\boldsymbol{x}}$ denotes the equilibrium state.

To find the equilibrium of (2.70), system (2.83), which consists of twelve equations (2.71) - (2.82) and twelve unknowns, must be solved. To find a solution to this system of equations, it is convenient to reduce the number of equations that must be solved simultaneously. Some of the twelve variables at equilibrium are known or can be recast in terms of other variables, and thus the number of equations that must be solved simultaneously for equilibrium can be reduced. The equilibrium solution for the vessel velocity vector ($\bar{u}$, $\bar{v}$, $\bar{r}$) can be derived by setting expressions (2.74) - (2.76) equal to zero (i.e. $\dot{x}=0$, $\dot{y}=0$, $\dot{\psi}=0$). This yields:

$$\bar{u} = -U_c \cos(\bar{\psi} - \alpha) \ , \tag{2.84}$$

$$\bar{v} = U_c \sin(\bar{\psi} - \alpha) \ , \tag{2.85}$$

$$\bar{r} = 0 \ . \tag{2.86}$$

In addition, by setting expression (2.82) equal to zero (i.e. $\dot{z}_B=0$), we have:

$$\bar{w}_B = 0 \ . \tag{2.87}$$

Thus, ($\bar{u}$, $\bar{v}$, $\bar{r}$, $\bar{w}_B$) can be eliminated, thus reducing the state variables and simultaneous equations from twelve to eight. The reduced system of equations includes (2.71) - (2.73) and (2.77) - (2.81). In these equations, the values for $\bar{u}$ and $\bar{v}$ are recast in terms of the vessel drift angle $\bar{\psi}$ using equations (2.84) and (2.85), while the values for $\bar{r}$ and $\bar{w}_B$ are zero.

Since the expressions for the horizontal tension terms at equilibrium $\bar{T}_{o1}$ and $\bar{T}_{o2}$ are unknown, six additional equations must be solved simultaneously with the eight equilibrium state space equations. Then, the fourteen equilibrium equations that need to be solved simultaneously are:

$$\bar{X}_H + \bar{T}_{o2}\cos\bar{\beta} - \bar{F}_{2BDX} + \bar{F}_{surge} = 0 \ , \tag{2.88}$$

$$\bar{Y}_H + \bar{T}_{o2}\sin\bar{\beta} - \bar{F}_{2BDY} + \bar{F}_{sway} = 0 \ , \tag{2.89}$$

$$\bar{N}_H + x_p\left(\bar{T}_{o2}\sin\bar{\beta} - \bar{F}_{2BDY}\right) - y_p\left(\bar{T}_{o2}\cos\bar{\beta} - \bar{F}_{2BDX}\right) + \bar{N}_{yaw} = 0 \ , \tag{2.90}$$

$$\bar{T}_{o1} + \bar{T}_{o2}\cos\bar{\beta}_B - \bar{F}_{BDx} - \bar{F}_{A1} - \bar{F}_{2ADX} = 0 \ , \tag{2.91}$$

$$\bar{T}_{o2}\sin\bar{\beta}_B - \bar{F}_{BDy} - \bar{F}_{L1} - \bar{F}_{2ADY} = 0 \ , \tag{2.92}$$

$$F_B - \bar{T}_{o1}\sinh\left(\frac{P\bar{\ell}_1}{\bar{T}_{o1}}\right) - \bar{T}_{o2}\sinh\left(\frac{P\bar{\ell}_{2A}}{\bar{T}_{o2}}\right) = 0 \ , \tag{2.93}$$

$$\bar{u}_B\cos\bar{\gamma}_B - \bar{v}_B\sin\bar{\gamma}_B + U_c\frac{\bar{z}_B}{h}\cos\alpha = 0 \ , \tag{2.94}$$

$$\bar{u}_B\sin\bar{\gamma}_B + \bar{v}_B\cos\bar{\gamma}_B + U_c\frac{\bar{z}_B}{h}\sin\alpha = 0 \ , \tag{2.95}$$

$$\sinh\left(\frac{P\bar{\ell}_1}{\bar{T}_{o1}}\right)-\frac{P}{\bar{T}_{o1}}\sqrt{\bar{z}_B\left(\bar{z}_B+2\frac{\bar{T}_{o1}}{P}\right)}=0\ , \tag{2.96}$$

$$\sinh\left(\frac{P\bar{\ell}_{2A}}{2\bar{T}_{o2}}\right)\cosh\left(\frac{P\bar{\ell}_{2B}}{2\bar{T}_{o2}}\right)+\cosh\left(\frac{P\bar{\ell}_{2A}}{2\bar{T}_{o2}}\right)\sinh\left(\frac{P\bar{\ell}_{2B}}{2\bar{T}_{o2}}\right)$$
$$-\frac{P}{2\bar{T}_{o2}}\sqrt{\ell_{w2}^2-(h-\bar{z}_B)^2}=0\ , \tag{2.97}$$

$$\ell_{w1}-\frac{\bar{T}_{o1}}{P}\sinh\left(\frac{P\bar{\ell}_1}{\bar{T}_{o1}}\right)-\bar{d}=0\ , \tag{2.98}$$

$$\ell_{w2}-\frac{\bar{T}_{o2}}{P}\sinh\left(\frac{P\bar{\ell}_{2A}}{\bar{T}_{o2}}\right)-\frac{\bar{T}_{o2}}{P}\sinh\left(\frac{P\bar{\ell}_{2B}}{2\bar{T}_{o2}}\right)=0\ , \tag{2.99}$$

$$\sqrt{(x_m-\bar{x}_B)^2+(y_m-\bar{y}_B)^2}-\bar{\ell}_1-\bar{d}=0\ , \tag{2.100}$$

$$\sqrt{(\bar{x}_B-\bar{x}_T)^2+(\bar{y}_B-\bar{y}_T)^2}-\bar{\ell}_{2A}-\bar{\ell}_{2B}=0\ , \tag{2.101}$$

for unknowns $\bar{x}$, $\bar{y}$, $\bar{\psi}$, $\bar{x}_B$, $\bar{y}_B$, $\bar{z}_B$, $\bar{u}_B$, $\bar{v}_B$, $\bar{T}_{o1}$, $\bar{T}_{o2}$, $\bar{d}$, $\bar{\ell}_1$, $\bar{\ell}_{2A}$, and $\bar{\ell}_{2B}$. In equation (2.100), $(x_m,\ y_m)=(0,\ 0)$ are the horizontal plane coordinates of the point where segment S1 is anchored to the sea floor, and $(\bar{x}_T, \bar{y}_T)$ are the horizontal plane attachment coordinates of segment 2B on the vessel:

$$\bar{x}_T=\bar{x}+x_p\cos\bar{\psi}-y_p\sin\bar{\psi}\ , \tag{2.102}$$

$$\bar{y}_T=\bar{y}+x_p\sin\bar{\psi}+y_p\cos\bar{\psi}\ . \tag{2.103}$$

It should be noted that the six additional equations introduced (2.96) - (2.101) correspond to unknowns for the horizontal tension components $\bar{T}_{o1}$, $\bar{T}_{o2}$, as well as the lengths of the horizontal projections of the mooring line segments $\bar{d}$, $\bar{\ell}_1$, $\bar{\ell}_{2A}$, and $\bar{\ell}_{2B}$. Unlike equations (2.18) - (2.23) where the touchdown length $\bar{d}$ was not required to derive the horizontal tension components at equilibrium, here we need to solve for it in order to define the exact location of the vessel and the buoy with respect to the mooring point on the ground. In addition, the value of h_1 is related to z_B as follows:

$$h_1=z_B-R_B\approx z_B\ . \tag{2.104}$$

Thus, we have exchanged h_1 for z_B in all equations where h_1 appears explicitly. The exact value for h_1 could be implemented without creating any complications to the solution algorithm. Practically, however, R_B is insignificantly small compared to z_B.

Equations (2.96) and (2.97) are used to solve for the values of $\overline{T}_{o1}$ and $\overline{T}_{o2}$. Equations (2.98) and (2.99) provide expressions for the total lengths ℓ_{w1} and ℓ_{w2} of each catenary segment in terms of auxiliary variables $\overline{T}_{o1}$, $\overline{T}_{o2}$, $\overline{\ell}_1$, $\overline{\ell}_{2A}$, and $\overline{\ell}_{2B}$. Finally, equations (2.100) and (2.101) provide auxiliary expressions for the lengths of the horizontal projections of segments S1 and S2.

To apply the concept of equilibrium, consider, as an example, the principal equilibrium of a SPM tanker [13] moored with a catenary chain [20] in 750 meters water depth under a current of velocity 2 knots (180° heading). The total length of the mooring line is 1600 meters, and the buoy is placed 600 meters from the top of S2B (i.e. ℓ_{w1}=1000 m; ℓ_{w2}=600 m). In this example, the net buoyancy of the buoy is F_B=886.5 kN, and the fairlead coordinates of attachment on the vessel are given by (x_p, y_p)=(60, 0) m. Table 2.1 shows the principal equilibrium values of the state space and auxiliary variables of equations (2.84) - (2.87) and (2.88) - (2.101). It is noteworthy to point out that this particular SPM configuration may have other equilibrium solutions. The complete solution to equilibrium equations (2.88) - (2.101) is, however, out of the scope of this report. Suffice to point out that all equilibria present in the system can be obtained by solving such equations.

2.5 Simulation of the Nonlinear SPM System Dynamics

Nonlinear solutions in time are used often to simulate the dynamical behavior that specific mooring systems exhibit. Simulations are further needed to understand the dynamics of mooring systems for design purposes. Simulations show the richness of the dynamics of mooring systems and can be performed directly on the system (2.71) - (2.82) by integrating in time using a Runge-Kutta or a similar algorithm [29]. Time integration of the nonlinear system requires that the system be bounded initially. Therefore, special attention must be paid when defining the initial conditions for simulation.

Even though it is not necessary to solve for the system equilibria in order to perform nonlinear time simulations, it is often desired and convenient to start a simulation near an equilibrium position, particularly its principal equilibrium. This assures that the initial geometry of the system, defined by the initial conditions, is bounded and does not induce excessive mooring line tensions. In addition, simulations near an equilibrium position provide useful information regarding the dynamics of the system near such equilibrium. It is important to point out, however, that inappropriate initial choices of conditions near an equilibrium

position may place the system inside a stable sub-manifold of the SPM [25] or even a spread mooring system [10]. In such a case, time simulations near an unstable equilibrium position may appear to be stable. Nonlinear time simulations, and even systematic simulations, reveal only a partial picture of the nonlinear system dynamics, and thus often times several simulations on the nonlinear system must be performed [3].

Table 2.1. Principal equilibrium of SPM: state space and auxiliary variables

State Space Variable		
$\overline{u}$	(m/s)	1.0296
$\overline{v}$	(m/s)	0.0000
$\overline{r}$	(r/s)	0.0000
$\overline{x}$	(m)	−760.7295
$\overline{y}$	(m)	0.0000
$\overline{\psi}$	(rad)	0.0000
$\overline{u}_B$	(m/s)	0.5927
$\overline{v}_B$	(m/s)	0.0000
$\overline{w}_B$	(m/s)	0.0000
$\overline{x}_B$	(m)	−613.7385
$\overline{y}_B$	(m)	0.0000
$\overline{z}_B$	(m)	431.7737
Auxiliary Variable		
$\overline{T}_{o1}$	(kN)	21.9343
$\overline{T}_{o2}$	(kN)	17.3255
$\overline{d}$	(m)	553.9436
$\overline{\ell}_1$	(m)	59.7949
$\overline{\ell}_{2A}$	(m)	36.7216
$\overline{\ell}_{2B}$	(m)	50.2695

To illustrate the behavior of the SPM system of our example near the equilibrium position in Table 2.1 using nonlinear time simulations, the drift angle of the SPM system is simulated in time in Figure 2.5. This simulation, whose initial conditions were close to the principal equilibrium position (zero drift angle equilibrium) of the system, shows divergence from it. Therefore, the principal equilibrium of the vessel is unstable, and the vessel drifts away from that equilibrium position.

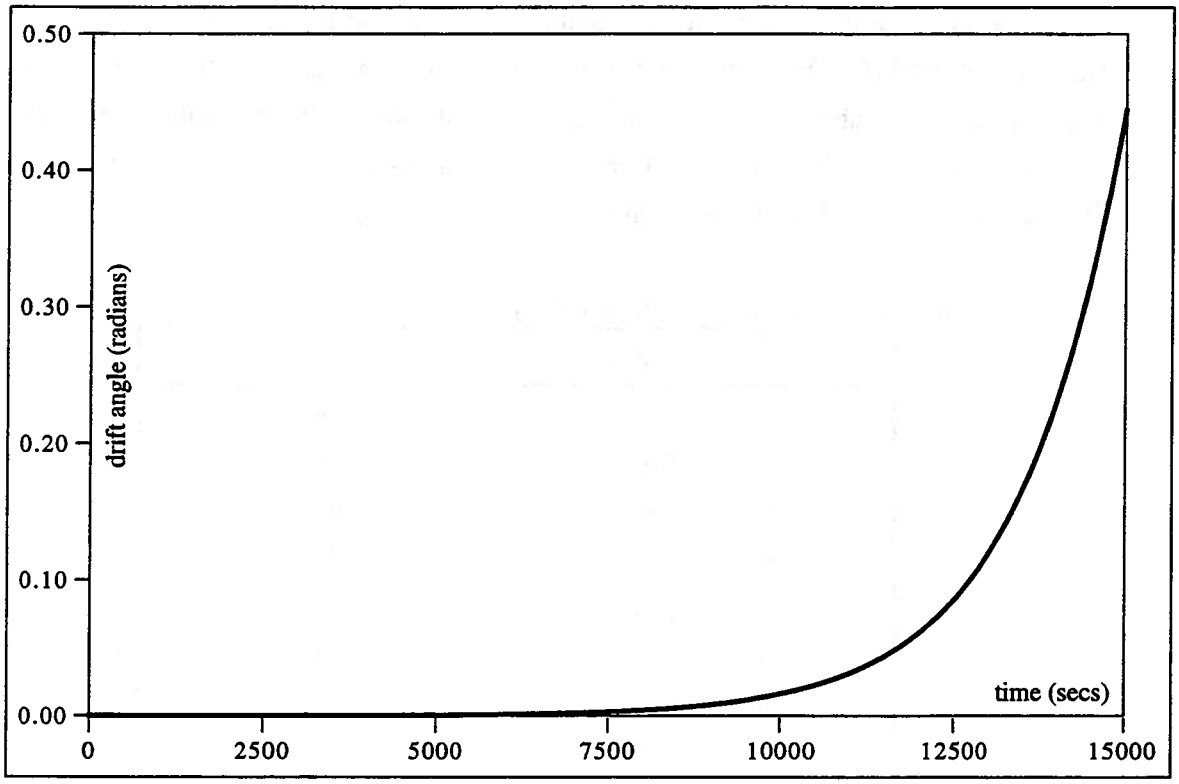

Figure 2.5. Time simulation of SPM - drift angle

In the following section, stability theory based on eigenvalue analysis is used to understand the qualitative behavior of mooring systems near an equilibrium. The concept and its usefulness are illustrated using the same numerical example of this section.

2.6 Introduction to Stability Analysis of Nonlinear SPM System

The qualitative dynamic behavior of the system about an equilibrium position is best described by nonlinear stability analysis as time simulations of the nonlinear system alone cannot reveal the complete picture of the system dynamics.

Stability in the sense of Liapunov defines the asymptotic behavior of trajectories of equation (2.70), provided that $f(x)$ is continuous with at least one continuous derivative, by studying the equivalent linear system near equilibrium:

$$\dot{\xi}=[A]\xi, \qquad \xi\in\Re^{12}, \qquad [A]\in\Re^{12\times12}, \tag{2.105}$$

where $\xi = \xi(t) = x(t) - \bar{x}$ is the deviation from equilibrium $\bar{x}$, and $[A] = Df(\bar{x})$ is the Jacobian matrix of the first partial derivatives of f evaluated at equilibrium:

$$[A] = \left[\frac{\partial f_i}{\partial x_j} \right] \Bigg|_{\bar{x}}, \qquad i, j = 1, 2, \ldots, 12 . \tag{2.106}$$

If [A] has exclusively hyperbolic eigenvalues (eigenvalues with nonzero real parts), the stability properties of the nonlinear system around equilibrium $\bar{x}$ can be obtained from the real parts of the eigenvalues of [A]. Stability of SPM and other types of mooring systems has been extensively studied in [2-5, 7, 8, 10, 11, 13-15, 17-19, 22, 25-27, 30], and will not be discussed in detail here. Suffice to say that if all eigenvalues have negative real parts, nearby trajectories approach $\bar{x}$ at an exponential rate in forward time; if at least one eigenvalue has a positive real part, $\bar{x}$ is unstable, and all trajectories initiated near $\bar{x}$ will deviate from it exponentially in forward time [33].

The goal of this section is to introduce this concept and apply it to the behavior of a particular SPM system with one buoy around a particular equilibrium solution. A complete description of general stability theory is provided by Guckenheimer and Holmes in [16].

Table 2.2 shows the twelve eigenvalues of the SPM system used in the previous section around the equilibrium in Table 2.1, that is, its principal equilibrium. The system possesses one positive real eigenvalue, which proves that the principal equilibrium of the system is unstable. Other equilibria that may attract these trajectories may exist. Thus, locally, the SPM system is unstable. A global analysis of the system dynamics is achieved by studying the stability properties of all system equilibria.

Important differences between the mooring systems treated in this report and other stability studies of mooring systems referenced above are the inclusion of buoys, and the dependence of mooring line tension and mooring line drag on the depth of submergence of the buoy. These differences affect the typical Jacobian matrix [A] of partial derivatives used for stability analysis of mooring systems. In the expressions for mooring line drag forces (2.32) - (2.33), (2.38) - (2.39), and (2.53) - (2.54), the buoy depth z_B (or h_1) appears as a variable, and thus partial derivatives of these expressions with respect to z_B can be readily taken. The changes in mooring line tension as a function of z_B, however, require extensive algebra. In Appendixes 1

and 2, expressions are derived for the changes in geometry and mooring line tension with changes in buoy depth.

Table 2.2. Eigenvalues of SPM system of Figure 2.5: Principal equilibrium

Eigenvalue	Real Part	Imaginary Part
λ_1	-0.8549×10^{-1}	$+i0.4167\times10^{-1}$
λ_2	-0.8549×10^{-1}	$-i0.4167\times10^{-1}$
λ_3	-0.1078×10^{-3}	$+i0.1070\times10^{-2}$
λ_4	-0.1078×10^{-3}	$-i0.1070\times10^{-2}$
λ_5	-0.3105×10^{-2}	$+i0.1849$
λ_6	-0.3105×10^{-2}	$-i0.1849$
λ_7	-0.4830×10^{-3}	$+i0.5135\times10^{-1}$
λ_8	-0.4830×10^{-3}	$-i0.5135\times10^{-1}$
λ_9	-0.9563×10^{-2}	0.0000
λ_{10}	-0.1516×10^{-3}	$+i0.4372\times10^{-3}$
λ_{11}	-0.1516×10^{-3}	$-i0.4372\times10^{-3}$
λ_{12}	$+0.6729\times10^{-3}$	0.0000

It is very unlikely that a single point, single line mooring system with one buoy would be deployed in deep water mooring operations. The hydrodynamic properties of tankers [9] make these types of systems unattractive. In addition, SPM systems without buoys may exhibit chaotic behavior [2, 27]. In deep water mooring operations, several mooring lines must be deployed to restrain the vessel from undergoing large amplitude motions. These types of systems, labeled as Spread Mooring Systems (SMS), are the subject of analysis in the next chapter.

III. SPREAD MOORING SYSTEMS WITH ONE BUOY PER LINE

In deep water operations, a single point, single line mooring system cannot be used because such system will not be able to restrict the motions of the vessel within bounds of safe operation. Thus, it is necessary to attach other lines to the system to help restrain the slow and intermediate motions of the vessel. These types of systems, known as Spread Mooring Systems (SMS), are the focus of this chapter. In this chapter, the equations of motion and kinematics of SPM systems are extended to SMS consisting of mooring lines with a single buoy per line. In addition, expressions for the state space representation, equilibria, and initial geometry of SMS are derived. Finally, an example of SMS is studied via nonlinear time simulations and stability analysis.

Figure 3.1 shows the general horizontal plane geometry of a SMS moored to several terminals. The system consists of n mooring lines and n_B buoys. In Figure 3.1, $n = n_B$, and $i = j$, where i is the line number and j is the buoy number. In addition to the inertial and ship body-fixed reference frames, each buoy has its own right handed reference frame (X_B, Y_B, Z_B) with X_B pointing horizontally in the direction of its corresponding mooring terminal (x_m, y_m, z_m) and Z_B pointing upwards. The conventions for the geometrical features of the SMS, the nomenclature, and the direction of excitation remain the same as those corresponding to the SPM system studied in Chapter 2.

3.1. SMS Equations of Motion and Kinematic Relations

The system shown in Figure 3.1 consists of $3+3n_B$ equations of motion and $3+3n_B$ kinematic relations. These correspond to the three horizontal plane vessel equations of motion and kinematics, and three equations of motion for each buoy in surge, sway, and heave as well as their corresponding kinematic relations.

The horizontal plane equations of motion for the vessel in surge, sway and yaw are:

$$(m+m_x)\dot{u} - (m+m_y)rv = X_H + \sum_{i=1}^{n}\left\{T_{o2}^{(i)}\cos\beta^{(i)} - F_{2BDX}^{(i)}\right\} + F_{surge}\ , \tag{3.1}$$

$$(m+m_y)\dot{v}+(m+m_x)ru = Y_H + \sum_{i=1}^{n}\left\{T_{o2}^{(i)}\sin\beta^{(i)} - F_{2BDY}^{(i)}\right\} + F_{sway}\ , \tag{3.2}$$

$$(I_{zz}+J_{zz})\dot{r} = N_H + \sum_{i=1}^{n}\left\{x_p^{(i)}\left[T_{o2}^{(i)}\sin\beta^{(i)} - F_{2BDY}^{(i)}\right] - y_p^{(i)}\left[T_{o2}^{(i)}\cos\beta^{(i)} - F_{2BDX}^{(i)}\right]\right\} + N_{yaw}\ . \tag{3.3}$$

The vessel kinematics are the same as those for SPM given by equations (2.61) - (2.63). Those equations are repeated below

$$\dot{x} = u\cos\psi - v\sin\psi + U_c\cos\alpha\ , \tag{3.4}$$

$$\dot{y} = u\sin\psi + v\cos\psi + U_c\sin\alpha\ , \tag{3.5}$$

$$\dot{\psi} = r\ . \tag{3.6}$$

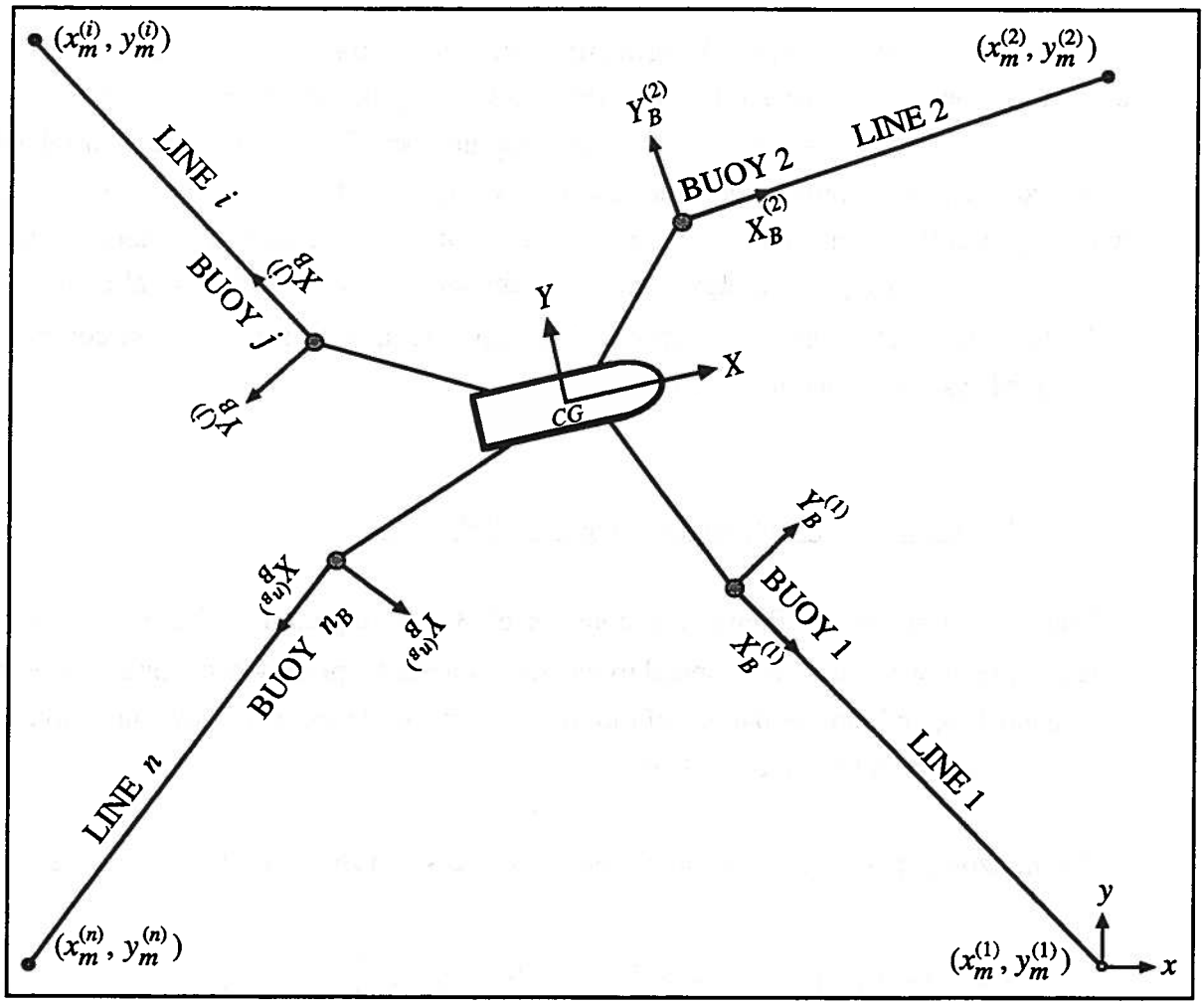

Figure 3.1. Geometry of Spread Mooring System with one buoy per line

The equations of motion for each of the buoys in surge, sway and heave are given by:

$$(m_B^{(i)} + A_{11}^{(i)})\dot{u}_B^{(i)} = T_{o1}^{(i)} + T_{o2}^{(i)} \cos\beta_B^{(i)} - F_{DBX}^{(i)} - F_{A1}^{(i)} - F_{2ADX}^{(i)}\ , \quad (i=1,\ \ldots\ ,\ n_B)\ , \tag{3.7}$$

$$(m_B^{(i)} + A_{22}^{(i)})\dot{v}_B^{(i)} = T_{o2}^{(i)} \cos\beta_B^{(i)} - F_{DBY}^{(i)} - F_{L1}^{(i)} - F_{2ADY}^{(i)}\ , \quad (i=1,\ \ldots\ ,\ n_B)\ , \tag{3.8}$$

$$(m_B^{(i)} + A_{33}^{(i)})\dot{w}_B^{(i)} = F_B^{(i)} - T_{o1}^{(i)} \sinh\left(\frac{P\ell_1^{(i)}}{T_{o1}^{(i)}}\right) - T_{o2}^{(i)} \sinh\left(\frac{P\ell_{2A}^{(i)}}{T_{o2}^{(i)}}\right),\quad (i=1,\ \ldots\ ,\ n_B)\ . \tag{3.9}$$

The associated $3n_B$ kinematic relations are:

$$\dot{x}_B^{(i)} = u_B^{(i)} \cos\gamma_B^{(i)} - v_B^{(i)} \sin\gamma_B^{(i)} + U_c \frac{z_B^{(i)}}{h} \cos\alpha\ , \quad (i=1,\ \ldots\ ,\ n_B)\ , \tag{3.10}$$

$$\dot{y}_B^{(i)} = u_B^{(i)} \sin\gamma_B^{(i)} + v_B^{(i)} \cos\gamma_B^{(i)} + U_c \frac{z_B^{(i)}}{h} \sin\alpha\ , \quad (i=1,\ \ldots\ ,\ n_B)\ , \tag{3.11}$$

$$\dot{z}_B^{(i)} = w_B^{(i)}\ , \quad (i=1,\ \ldots\ ,\ n_B)\ . \tag{3.12}$$

The three equations of motion for the vessel (3.1) - (3.3), buoys (3.7) - (3.9), and their corresponding kinematic relations (3.4) - (3.6) and (3.10) - (3.13) provide the mathematical model used to describe the slow motion dynamics of the SMS.

3.2. State Space Representation and Equilibria of SMS

The nonlinear SMS model presented in the previous section consists of $3+3n_B$ equations of motion as follows: 3 vessel equations in surge, sway and yaw, and 3 equations for each buoy in surge, sway and heave; and their corresponding $3+3n_B$ kinematic relations. Following the representation of the SPM system in Section 2.4, the SMS equations are recast into a set of $6(1+n_B)$ first order nonlinear coupled differential equations of the form:

$$\dot{\boldsymbol{x}} = \boldsymbol{f}(\boldsymbol{x}), \qquad \boldsymbol{x} \in \Re^{6(1+n_B)}\ . \tag{3.13}$$

For $n_B = n = 1$, the state space representation for the SPM model is recovered.

The SMS state space variable vector can be represented with the "Ship Motions Flow" to yield $6+6n_B$ state space variables as follows: $[u,\ v,\ r,\ x,\ y,\ \psi,\ u_B^{(i)},\ v_B^{(i)},\ w_B^{(i)},\ x_B^{(i)},\ y_B^{(i)},\ z_B^{(i)},\ i=1,\ldots,n_B]^{\mathrm{T}}$. The SMS nonlinear model in Cauchy standard form becomes:

$$\dot{u} = \frac{X_H + (m+m_y)rv + \sum_{i=1}^{n}\left\{T_{o2}^{(i)}\cos\beta^{(i)} - F_{2BDX}^{(i)}\right\} + F_{surge}}{(m+m_x)}\ , \tag{3.14}$$

$$\dot{v} = \frac{Y_H - (m+m_x)ru + \sum_{i=1}^{n}\left\{T_{o2}^{(i)}\sin\beta^{(i)} - F_{2BDY}^{(i)}\right\} + F_{sway}}{(m+m_y)}\ , \tag{3.15}$$

$$\dot{r} = \frac{N_H + \sum_{i=1}^{n}\left\{x_p^{(i)}\left[T_{o2}^{(i)}\sin\beta^{(i)} - F_{2BDY}^{(i)}\right] - y_p^{(i)}\left[T_{o2}^{(i)}\cos\beta^{(i)} - F_{2BDX}^{(i)}\right]\right\} + N_{yaw}}{(I_{zz}+J_{zz})}\ , \tag{3.16}$$

$$\dot{x} = u\cos\psi - v\sin\psi + U_c\cos\alpha\ , \tag{3.17}$$

$$\dot{y} = u\sin\psi + v\cos\psi + U_c\sin\alpha\ , \tag{3.18}$$

$$\dot{\psi} = r\ , \tag{3.19}$$

$$\dot{u}_B^{(i)} = \frac{T_{o1}^{(i)} + T_{o2}^{(i)}\cos\beta_B^{(i)} - F_{DBX}^{(i)} - F_{A1}^{(i)} - F_{2ADX}^{(i)}}{(m_B^{(i)} + A_{11}^{(i)})}\ ,\ (i=1,\ \ldots.\ ,\ n_B)\ , \tag{3.20}$$

$$\dot{v}_B^{(i)} = \frac{T_{o2}^{(i)}\cos\beta_B^{(i)} - F_{DBY}^{(i)} - F_{L1}^{(i)} - F_{2ADY}^{(i)}}{(m_B^{(i)} + A_{22}^{(i)})}\ ,\ (i=1,\ \ldots.\ ,\ n_B)\ , \tag{3.21}$$

$$\dot{w}_B^{(i)} = \frac{F_B^{(i)} - T_{o1}^{(i)}\sinh\left(\frac{P\ell_1^{(i)}}{T_{o1}^{(i)}}\right) - T_{o2}^{(i)}\sinh\left(\frac{P\ell_{2A}^{(i)}}{T_{o2}^{(i)}}\right)}{(m_B^{(i)} + A_{33}^{(i)})}\ ,\ (i=1,\ \ldots.\ ,\ n_B)\ , \tag{3.22}$$

$$\dot{x}_B^{(i)} = u_B^{(i)}\cos\gamma_B^{(i)} - v_B^{(i)}\sin\gamma_B^{(i)} + U_c\frac{z_B^{(i)}}{h}\cos\alpha\ ,\ (i=1,\ \ldots.\ ,\ n_B)\ , \tag{3.23}$$

$$\dot{y}_B^{(i)} = u_B^{(i)}\sin\gamma_B^{(i)} + v_B^{(i)}\cos\gamma_B^{(i)} + U_c\frac{z_B^{(i)}}{h}\sin\alpha\ ,\ (i=1,\ \ldots.\ ,\ n_B)\ , \tag{3.24}$$

$$\dot{z}_B^{(i)} = w_B^{(i)},\ \ (i=1,\ \ldots.\ ,\ n_B)\ . \tag{3.25}$$

Equations (3.14) - (3.25) are in the form (3.13). The equilibria of the SMS can be found by setting the time derivative of the state variable vector equal to zero; i.e.

$$\bar{x} \in \Re^{6(1+n_B)} \ \text{ is an equilibrium of } \ \dot{x} = f(x) \quad \Leftrightarrow \quad f(\bar{x}) = 0\ . \tag{3.26}$$

As with SPM systems, the number of state space equations can and should be reduced when solving for equilibrium. The vessel velocity vector at equilibrium ($\overline{u}$, $\overline{v}$, $\overline{r}$) is recast as a function of the drift angle at equilibrium $\overline{\psi}$ as in Chapter 2 as follows:

$$\overline{u} = -U_c \cos(\overline{\psi} - \alpha) \ , \tag{3.27}$$

$$\overline{v} = U_c \sin(\overline{\psi} - \alpha) \ , \tag{3.28}$$

$$\overline{r} = 0 \ . \tag{3.29}$$

In addition, by setting expressions (3.25) to zero - i.e. $\dot{z}_B^{(i)} = 0$, ($i = 1, \ldots, n_B$), - we have:

$$\overline{w}_B^{(i)} = 0 \ , \quad (i = 1, \ldots, n_B) \ . \tag{3.30}$$

The number of unknown state variables in the equilibrium equations of the system (3.14) - (3.25) has been reduced from $6(1+n_B)$ to $3+5n_B$. The SMS equilibrium equations can be reduced to the zero solution of equations (3.14) - (3.16) and (3.20) - (3.24), provided that the appropriate expressions for $\overline{u}$ and $\overline{v}$ (3.27) and (3.28) are substituted in equations (3.14) - (3.16). Derivation of equilibria requires that those equations be solved simultaneously.

Since the expressions for $\overline{T}_{o1}^{(i)}$ and $\overline{T}_{o2}^{(i)}$ in equations (3.14) - (3.16) and (3.20) - (3.22) are unknown, $6n_B$ additional equations must be solved simultaneously with the $3+5n_B$ state space equations as shown in the previous chapter. These equations, which are equivalent to the six auxiliary equations used to solve for the SPM equilibrium, are introduced to solve for the horizontal tension terms $\overline{T}_{o1}^{(i)}$ and $\overline{T}_{o2}^{(i)}$, as well as the horizontal distances $\overline{d}^{(i)}$, $\overline{\ell}_1^{(i)}$, $\overline{\ell}_{2A}^{(i)}$, and $\overline{\ell}_{2B}^{(i)}$, ($i = 1, \ldots, n_B$). The total number of equations that must be solved for equilibrium is therefore $3+11n_B$. The equilibrium equations are:

$$\overline{X}_H + \sum_{i=1}^{n} \left\{ \overline{T}_{o2}^{(i)} \cos\overline{\beta}^{(i)} - \overline{F}_{2BDX}^{(i)} \right\} + \overline{F}_{surge} = 0 \ , \tag{3.31}$$

$$\overline{Y}_H + \sum_{i=1}^{n} \left\{ \overline{T}_{o2}^{(i)} \sin\overline{\beta}^{(i)} - \overline{F}_{2BDY}^{(i)} \right\} + \overline{F}_{sway} = 0 \ , \tag{3.32}$$

$$\begin{aligned} \overline{N}_H &+ \sum_{i=1}^{n} x_p^{(i)} \left\{ \overline{T}_{o2}^{(i)} \sin\overline{\beta}^{(i)} - \overline{F}_{2BDY}^{(i)} \right\} \\ &- \sum_{i=1}^{n} y_p^{(i)} \left\{ \overline{T}_{o2}^{(i)} \cos\overline{\beta}^{(i)} - \overline{F}_{2BDX}^{(i)} \right\} + \overline{N}_{yaw} = 0 \ . \end{aligned} \tag{3.33}$$

For $i = 1, \ldots, n_B$

$$\bar{T}_{o1}^{(i)} + \bar{T}_{o2}^{(i)} \cos\bar{\beta}_B^{(i)} - \bar{F}_{BDx}^{(i)} - \bar{F}_{A1}^{(i)} - \bar{F}_{2ADX}^{(i)} = 0 \ , \tag{3.34}$$

$$\bar{T}_{o2}^{(i)} \sin\bar{\beta}_B^{(i)} - \bar{F}_{BDy}^{(i)} - \bar{F}_{L1}^{(i)} - \bar{F}_{2ADY}^{(i)} = 0 \ , \tag{3.35}$$

$$F_B^{(i)} - \bar{T}_{o1}^{(i)} \sinh\left(\frac{P\bar{\ell}_1^{(i)}}{\bar{T}_{o1}^{(i)}}\right) - \bar{T}_{o2}^{(i)} \sinh\left(\frac{P\bar{\ell}_{2A}^{(i)}}{\bar{T}_{o2}^{(i)}}\right) = 0 \ , \tag{3.36}$$

$$\bar{u}_B^{(i)} \cos\bar{\gamma}_B^{(i)} - \bar{v}_B^{(i)} \sin\bar{\gamma}_B^{(i)} + U_c \frac{\bar{z}_B^{(i)}}{h} \cos\alpha = 0 \ , \tag{3.37}$$

$$\bar{u}_B^{(i)} \sin\bar{\gamma}_B^{(i)} + \bar{v}_B^{(i)} \cos\bar{\gamma}_B^{(i)} + U_c \frac{\bar{z}_B^{(i)}}{h} \sin\alpha = 0 \ , \tag{3.38}$$

$$\sinh\left(\frac{P\bar{\ell}_1^{(i)}}{\bar{T}_{o1}^{(i)}}\right) - \frac{P}{\bar{T}_{o1}^{(i)}} \sqrt{\bar{z}_B^{(i)}\left(\bar{z}_B^{(i)} + 2\frac{\bar{T}_{o1}^{(i)}}{P}\right)} = 0 \ , \tag{3.39}$$

$$\sinh\left(\frac{P\bar{\ell}_{2A}^{(i)}}{2\bar{T}_{o2}^{(i)}}\right)\cosh\left(\frac{P\bar{\ell}_{2B}^{(i)}}{2\bar{T}_{o2}^{(i)}}\right) + \cosh\left(\frac{P\bar{\ell}_{2A}^{(i)}}{2\bar{T}_{o2}^{(i)}}\right)\sinh\left(\frac{P\bar{\ell}_{2B}^{(i)}}{2\bar{T}_{o2}^{(i)}}\right)$$
$$- \frac{P}{2\bar{T}_{o2}^{(i)}} \sqrt{\ell_{w2}^{(i)2} - (h - \bar{z}_B^{(i)})^2} = 0 \ , \tag{3.40}$$

$$\ell_{w1}^{(i)} - \frac{\bar{T}_{o1}^{(i)}}{P} \sinh\left(\frac{P\bar{\ell}_1^{(i)}}{\bar{T}_{o1}^{(i)}}\right) - \bar{d}^{(i)} = 0 \ , \tag{3.41}$$

$$\ell_{w2}^{(i)} - \frac{\bar{T}_{o2}^{(i)}}{P} \sinh\left(\frac{P\bar{\ell}_{2A}^{(i)}}{\bar{T}_{o2}^{(i)}}\right) - \frac{\bar{T}_{o2}^{(i)}}{P} \sinh\left(\frac{P\bar{\ell}_{2B}^{(i)}}{2\bar{T}_{o2}^{(i)}}\right) = 0 \ , \tag{3.42}$$

$$\sqrt{\left(x_m^{(i)} - \bar{x}_B^{(i)}\right)^2 + \left(y_m^{(i)} - \bar{y}_B^{(i)}\right)^2} - \bar{\ell}_1^{(i)} - \bar{d}^{(i)} = 0 \ , \tag{3.43}$$

$$\sqrt{\left(\bar{x}_B^{(i)} - \bar{x}_T^{(i)}\right)^2 + \left(\bar{y}_B^{(i)} - \bar{y}_T^{(i)}\right)^2} - \bar{\ell}_{2A}^{(i)} - \bar{\ell}_{2B}^{(i)} = 0 \ . \tag{3.44}$$

In expressions (3.43) and (3.44), $(x_m^{(i)},\ y_m^{(i)})$ and $(\bar{x}_T^{(i)},\ \bar{y}_T^{(i)})$ are the anchoring coordinates of mooring line i on the sea floor and attachment coordinates of mooring line i on the vessel with respect to the inertial reference frame $(x,\ y)$.

Note that equations (3.31) - (3.44) are the counterpart expressions for relations (2.88) - (2.101) of the SPM case. The main difference between these two types of systems is the addition of a finite number of mooring lines to the vessel, and therefore the addition of an equal number of buoys. This increases the dimension of the state space by a factor of F_l with respect to the single point, single buoy case, where

$$F_I = \frac{1}{2}(1+n_B) \ , \tag{3.45}$$

thus resulting in more complicated system dynamics.

3.3. SMS Pretension and Geometry Definition

SMS need to be deployed with certain geometrical specifications, such as number, length, orientation and pretension of the mooring lines, size and location of each buoy along a line, etc. The dynamic characteristics of a SMS depend to a large extent on its geometry. The geometry of single line SPM systems, although important, does not severely affect the dynamic behavior as the system tends to weathervane in response to the external excitation. SMS, on the other hand, are deployed to restrict the slow and intermediate motions of the vessel, and therefore a small change in mooring line pretension, for example, may affect the dynamics of the system considerably [3].

Consider a SMS with n mooring lines and one buoy per line ($n = n_B$) that is to be deployed at a specific site and oriented in a specific direction. The system pretension must be specified in order to define the geometry of the system. The total pretension of a catenary segment T_P can be calculated once the horizontal pretension of that segment T_{oP}, and the vertical pretension T_{vP}, are known, as

$$T_P = \sqrt{T_{oP} + T_{vP}} \ . \tag{3.46}$$

According to equation (3.46), the pretension is given by the vectorial sum of the two pretension components T_{oP} and T_{vP}. It is difficult to define T_P a priori, because we do not know the depths of submergence of each of the buoys.

To simplify the problem, and since we are dealing with the horizontal plane motion dynamics of the vessel, we specify the "horizontal plane" pretension T_{oP} to define the initial SMS geometric configuration (set-up).

Assuming that the following are known for every mooring line

- total length of AC,

- total length of SC,
- buoy characteristics,
- horizontal pretension of the system $T_{oP} = T_{o1} = T_{o2}$ (Note: T_{o1} and T_{o2} do not have to be equal; we set them equal to simplify the problem),
- water depth,

we can define the complete three-dimensional geometry of the SMS, by solving for the depth of each buoy, and for the various geometric configurations of the mooring lines.

First, we need to find the depth at which each of the buoys is in static equilibrium in calm water (z_B). To do that, we combine the following four equations

$$\sinh\left(\frac{P\ell_1}{T_{oP}}\right) - \frac{P}{T_{oP}}\sqrt{z_B\left(z_B + 2\frac{T_{oP}}{P}\right)} = 0\,, \tag{3.47}$$

$$\sinh\left(\frac{P\ell_{2A}}{2T_{oP}}\right)\cosh\left(\frac{P\ell_{2B}}{2T_{oP}}\right) + \cosh\left(\frac{P\ell_{2A}}{2T_{oP}}\right)\sinh\left(\frac{P\ell_{2B}}{2T_{oP}}\right) - \frac{P}{2T_{oP}}\sqrt{\ell_{w2}^2 - (h - z_B)^2} = 0\,, \tag{3.48}$$

$$F_B - T_{oP}\left[\sinh\left(\frac{P\ell_1}{T_{oP}}\right) + \sinh\left(\frac{P\ell_{2A}}{T_{oP}}\right)\right] = 0\,, \tag{3.49}$$

$$P\ell_{w2} - T_{oP}\left[\sinh\left(\frac{P\ell_{2A}}{2T_{oP}}\right) + \sinh\left(\frac{P\ell_{2B}}{2T_{oP}}\right)\right] = 0\,, \tag{3.50}$$

for unknowns ℓ_1, ℓ_{2A}, ℓ_{2B} and z_B into a single equation in terms of z_B (notice that T_{oP}, the horizontal pretension, is known). This is done for each mooring line as follows.

We combine equations (3.47) and (3.49) to obtain the expression

$$\sinh\left(\frac{P\ell_{2A}}{T_{oP}}\right) = A = \frac{F_B - P\sqrt{z_B\left(z_B + 2\frac{T_{oP}}{P}\right)}}{T_{oP}}\,. \tag{3.51}$$

Then, equation (3.51) is combined with equation (3.50) to obtain

$$\sinh\left(\frac{P\ell_{2B}}{T_{oP}}\right)=B=\frac{P\ell_{w2}-F_B+P\sqrt{z_B\left(z_B+2\frac{T_{oP}}{P}\right)}}{T_{oP}}=\frac{P\ell_{w2}}{T_{oP}}-A\ . \tag{3.52}$$

Note that A and B are functions of the only unknown z_B. Letting

$$\alpha=\frac{P\ell_{2A}}{T_{oP}}=\sinh^{-1}A\ , \tag{3.53}$$

$$\beta=\frac{P\ell_{2B}}{T_{oP}}=\sinh^{-1}B\ , \tag{3.54}$$

equation (3.48) above can be recast in terms of α and β as follows

$$f=\sinh\frac{\alpha}{2}\cosh\frac{\beta}{2}+\cosh\frac{\alpha}{2}\sinh\frac{\beta}{2}-C=0\ , \tag{3.55}$$

where

$$C=\frac{P}{2T_{oP}}\sqrt{\ell_{w2}^2-(h-z_B)^2}\ . \tag{3.56}$$

Notice that α and β in equation (3.55) are recast in terms of A and B which are functions of z_B exclusively. Equation (3.55) is therefore in terms of a single unknown z_B.

A relatively simple solution to equation (3.55), can be found using a Newton-Rapson method of the form [29]:

$$f(x+\delta)=f(x)+f'(x)+\frac{1}{2}f''(x)\delta^2+\cdots\ , \tag{3.57}$$

where f is the function of equation (3.55), x is the variable we need to solve for (z_B); δ is a small perturbation number; f' is the first derivative with respect to x; f'' is the second derivative with respect to x. For small values of δ, and for well defined functions, the terms beyond linear are not important. Hence, $f(x+\delta)=0$ implies that

$$\delta=-\frac{f(x)}{f'(x)}\ , \tag{3.58}$$

and the solution for the unknown x requires an iterative process of the form

$$x_{i+1} = x_i - \frac{f(x_i)}{f'(x_i)} \ . \tag{3.59}$$

The first derivative f' with respect to the unknown is required. It is given by

$$\begin{aligned} f' = \frac{df}{dz_B} = &\frac{1}{2}\cosh\frac{\alpha}{2}\cosh\frac{\beta}{2}\left(\frac{d}{dz_B}\sinh^{-1}A\right) + \frac{1}{2}\sinh\frac{\alpha}{2}\sinh\frac{\beta}{2}\left(\frac{d}{dz_B}\sinh^{-1}B\right) \\ &+ \frac{1}{2}\cosh\frac{\alpha}{2}\cosh\frac{\beta}{2}\left(\frac{d}{dz_B}\sinh^{-1}B\right) + \frac{1}{2}\sinh\frac{\alpha}{2}\sinh\frac{\beta}{2}\left(\frac{d}{dz_B}\sinh^{-1}A\right) \\ &- \frac{dC}{dz_B} \ , \end{aligned} \tag{3.60}$$

where

$$\frac{d}{dz_B}\sinh^{-1}A = \frac{1}{\sqrt{A^2+1}}\frac{dA}{dz_B} =, \quad \frac{dA}{dz_B} = -\frac{\left(1+\dfrac{Pz_B}{T_{oP}}\right)}{\sqrt{z_B\left(z_B+2\dfrac{T_{oP}}{P}\right)}} \ , \tag{3.61}$$

$$\frac{d}{dz_B}\sinh^{-1}B = \frac{1}{\sqrt{B^2+1}}\frac{dB}{dz_B} =, \quad \frac{dB}{dz_B} = \frac{\left(1+\dfrac{Pz_B}{T_{oP}}\right)}{\sqrt{z_B\left(z_B+2\dfrac{T_{oP}}{P}\right)}} \ . \tag{3.62}$$

Therefore,

$$\begin{aligned} f' = \frac{df}{dz_B} = &\frac{1}{2}\left[\cosh\frac{\alpha}{2}\cosh\frac{\beta}{2} + \sinh\frac{\alpha}{2}\sinh\frac{\beta}{2}\right]\left(\frac{1}{\sqrt{B^2+1}} - \frac{1}{\sqrt{A^2+1}}\right)\frac{\left(1+\dfrac{Pz_B}{T_{oP}}\right)}{\sqrt{z_B\left(z_B+2\dfrac{T_{oP}}{P}\right)}} \\ &- \frac{P}{2T_{oP}}\frac{(h-z_B)}{\sqrt{\ell_{w2}^2-(h-z_B)^2}} \ . \end{aligned} \tag{3.63}$$

An initial value for the buoy depth z_{Bo} needs to be given for the iterative process (3.59).

Once the buoy depth z_B is calculated, the rest of the geometrical properties of the mooring line (namely d, ℓ_1, ℓ_{2A} and ℓ_{2B}) can be calculated as follows:

For each mooring line, we obtain ℓ_1 from (3.47):

$$\ell_1 = \frac{T_{oP}}{P}\sinh^{-1}\left(\frac{P\sqrt{z_B\left(z_B+2\frac{T_{oP}}{P}\right)}}{T_{oP}}\right). \tag{3.64}$$

Obtain ℓ_{2A} from (3.51)

$$\ell_{2A} = \frac{T_{oP}}{P}\sinh^{-1}\left(\frac{F_B - P\sqrt{z_B\left(z_B+2\frac{T_{oP}}{P}\right)}}{T_{oP}}\right). \tag{3.65}$$

Next, obtain ℓ_{2B} from equation (3.52)

$$\ell_{2B} = \frac{T_{oP}}{P}\sinh^{-1}\left(\frac{P\ell_{w2} - F_B + P\sqrt{z_B\left(z_B+2\frac{T_{oP}}{P}\right)}}{T_{oP}}\right). \tag{3.66}$$

The horizontal distance d is given, from (2.8) as

$$d = \ell_{w1} - \ell_{eff1} = \ell_{w1} - \sqrt{z_B\left(z_B+2\frac{T_{oP}}{P}\right)}\,, \tag{3.67}$$

and the total horizontal length of AC, ℓ_1', is given by (2.1) by

$$\ell_1' = \ell_1 + d = \frac{T_{oP}}{P}\sinh^{-1}\left(\frac{P\sqrt{z_B\left(z_B+2\frac{T_{oP}}{P}\right)}}{T_{oP}}\right) + \ell_{w1} - \sqrt{z_B\left(z_B+2\frac{T_{oP}}{P}\right)}\,. \tag{3.68}$$

Once the quantities d, ℓ_1, ℓ_{2A}, ℓ_{2B} and z_B for each mooring line are known, the system geometry can be defined, and the desired system configuration obtained. The system set-up discussed in this section is used to define the pretension and initial geometry of the system under no external excitation from current, wind, and second order mean wave drift (i.e. calm water conditions). Notice that this configuration does not correspond to the equilibrium position of the system in calm water or otherwise under external excitation, nor will it in general be in static equilibrium.

To illustrate the concepts of definition of system geometry and equilibrium, consider a 4-line SMS tanker [13] moored with catenary chains [20] in 750 meters water depth in a 2 knot head current ($\alpha = 180°$). In this example, the net buoyancy of each buoy is $F_B = 886.5$ kN.

Table 3.1 shows the mooring line particulars and the values of the system design parameters in terms of mooring line orientation, fairlead coordinates, and horizontal mooring line pretension which is equal for both segments of each catenary. The initial system configuration as specified by the requirements in Table 3.1 in terms of its state space and other geometrical specifications (system set-up) is given in Table 3.2.

Table 3.1. Mooring line and geometry specifications of 4-line tanker SMS

	Line 1	Line 2	Line 3	Line 4
Horizontal pretension T_{OP} (kN)	260.6	260.6	104.2	104.2
Total length: ℓ_{wT} (m)	1600.0	1600.0	1600.0	1600.0
Length of S1: ℓ_{w1} (m)	1000.0	1000.0	1000.0	1000.0
Length of S2: ℓ_{w2} (m)	600.0	600.0	600.0	600.0
Orientation of S1: γ_B (deg)	340.0	20.0	160.0	200.0
Orientation of S2: γ (deg)	340.0	20.0	160.0	200.0
Fairlead Coordinates:				
x_p (m)	125.0	125.0	−129.7	−129.7
y_p (m)	−4.1	4.1	0.0	0.0

Note that the values of the state space variables and other geometrical properties of Table 3.2 correspond to the geometry of the mooring system obtained from the specifications of Table 3.1 subject to hydrostatic forces only, as mentioned previously. The values of Table 3.2 are exclusively used to define the geometry of the system based on specific requirements (initial

pretension and configuration). The equilibria of the mooring system under external excitation are calculated using equations (3.31) - (3.44).

Table 3.3 shows the solution to the principal equilibrium in terms of the state space and auxiliary variables of the system of Tables 3.1 and 3.2 under the external excitation specified above.

Table 3.2. Set-up of 4-line tanker SMS of Table 3.1

State Space Variable					
x	(m)		−1232.633		
y	(m)		407.248		
ψ	(rad)		0.000		
		Line 1	Line 2	Line 3	Line 4
x_B	(m)	−746.779	−746.779	−1618.890	−1618.890
y_B	(m)	271.805	542.690	500.630	313.865
z_B	(m)	375.026	375.026	403.079	403.079
Auxiliary Variable					
d	(m)	480.376	480.376	532.999	532.999
ℓ_1	(m)	314.329	314.329	180.127	180.127
ℓ_{2A}	(m)	65.567	65.567	91.000	91.000
ℓ_{2B}	(m)	318.446	318.446	182.033	182.033
x_m	(m)	0.000	0.000	−2289.010	−2289.010
y_m	(m)	0.000	814.496	744.534	69.961

Notice that the equilibrium solution given in Table 3.3 differs considerably from the set-up geometry of the system given in Table 3.2. The tanker at equilibrium under the action of external excitation and line pretension has moved forward, therefore decreasing the horizontal tension in the forward mooring lines, and increasing it in the aft mooring lines. This occurs because of the high horizontal pretension values used in the forward mooring lines (see Table 3.1) as initial conditions. At equilibrium, the sum of all external forces and moments must be zero, thus resulting in higher horizontal tensions in the aft mooring lines with respect to the initial conditions in Table 3.2.

Table 3.3. Principal equilibrium of SMS: state space and auxiliary variables

State Space Variable					
$\bar{u}$	(m/s)		1.0296		
$\bar{v}$	(m/s)		0.0000		
$\bar{r}$	(r/s)		0.0000		
$\bar{x}$	(m)		−1142.7415		
$\bar{y}$	(m)		407.2478		
$\bar{\psi}$	(rad)		0.0000		
		Line 1	Line 2	Line 3	Line 4
$\bar{u}_B$	(m/s)	0.4936	0.4936	−0.5103	−0.5103
$\bar{v}_B$	(m/s)	0.1949	−0.1949	−0.1698	0.1698
$\bar{w}_B$	(m/s)	0.0000	0.0000	0.0000	0.0000
$\bar{x}_B$	(m)	−705.7964	−705.7964	−1581.2816	−1581.2816
$\bar{y}_B$	(m)	278.6886	535.8071	509.0087	305.4870
$\bar{z}_B$	(m)	386.5390	386.5390	391.7862	391.7862
Auxiliary Variable					
$\bar{T}_{o1}$	(kN)	172.3221	172.3221	150.7239	150.7239
$\bar{T}_{o2}$	(kN)	168.7913	168.7913	154.1621	154.1621
$\bar{d}$	(m)	512.5646	512.5646	518.6767	518.6767
$\bar{\ell}_1$	(m)	246.2607	246.2607	227.2131	227.2131
$\bar{\ell}_{2A}$	(m)	89.4719	89.4719	92.3331	92.3331
$\bar{\ell}_{2B}$	(m)	246.3842	246.3842	232.8495	232.8495

3.4. Simulation of the Nonlinear SMS Dynamics and Stability of Equilibria

As with SPM systems, the nonlinear SMS model presented in the previous sections of this chapter can be simulated in time and its stability determined using eigenvalue analysis. To illustrate the behavior of the 4-line tanker SMS described in the previous section around the principal equilibrium, a select number of nonlinear time simulations are shown in Figures 3.2 - 3.5. Figure 3.2 shows the time simulation of the vessel drift angle; Figure 3.3 shows the time simulation corresponding to the depth of each of the four buoys; Figures 3.4 and 3.5 show the horizontal tension components of each SC and AC. These time simulations show that the system converges to its principal equilibrium position.

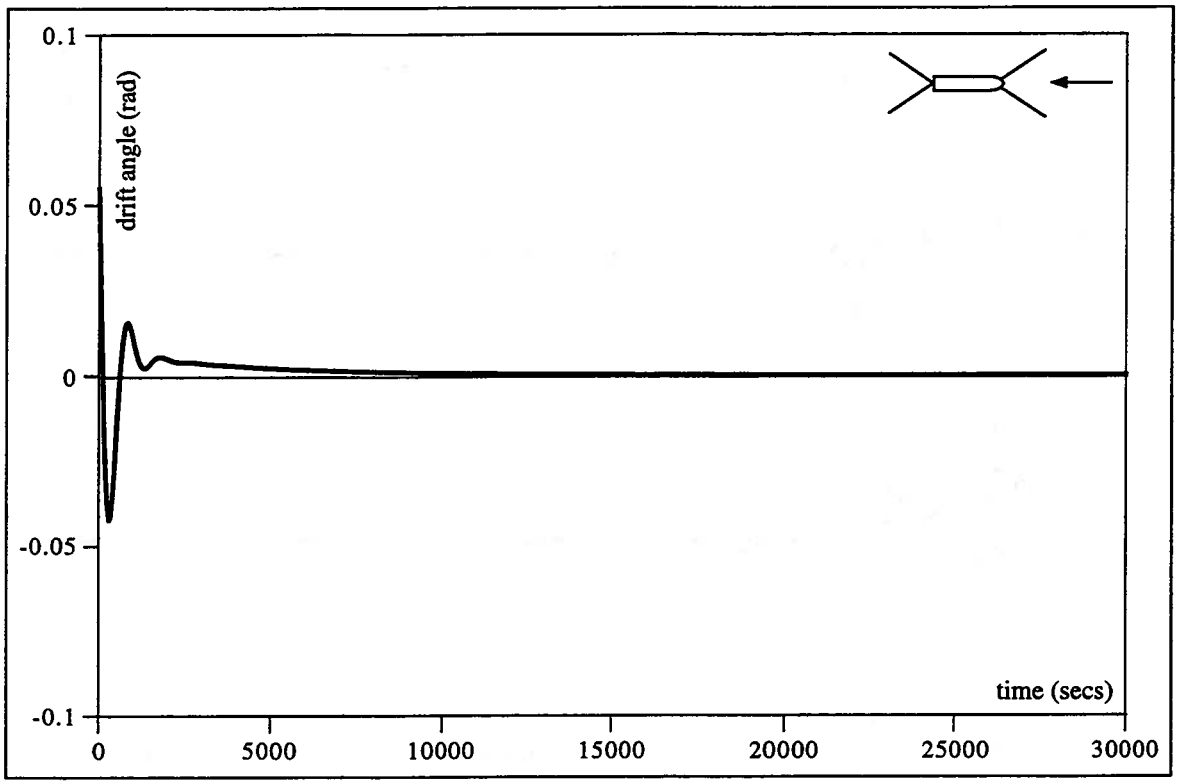

Figure 3.2. Time simulation of 4-line tanker SMS - drift angle

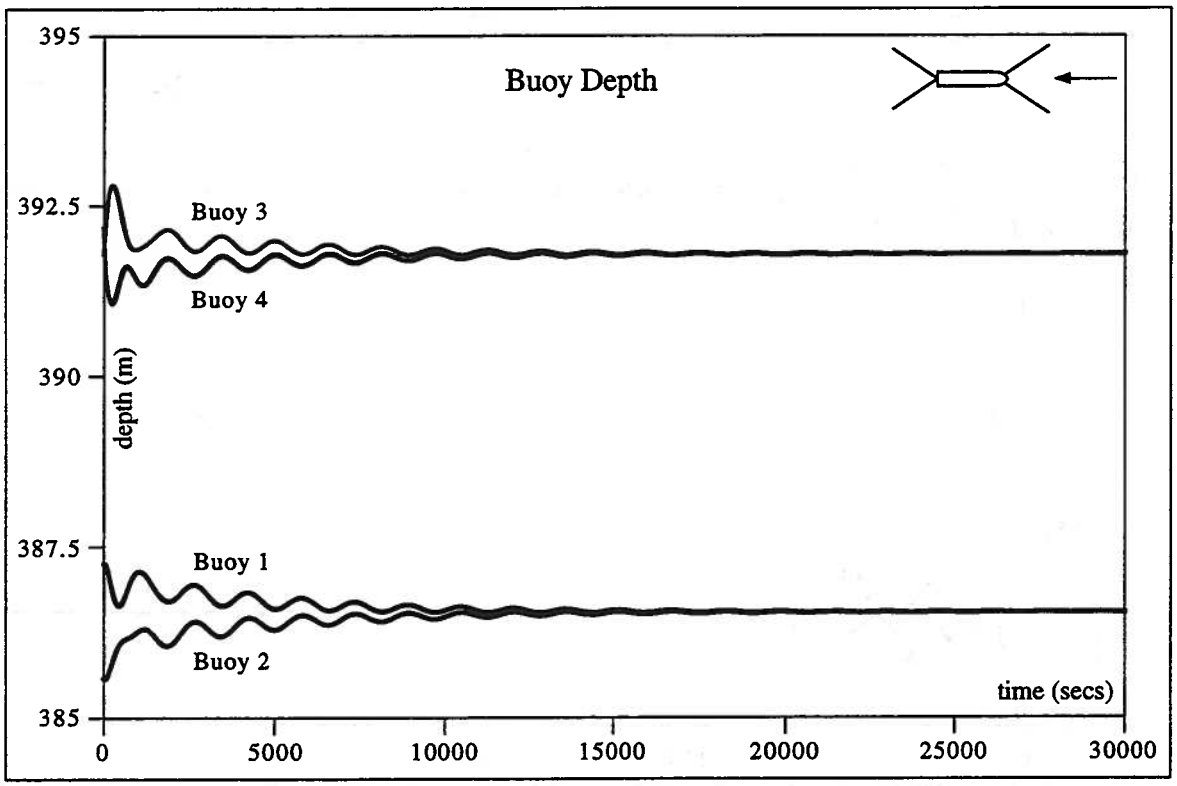

Figure 3.3. Time simulation of 4-line tanker SMS - buoy depth

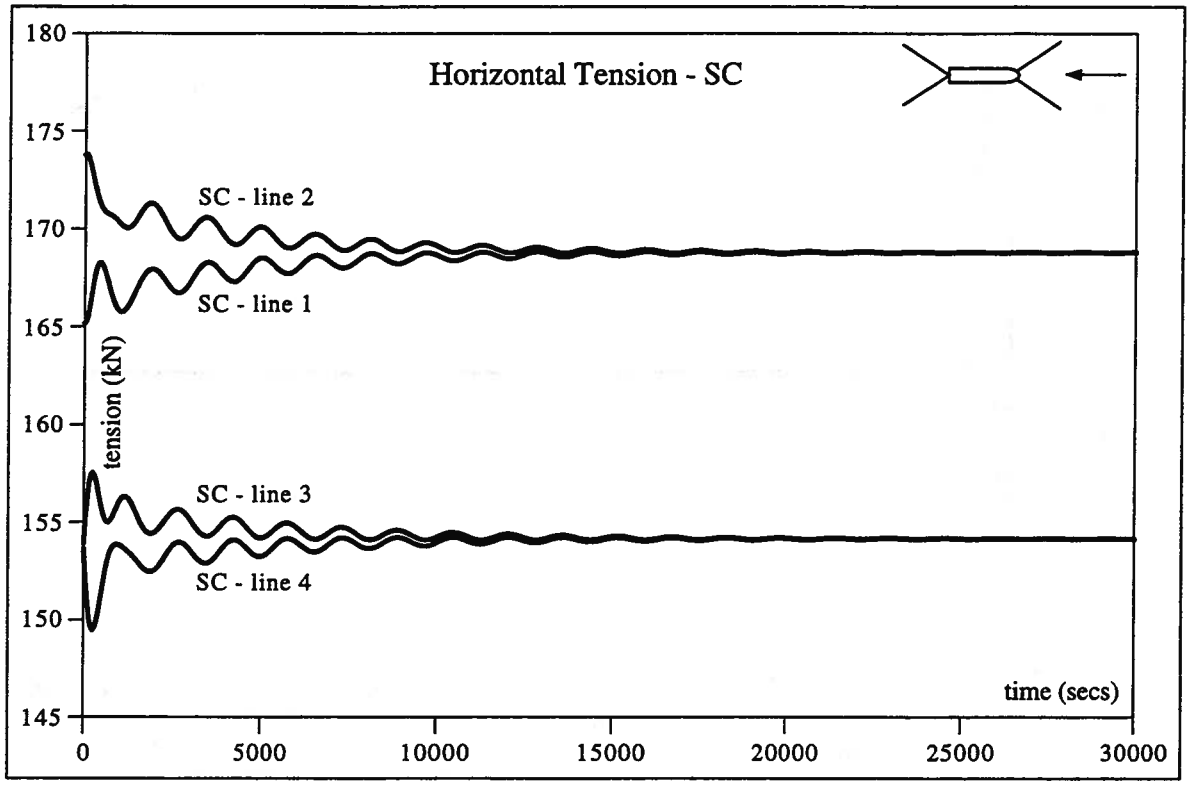

Figure 3.4. Time simulation of 4-line tanker SMS - horizontal tension in SC

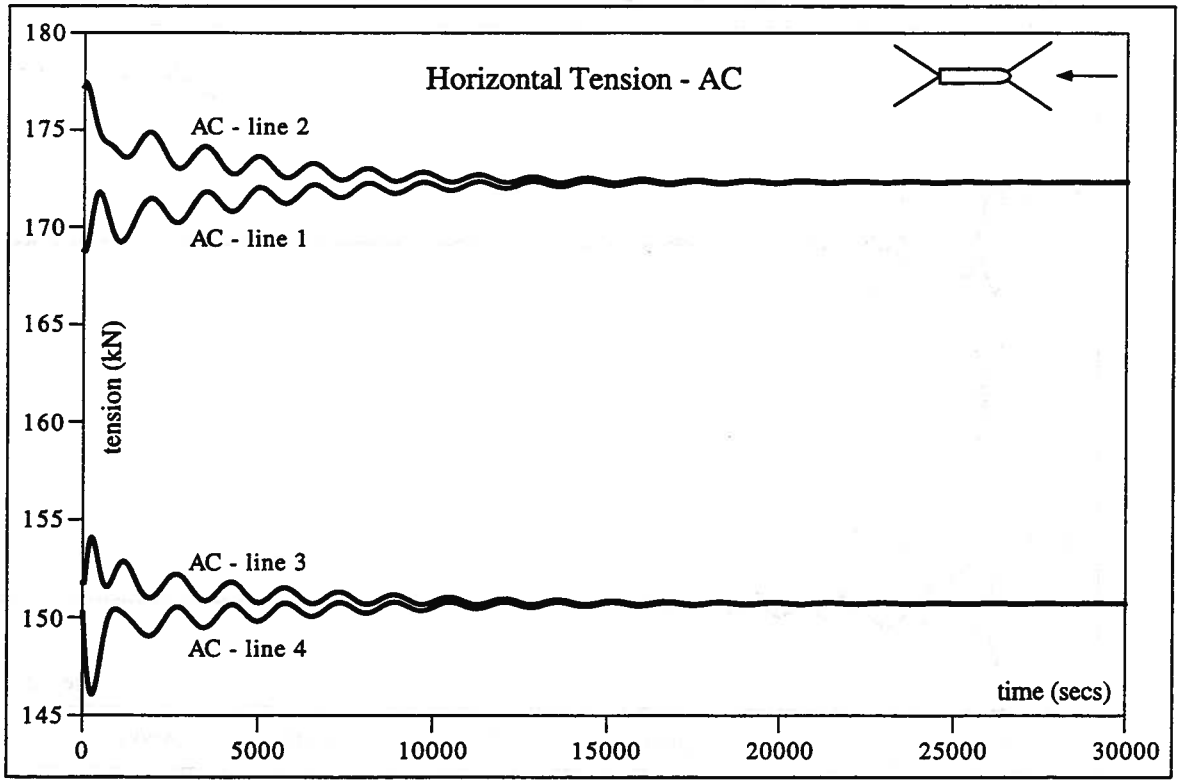

Figure 3.5. Time simulation of 4-line tanker SMS - horizontal tension in AC

The nonlinear time simulations of Figures 3.2 - 3.5 show convergence to the principal equilibrium given in Table 3.3. Convergence to the principal equilibrium implies that all the real parts of all eigenvalues of the system around that particular equilibrium are negative. This is indeed the case, as shown by the system eigenvalues given in Table 3.4.

Table 3.4. Eigenvalues of principal equilibrium of SMS defined in Table 3.3

Eigenvalue	Real Part	Imaginary Part
λ_1	-0.3149×10^{-1}	$+i0.2561$
λ_2	-0.3149×10^{-1}	$-i0.2561$
λ_3	-0.2705×10^{-1}	$+i0.2451$
λ_4	-0.2705×10^{-1}	$-i0.2451$
λ_5	-0.3149×10^{-1}	$+i0.2561$
λ_6	-0.3149×10^{-1}	$-i0.2561$
λ_7	-0.2705×10^{-1}	$+i0.2451$
λ_8	-0.2705×10^{-1}	$-i0.2451$
λ_9	-0.1524×10^{-3}	$+i0.4021\times10^{-2}$
λ_{10}	-0.1524×10^{-3}	$-i0.4021\times10^{-2}$
λ_{11}	-0.5008×10^{-1}	$+i0.1341$
λ_{12}	-0.5008×10^{-1}	$-i0.1341$
λ_{13}	-0.4969×10^{-1}	$+i0.1295$
λ_{14}	-0.4969×10^{-1}	$-i0.1295$
λ_{15}	-0.5008×10^{-1}	$+i0.1341$
λ_{16}	-0.5008×10^{-1}	$-i0.1341$
λ_{17}	-0.4969×10^{-1}	$+i0.1295$
λ_{18}	-0.4969×10^{-1}	$-i0.1295$
λ_{19}	-0.3038×10^{-1}	$+i0.8230\times10^{-1}$
λ_{20}	-0.3038×10^{-1}	$-i0.8230\times10^{-1}$
λ_{21}	-0.3557×10^{-1}	$+i0.8410\times10^{-1}$
λ_{22}	-0.3557×10^{-1}	$-i0.8410\times10^{-1}$
λ_{23}	-0.3035×10^{-1}	$+i0.8235\times10^{-1}$
λ_{24}	-0.3035×10^{-1}	$-i0.8235\times10^{-1}$
λ_{25}	-0.3553×10^{-1}	$+i0.8414\times10^{-1}$
λ_{26}	-0.3553×10^{-1}	$-i0.8414\times10^{-1}$
λ_{27}	-0.2577×10^{-2}	$+i0.6367\times10^{-2}$
λ_{28}	-0.2577×10^{-2}	$-i0.6367\times10^{-2}$
λ_{29}	-0.2402×10^{-3}	0.0000
λ_{30}	-0.4278×10^{-2}	0.0000

In this particular case, as shown by the eigenvalues of Table 3.4, the principal equilibrium position is stable, and all trajectories initiated sufficiently close to the principal equilibrium converge toward it in forward time. Since there are no other attainable equilibria that may attract the trajectories, the system converges to the principal equilibrium for all bounded initial conditions.

The 4-line tanker SMS example of this chapter shows that a system can be stable for appropriate choices of system parameters. Eigenvalue analysis is thus a very powerful tool to determine the qualitative behavior of the system without the need to resort to trial and error and systematic nonlinear time simulations.

IV. INTRODUCTION TO MULTI-BUOY MOORING SYSTEMS

In deeper waters, the implementation of one buoy connecting two segments of a catenary line may not be sufficient to withstand the vertical forces that are exerted by the weight of each chain. This problem can be solved by distributing more than one buoy along the catenary to support its weight. In this chapter, an introduction to the nonlinear mathematical model for Multi-Buoy Spread Mooring Systems (MBSMS) is presented by formulating the mathematical model for the dynamical system and by deriving its equilibrium equations. Nonlinear time simulations and stability analysis for these types of systems are beyond the scope of this report.

To understand how the MBSMS model is derived, the catenary model with two buoys is first considered, and then implemented to a spread mooring system. A natural extension to this system results in the mathematical model for the MBSMS.

4.1. Equations for Catenary Model with Two Buoys

Consider the mooring line with two buoys shown in Figure 4.1. The resulting catenary is composed of three segments: Segment S1 consists of an Anchored Catenary (AC), and connects the lower buoy, B1, to the sea floor; segments S2 and S3 consist of Suspended Catenaries (SCs), with segment S2 connecting the lower buoy to the upper buoy, B2, and segment S3 connecting the upper buoy to the floating vessel. Segments S2 and S3 are further divided into segments S2A, S2B and S3A, S3B, respectively. Segment S2A extends from B1 to the lowest point of S2; S2B runs from the lowest point of S2 to B2; S3A extends from B2 to the lowest point of S3; and S3B extends from the lowest point of S3 to the point of attachment of the upper SC on the floating body.

Using in Figure 4.1 notation similar to that in Figure 2.1, we have: (x,z) is the inertial reference frame of the catenary; ℓ_1', ℓ_1, d, ℓ_2, ℓ_{2A} and ℓ_{2B} are the same as those defined in Chapter 2; ℓ_3 is the length of the horizontal projection of the upper SC; ℓ_{3A} is the length of the horizontal projection of segment S3A; ℓ_{3B} is the length of the horizontal projection of segment S3B:

$$\ell_3 = \ell_{3A} + \ell_{3B} \ . \tag{4.1}$$

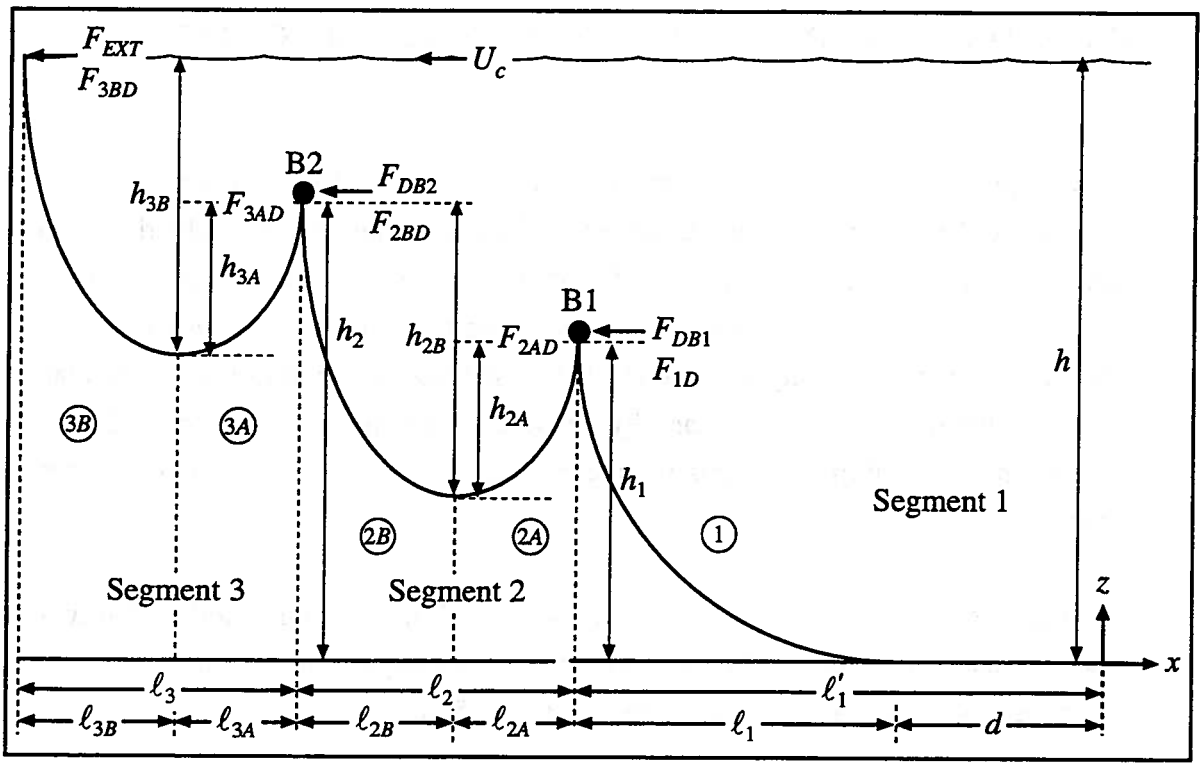

Figure 4.1. Geometry of deep water catenary with two buoys

In addition, h_1 is the vertical distance from the sea bed to the lower point of B1; h_2 is the vertical distance from the sea bed to the lower point of B2; h_{2A} is the vertical distance from the lower point of the lower SC to the lower point of B1; h_{2B} is the vertical distance from the lower point of the lower SC to the lower point of B2; h_{3A} is the vertical distance from the lower point of the upper SC to the lower point of B2; h_{3B} is the vertical distance from the lower point of upper SC to the point of attachment on the floating body. The relationship between the vertical ordinates of Buoys B1 and B2 is given by:

$$h_2 = h_1 - h_{2A} + h_{2B} \ , \tag{4.2}$$

and the total depth h is related to the various vertical ordinates by

$$h = h_2 - h_{3A} + h_{3B} \ , \tag{4.3}$$

where, following equations (2.5) and (2.6), we have

$$h_{3A} = \frac{T_{o3}}{P}\left[\cosh\left(\frac{P\ell_{3A}}{T_{o1}}\right) - 1\right], \tag{4.4}$$

$$h_{3B} = \frac{T_{o3}}{P}\left[\cosh\left(\frac{P\ell_{3B}}{T_{o1}}\right) - 1\right], \tag{4.5}$$

and T_{o3} is the horizontal tension of segment S3.

The total length of the mooring line, ℓ_{wT}, is the sum of its component lengths ℓ_{w1}, ℓ_{w2} and ℓ_{w3}:

$$\ell_{wT} = \ell_{w1} + \ell_{w2} + \ell_{w3} \ . \tag{4.6}$$

The drag forces acting on the buoy and the catenary, and the external forces are defined as in Chapter 2. The forces acting on each of the two buoys are shown in Figure 4.2. Symbols and nomenclature in Figure 4.2 follow those of Figure 2.2 in Chapter 2. Thus, R_{B1} and R_{B2} are the radii of Buoys B1 and B2; F_{B1} and F_{B2} are the net buoyancy forces acting on Buoys B1 and B2; F_{1D}, F_{2AD}, F_{2BD}, and F_{3AD} , are the drag forces acting on each of the catenary segments S1, S2A, S2B and S3A, respectively. The drag forces on the buoys and catenary segments follow the concepts introduced in Chapter 2. All drag forces on the various SCs can be calculated following [12, 21] after decomposing each SC segment into two AC segments.

As shown in Figure 4.2, each of the buoys has its own coordinate system: (X_{B1}, Z_{B1}) has its origin at the center of gravity of Buoy B1, and (X_{B2}, Z_{B2}) at the center of gravity of Buoy B2.

The equations of motion of Buoy B1 in the horizontal (surge) and vertical (heave) planes are:

$$(m_{B1} + A_{11-1})\ddot{x}_{B1} = T_{o1} - T_{o2} - F_{DB1} - F_{1D} - F_{2AD} \ , \tag{4.7}$$

$$(m_{B1} + A_{33-1})\ddot{z}_{B1} = F_{B1} - T_{v1} - T_{v2A} \ . \tag{4.8}$$

Equations (4.7) and (4.8) are the equivalent expressions for the one buoy case (2.13) and (2.14). The equations of motion of Buoy B2 in surge and heave are:

$$(m_{B2} + A_{11-2})\ddot{x}_{B2} = T_{o2} - T_{o3} - F_{DB2} - F_{2BD} - F_{3AD} \ , \tag{4.9}$$

$$(m_{B2} + A_{33-2})\ddot{z}_{B2} = F_{B2} - T_{v2B} - T_{v3A} \ , \tag{4.10}$$

where T_{v3A} is the vertical tension in segment S3A, and

$$T_{v3A} = T_{o3} \sinh\left(\frac{P\ell_{3A}}{T_{o3}}\right) . \tag{4.11}$$

The vertical tension in segment S3B is denoted by T_{v3B} and acts on the moored vessel. It is given by

$$T_{v3B} = T_{o3} \sinh\left(\frac{P\ell_{3B}}{T_{o3}}\right) . \tag{4.12}$$

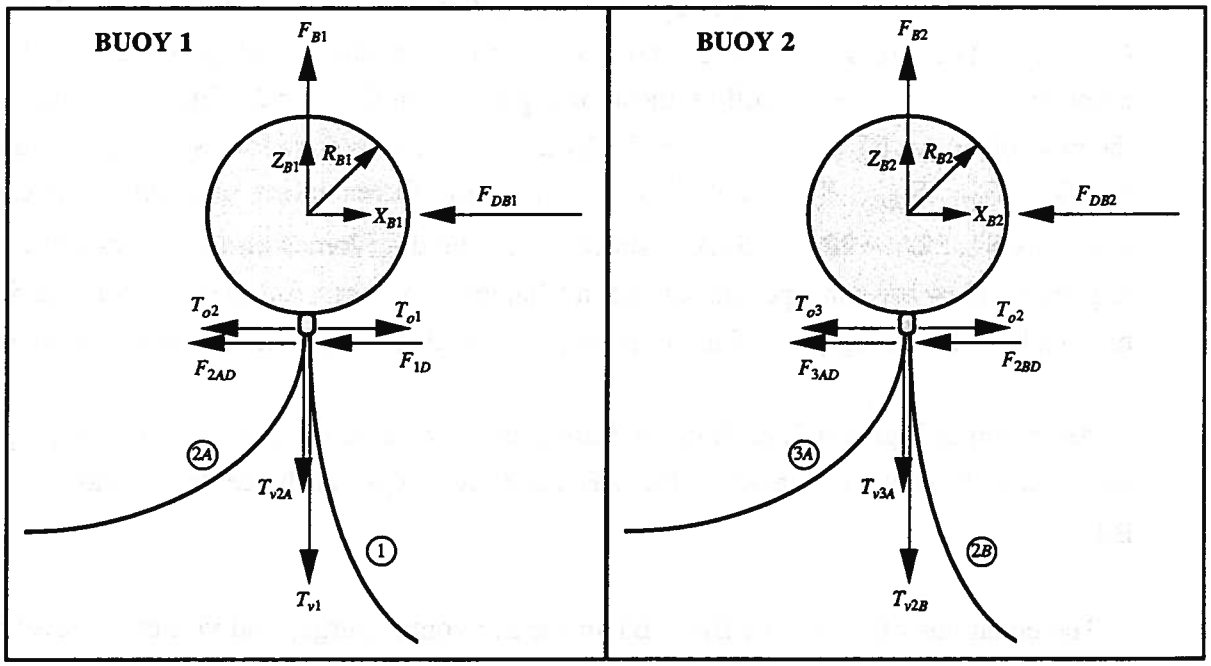

Figure 4.2. Forces acting on each buoy

4.2. Three-Dimensional Deformation of Catenaries with Two Buoys

Figure 4.3 shows the horizontal plane deformation of the two-buoy catenary due to the action of drag forces applied to the buoys. In this figure, each buoy has a right hand coordinate reference frame (X_{B1}, Y_{B1}, Z_{B1}) and (X_{B2}, Y_{B2}, Z_{B2}), with Z_{B1} and Z_{B2} pointing upwards, X_{B1} pointing horizontally in the plane of AC, and X_{B2} pointing horizontally in the

plane of S2. The position of B1 with respect to the inertial reference frame is given by (x_{B1}, y_{B1}, z_{B1}), and the position of B2 is given by (x_{B2}, y_{B2}, z_{B2}).

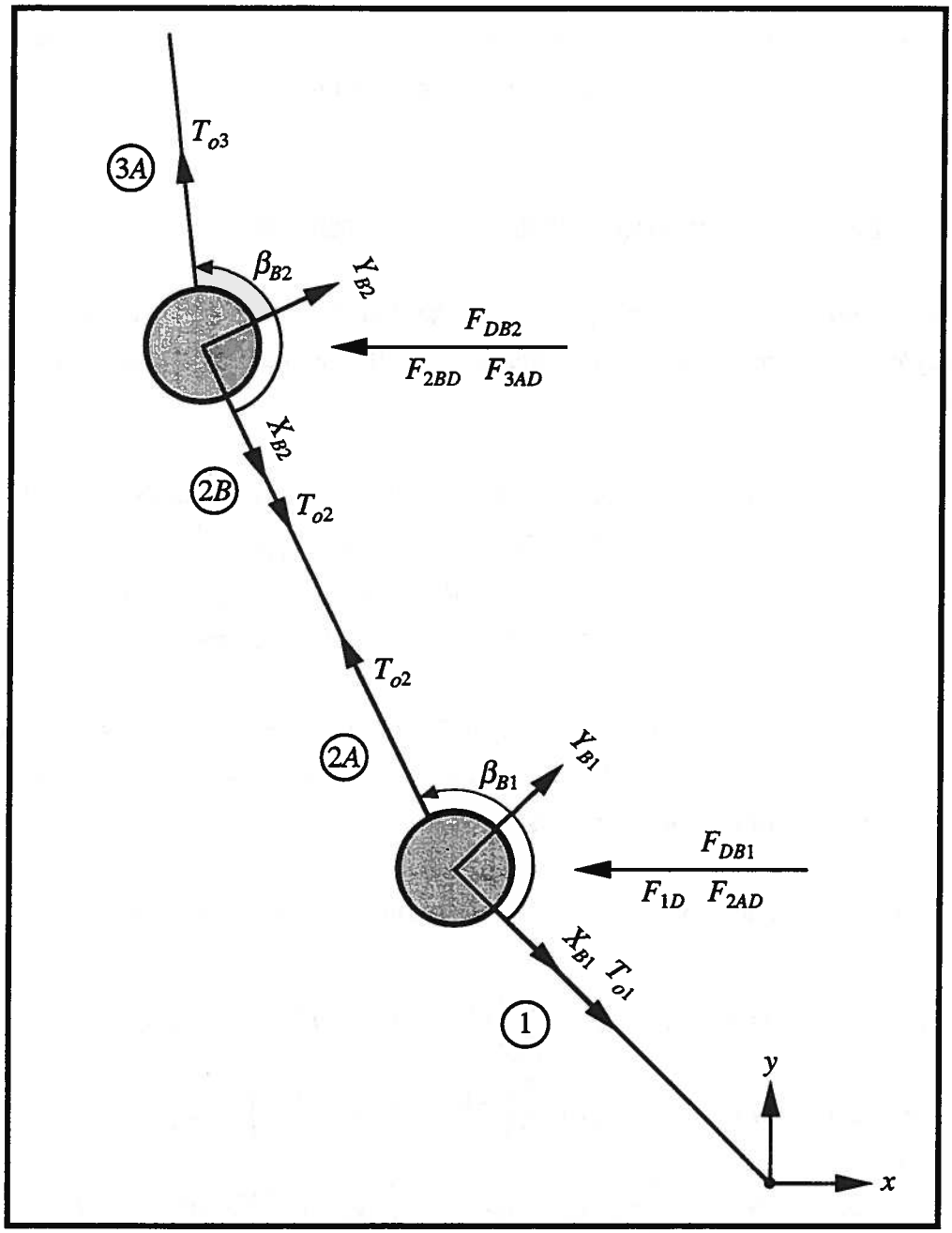

Figure 4.3. Three-dimensional catenary deformation with two buoys

In Figure 4.3, the horizontal angle between segments S1 and S2A is denoted by β_{B1}, and is measured counterclockwise from X_{B1}. The horizontal angle between segments S2B and S3A is denoted by β_{B2}, measured counterclockwise from X_{B2}. These are given by

$$\beta_{B1} = \gamma_{B2} - \gamma_{B1} + \pi \ , \tag{4.13}$$

$$\beta_{B2} = \gamma - \gamma_{B2} + \pi \ , \tag{4.14}$$

where γ_{B1} and γ_{B2} are the horizontal angles between the $x-$axis and segments S1 and S2B respectively, measured counterclockwise from the buoy.

4.3. Spread Mooring Systems with Two Buoys per Line

Once the geometrical properties of the two-buoy catenary have been defined, the buoy/catenary model can be incorporated into the mathematical model for spread mooring systems.

Figure 4.4 shows the general geometry of a SMS with two buoys per mooring line. Each buoy has its own right hand reference frame ($X^{(i)}_{B(j)}$, $Y^{(i)}_{B(j)}$, $Z^{(i)}_{B(j)}$), ($i=1, \ldots, n$; $j=1, 2$). The geometric properties of the SMS of Figure 4.4 are defined as in the previous chapters. The total number of buoys in the system of Figure 4.4 is thus $n_B=2n$.

The mathematical model for the system shown in Figure 4.4 consists of 3+3n_B equations of motion and their associated kinematic equations. Since $n_B=2n$, the system is modeled by 3+6n equations of motion as follows:

The three equations of motion for the vessel in surge, sway and yaw are:

$$(m+m_x)\dot{u} - (m+m_y)rv = X_H + \sum_{i=1}^{n}\left\{T^{(i)}_{o3}\cos\beta^{(i)} - F^{(i)}_{3BDX}\right\} + F_{surge} \ , \tag{4.15}$$

$$(m+m_y)\dot{v} + (m+m_x)ru = Y_H + \sum_{i=1}^{n}\left\{T^{(i)}_{o3}\sin\beta^{(i)} - F^{(i)}_{3BDY}\right\} + F_{sway} \ , \tag{4.16}$$

$$(I_{zz}+J_{zz})\dot{r} = N_H + \sum_{i=1}^{n}\left\{x^{(i)}_p\left[T^{(i)}_{o3}\sin\beta^{(i)} - F^{(i)}_{3BDY}\right] - y^{(i)}_p\left[T^{(i)}_{o3}\cos\beta^{(i)} - F^{(i)}_{3BDX}\right]\right\} + N_{yaw} \ , \tag{4.17}$$

while their corresponding kinematic relations remain as in (2.61) - (2.63). The 6n equations of motion in surge, sway and heave for the buoys are given by:

Buoy B1:

$$(m_{B1}^{(i)} + A_{11-1}^{(i)})\dot{u}_{B1}^{(i)} = T_{o1}^{(i)} + T_{o2}^{(i)} \cos\beta_{B1}^{(i)} - F_{DBX1}^{(i)} - F_{A1}^{(i)} - F_{2ADX}^{(i)} \ , \tag{4.18}$$

$$(m_{B1}^{(i)} + A_{22-1}^{(i)})\dot{v}_{B1}^{(i)} = T_{o2}^{(i)} \sin\beta_{B1}^{(i)} - F_{DBY1}^{(i)} - F_{L1}^{(i)} - F_{2ADY}^{(i)} \ , \tag{4.19}$$

$$(m_{B1}^{(i)} + A_{33-1}^{(i)})\dot{w}_{B1}^{(i)} = F_{B1}^{(i)} - T_{o1}^{(i)} \sinh\left(\frac{P\ell_1^{(i)}}{T_{o1}^{(i)}}\right) - T_{o2}^{(i)} \sinh\left(\frac{P\ell_{2A}^{(i)}}{T_{o2}^{(i)}}\right) , \tag{4.20}$$

for $i = 1, \ldots . , n$.

Buoy B2:

$$(m_{B2}^{(i)} + A_{11-2}^{(i)})\dot{u}_{B2}^{(i)} = T_{o2}^{(i)} + T_{o3}^{(i)} \cos\beta_{B2}^{(i)} - F_{DBX2}^{(i)} - F_{A2B}^{(i)} - F_{3ADX}^{(i)} \ , \tag{4.21}$$

$$(m_{B2}^{(i)} + A_{22-2}^{(i)})\dot{v}_{B2}^{(i)} = T_{o3}^{(i)} \sin\beta_{B2}^{(i)} - F_{DBY2}^{(i)} - F_{L2B}^{(i)} - F_{3ADY}^{(i)} \ , \tag{4.22}$$

$$(m_{B2}^{(i)} + A_{33-2}^{(i)})\dot{w}_{B2}^{(i)} = F_{B2}^{(i)} - T_{o2}^{(i)} \sinh\left(\frac{P\ell_{2B}^{(i)}}{T_{o2}^{(i)}}\right) - T_{o3}^{(i)} \sinh\left(\frac{P\ell_{3A}^{(i)}}{T_{o3}^{(i)}}\right) , \tag{4.23}$$

for $i = 1, \ldots . , n$.

The associated $6n$ kinematic conditions are:

Buoy B1:

$$\dot{x}_{B1}^{(i)} = u_{B1}^{(i)} \cos\gamma_{B1}^{(i)} - v_{B1}^{(i)} \sin\gamma_{B1}^{(i)} + U_c \frac{z_{B1}^{(i)}}{h} \cos\alpha \ , \tag{4.24}$$

$$\dot{y}_{B1}^{(i)} = u_{B1}^{(i)} \sin\gamma_{B1}^{(i)} + v_{B1}^{(i)} \cos\gamma_{B1}^{(i)} + U_c \frac{z_{B1}^{(i)}}{h} \sin\alpha \ , \tag{4.25}$$

$$\dot{z}_{B1}^{(i)} = w_{B1}^{(i)} \ , \tag{4.26}$$

for $i = 1, \ldots . , n$.

Buoy B2:

$$\dot{x}_{B2}^{(i)} = u_{B2}^{(i)} \cos\gamma_{B2}^{(i)} - v_{B2}^{(i)} \sin\gamma_{B2}^{(i)} + U_c \frac{z_{B2}^{(i)}}{h} \cos\alpha \ , \tag{4.27}$$

$$\dot{y}_{B2}^{(i)} = u_{B2}^{(i)} \sin\gamma_{B2}^{(i)} + v_{B2}^{(i)} \cos\gamma_{B2}^{(i)} + U_c \frac{z_{B2}^{(i)}}{h} \sin\alpha \ , \tag{4.28}$$

$$\dot{z}_{B2}^{(i)} = w_{B2}^{(i)}, \quad (i=1, \ldots, n), \tag{4.29}$$

for $i=1, \ldots, n$.

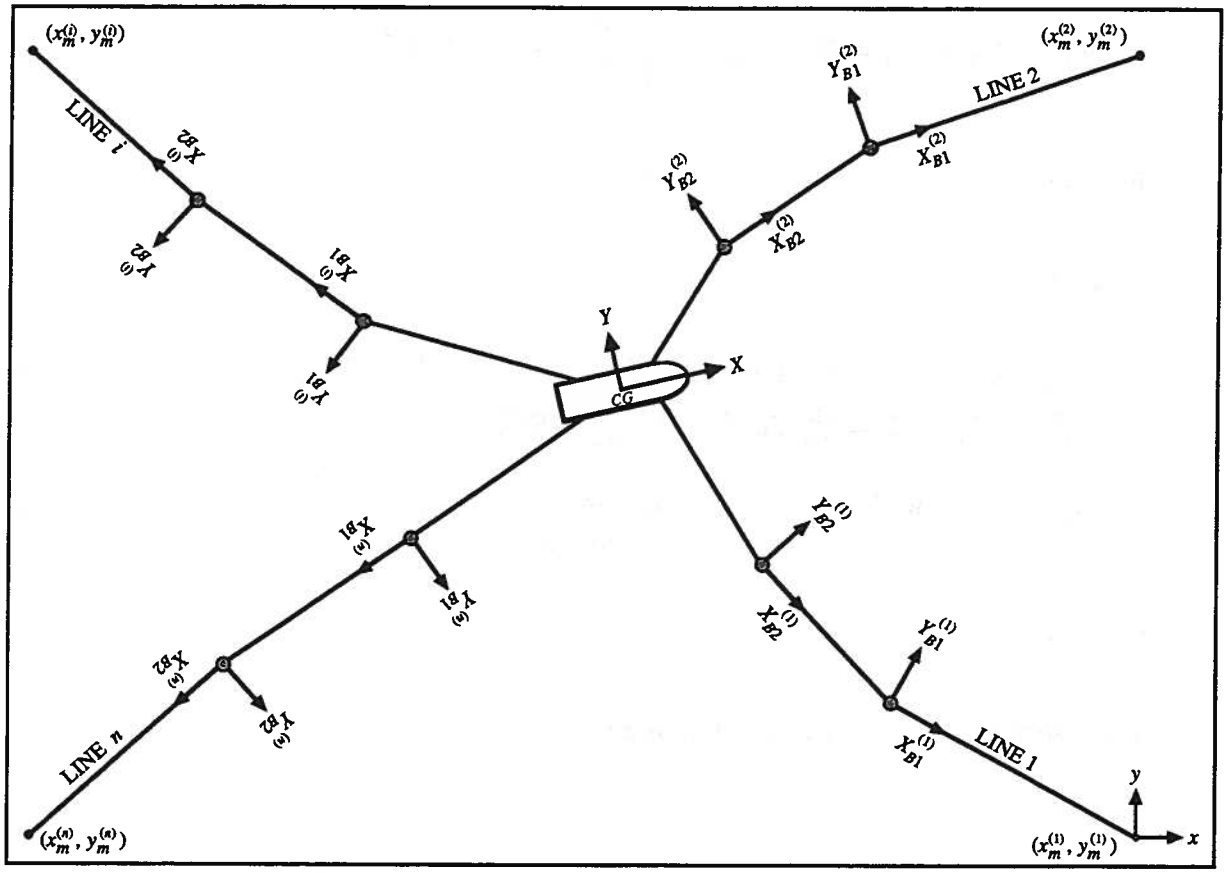

Figure 4.4. Geometry of multi-buoy Spread Mooring System

4.4. State Space Representation and Equilibria of SMS with Two Buoys per Line

Equilibrium of the system governed by equations of motion (4.15) - (4.23) and kinematics (2.61) - (2.63) and (4.24) - (4.29) is solved following the solution approach presented in Chapters 2 and 3. The state space representation for this type of systems can be recast in a $6(1+n_B)$ state space, as discussed in the previous chapter. Notice, however, that in this case $n_B=2n$, resulting in increased number of dimensions of the state space. Following the "Ship Motions Flow," the state space is defined by the following variables: $[u,\ v,\ r,\ x,\ y,\ \psi,\ u_{B(j)}^{(i)},\ v_{B(j)}^{(i)},\ w_{B(j)}^{(i)},\ x_{B(j)}^{(i)},\ y_{B(j)}^{(i)},\ z_{B(j)}^{(i)},\ i=1, \ldots, n;\ j=1, 2]^{\mathrm{T}}$. The nonlinear system is represented in Cauchy standard form by simply extending the concepts of Chapter 3 as:

$$\dot{u} = \frac{X_H + (m+m_y)rv + \sum_{i=1}^{n}\left\{T_{o3}^{(i)}\cos\beta^{(i)} - F_{3BDX}^{(i)}\right\} + F_{surge}}{(m+m_x)}, \tag{4.30}$$

$$\dot{v} = \frac{Y_H - (m+m_x)ru + \sum_{i=1}^{n}\left\{T_{o3}^{(i)}\sin\beta^{(i)} - F_{3BDY}^{(i)}\right\} + F_{sway}}{(m+m_y)}, \tag{4.31}$$

$$\dot{r} = \frac{N_H + \sum_{i=1}^{n}\left\{x_p^{(i)}\left[T_{o3}^{(i)}\sin\beta^{(i)} - F_{3BDY}^{(i)}\right] - y_p^{(i)}\left[T_{o3}^{(i)}\cos\beta^{(i)} - F_{3BDX}^{(i)}\right]\right\} + N_{yaw}}{(I_{zz}+J_{zz})}, \tag{4.32}$$

$$\dot{x} = u\cos\psi - v\sin\psi + U_c\cos\alpha\ , \tag{4.33}$$

$$\dot{y} = u\sin\psi + v\cos\psi + U_c\sin\alpha\ , \tag{4.34}$$

$$\dot{\psi} = r\ , \tag{4.35}$$

$$\dot{u}_{B1}^{(i)} = \frac{T_{o1}^{(i)} + T_{o2}^{(i)}\cos\beta_{B1}^{(i)} - F_{DBX1}^{(i)} - F_{A1}^{(i)} - F_{2ADX}^{(i)}}{(m_{B1}^{(i)} + A_{11-1}^{(i)})}, \tag{4.36}$$

$$\dot{v}_{B1}^{(i)} = \frac{T_{o2}^{(i)}\sin\beta_{B1}^{(i)} - F_{DBY1}^{(i)} - F_{L1}^{(i)} - F_{2ADY}^{(i)}}{(m_{B1}^{(i)} + A_{22-1}^{(i)})}, \tag{4.37}$$

$$\dot{w}_{B1}^{(i)} = \frac{F_{B1}^{(i)} - T_{o1}^{(i)}\sinh\left(\frac{P\ell_1^{(i)}}{T_{o1}^{(i)}}\right) - T_{o2}^{(i)}\sinh\left(\frac{P\ell_{2A}^{(i)}}{T_{o2}^{(i)}}\right)}{(m_{B1}^{(i)} + A_{33-1}^{(i)})}, \tag{4.38}$$

$$\dot{u}_{B2}^{(i)} = \frac{T_{o2}^{(i)} + T_{o3}^{(i)}\cos\beta_{B2}^{(i)} - F_{DBX2}^{(i)} - F_{A2B}^{(i)} - F_{3ADX}^{(i)}}{(m_{B2}^{(i)} + A_{11-2}^{(i)})}, \tag{4.39}$$

$$\dot{v}_{B2}^{(i)} = \frac{T_{o3}^{(i)}\sin\beta_{B2}^{(i)} - F_{DBY2}^{(i)} - F_{L2B}^{(i)} - F_{3ADY}^{(i)}}{(m_{B2}^{(i)} + A_{22-2}^{(i)})}, \tag{4.40}$$

$$\dot{w}_{B2}^{(i)} = \frac{F_{B2}^{(i)} - T_{o2}^{(i)}\sinh\left(\frac{P\ell_{2B}^{(i)}}{T_{o2}^{(i)}}\right) - T_{o3}^{(i)}\sinh\left(\frac{P\ell_{3A}^{(i)}}{T_{o3}^{(i)}}\right)}{(m_{B2}^{(i)} + A_{33-2}^{(i)})}, \tag{4.41}$$

$$\dot{x}_{B1}^{(i)} = u_{B1}^{(i)}\cos\gamma_{B1}^{(i)} - v_{B1}^{(i)}\sin\gamma_{B1}^{(i)} + U_c\frac{z_{B1}^{(i)}}{h}\cos\alpha\ , \tag{4.42}$$

$$\dot{y}_{B1}^{(i)} = u_{B1}^{(i)}\sin\gamma_{B1}^{(i)} + v_{B1}^{(i)}\cos\gamma_{B1}^{(i)} + U_c\frac{z_{B1}^{(i)}}{h}\sin\alpha\ , \tag{4.43}$$

$$\dot{z}_{B1}^{(i)} = w_{B1}^{(i)}\ , \tag{4.44}$$

$$\dot{x}_{B2}^{(i)} = u_{B2}^{(i)}\cos\gamma_{B2}^{(i)} - v_{B2}^{(i)}\sin\gamma_{B2}^{(i)} + U_c\frac{z_{B2}^{(i)}}{h}\cos\alpha\ , \tag{4.45}$$

$$\dot{y}_{B2}^{(i)} = u_{B2}^{(i)} \sin\gamma_{B2}^{(i)} + v_{B2}^{(i)} \cos\gamma_{B2}^{(i)} + U_c \frac{z_{B2}^{(i)}}{h} \sin\alpha \ , \tag{4.46}$$

$$\dot{z}_{B2}^{(i)} = w_{B2}^{(i)} \ , \tag{4.47}$$

for $i = 1, \ldots, n$.

The equilibria of the nonlinear system can be found by setting the left hand sides in equations (4.30) - (4.47) equal to zero. As seen in Chapters 2 and 3, some of the equations above can be either eliminated or recast in terms of other state space variables at equilibrium. The linear velocity vector of the vessel at equilibrium $(u, v) = (\overline{u}, \overline{v})$ can be recast in terms of the drift angle at equilibrium $\overline{\psi}$ as in expressions (2.84) and (2.85). In addition, equations (4.35), (4.38) and (4.47) yield $\overline{r} = 0$, and $\overline{w}_{B1}^{(i)} = \overline{w}_{B2}^{(i)} = 0$, $(i = 1, \ldots, n)$. The state space unknowns at equilibrium is therefore decreased from $6+6n_B$ to $3+5n_B$, and the equilibrium equations that must be solved simultaneously have been reduced to (4.30) - (4.32), (4.36), (4.37), (4.39), (4.40), and (4.42) - (4.47), provided the appropriate values for $\overline{u}$ and $\overline{v}$ are substituted from equations (3.27) and (3.28). In addition to these equations, the solution for equilibrium requires that we solve equations for the auxiliary unknowns $\overline{T}_{o1}^{(i)}$, $\overline{T}_{o2}^{(i)}$, $\overline{T}_{o3}^{(i)}$, $d^{(i)}$, $\overline{\ell}_1^{(i)}$, $\overline{\ell}_{2A}^{(i)}$, $\overline{\ell}_{2B}^{(i)}$, $\overline{\ell}_{3A}^{(i)}$, and $\overline{\ell}_{3B}^{(i)}$, $(i = 1, \ldots, n)$, thus introducing an additional $9n$ equations. The total number of equilibrium equations for the $n_B = 2n$ system is therefore

$$N_{EQ} = 3 + 5n_B + 9n = 3 + 10n + 9n = 3 + 19n \ . \tag{4.48}$$

The above number can also be recast as follows

$$N_{EQ} = 3 + 5n_B + 3(n_B + n) = 3 + 8n_B + 3n \ , \tag{4.49}$$

where 3 is the number of vessel state space variables; $5n_B$ is the number of the buoy state space variables; and $3(n_B + n)$ is the number of auxiliary variables representing unknowns for the horizontal tension and horizontal distance components. Thus, we have the following $N_{EQ} = 3 + 19n$ simultaneous equations to solve for the system equilibria

$$\overline{X}_H + \sum_{i=1}^{n} \left\{ \overline{T}_{o3}^{(i)} \cos\overline{\beta}^{(i)} - \overline{F}_{3BDX}^{(i)} \right\} + \overline{F}_{surge} = 0 \ , \tag{4.50}$$

$$\overline{Y}_H + \sum_{i=1}^{n} \left\{ \overline{T}_{o3}^{(i)} \sin\overline{\beta}^{(i)} - \overline{F}_{3BDY}^{(i)} \right\} + \overline{F}_{sway} = 0 \ , \tag{4.51}$$

$$\overline{N}_H + \sum_{i=1}^{n}\left\{x_p^{(i)}\left[\overline{T}_{o3}^{(i)}\sin\overline{\beta}^{(i)} - \overline{F}_{3BDY}^{(i)}\right] - y_p^{(i)}\left[\overline{T}_{o3}^{(i)}\cos\overline{\beta}^{(i)} - \overline{F}_{3BDX}^{(i)}\right]\right\} + \overline{N}_{yaw} = 0\,, \tag{4.52}$$

$$\overline{T}_{o1}^{(i)} + \overline{T}_{o2}^{(i)}\cos\overline{\beta}_{B1}^{(i)} - \overline{F}_{DBX1}^{(i)} - \overline{F}_{A1}^{(i)} - \overline{F}_{2ADX}^{(i)} = 0\,, \tag{4.53}$$

$$\overline{T}_{o2}^{(i)}\sin\overline{\beta}_{B1}^{(i)} - \overline{F}_{DBY1}^{(i)} - \overline{F}_{L1}^{(i)} - \overline{F}_{2ADY}^{(i)} = 0\,, \tag{4.54}$$

$$F_{B1}^{(i)} - \overline{T}_{o1}^{(i)}\sinh\left(\frac{P\overline{\ell}_1^{(i)}}{\overline{T}_{o1}^{(i)}}\right) - \overline{T}_{o2}^{(i)}\sinh\left(\frac{P\overline{\ell}_{2A}^{(i)}}{\overline{T}_{o2}^{(i)}}\right) = 0\,, \tag{4.55}$$

$$\overline{T}_{o2}^{(i)} + \overline{T}_{o3}^{(i)}\cos\overline{\beta}_{B2}^{(i)} - \overline{F}_{DBX2}^{(i)} - \overline{F}_{A2B}^{(i)} - \overline{F}_{3ADX}^{(i)} = 0\,, \tag{4.56}$$

$$\overline{T}_{o3}^{(i)}\sin\overline{\beta}_{B2}^{(i)} - \overline{F}_{DBY2}^{(i)} - \overline{F}_{L2B}^{(i)} - \overline{F}_{3ADY}^{(i)} = 0\,, \tag{4.57}$$

$$F_{B2}^{(i)} - \overline{T}_{o2}^{(i)}\sinh\left(\frac{P\overline{\ell}_{2B}^{(i)}}{\overline{T}_{o2}^{(i)}}\right) - \overline{T}_{o3}^{(i)}\sinh\left(\frac{P\overline{\ell}_{3A}^{(i)}}{\overline{T}_{o3}^{(i)}}\right) = 0\,, \tag{4.58}$$

$$\overline{u}_{B1}^{(i)}\cos\overline{\gamma}_{B1}^{(i)} - \overline{v}_{B1}^{(i)}\sin\overline{\gamma}_{B1}^{(i)} + U_c\frac{\overline{z}_{B1}^{(i)}}{h}\cos\alpha = 0\,, \tag{4.59}$$

$$\overline{u}_{B1}^{(i)}\sin\overline{\gamma}_{B1}^{(i)} + \overline{v}_{B1}^{(i)}\cos\overline{\gamma}_{B1}^{(i)} + U_c\frac{\overline{z}_{B1}^{(i)}}{h}\sin\alpha = 0\,, \tag{4.60}$$

$$\overline{u}_{B2}^{(i)}\cos\overline{\gamma}_{B2}^{(i)} - \overline{v}_{B2}^{(i)}\sin\overline{\gamma}_{B2}^{(i)} + U_c\frac{\overline{z}_{B2}^{(i)}}{h}\cos\alpha = 0\,, \tag{4.61}$$

$$\overline{u}_{B2}^{(i)}\sin\overline{\gamma}_{B2}^{(i)} + \overline{v}_{B2}^{(i)}\cos\overline{\gamma}_{B2}^{(i)} + U_c\frac{\overline{z}_{B2}^{(i)}}{h}\sin\alpha = 0\,, \tag{4.62}$$

$$\sinh\left(\frac{P\overline{\ell}_1^{(i)}}{\overline{T}_{o1}^{(i)}}\right) - \frac{P}{\overline{T}_{o1}^{(i)}}\sqrt{\overline{z}_{B1}^{(i)}\left(\overline{z}_{B1}^{(i)} + 2\frac{\overline{T}_{o1}^{(i)}}{P}\right)} = 0\,, \tag{4.63}$$

$$\sinh\left(\frac{P\overline{\ell}_{2A}^{(i)}}{2\overline{T}_{o2}^{(i)}}\right)\cosh\left(\frac{P\overline{\ell}_{2B}^{(i)}}{2\overline{T}_{o2}^{(i)}}\right) + \cosh\left(\frac{P\overline{\ell}_{2A}^{(i)}}{2\overline{T}_{o2}^{(i)}}\right)\sinh\left(\frac{P\overline{\ell}_{2B}^{(i)}}{2\overline{T}_{o2}^{(i)}}\right) - \frac{P}{2\overline{T}_{o2}^{(i)}}\sqrt{\ell_{w2}^{(i)2} - (\overline{z}_{B2}^{(i)} - \overline{z}_{B1}^{(i)})^2} = 0\,, \tag{4.64}$$

$$\sinh\left(\frac{P\overline{\ell}_{3A}^{(i)}}{2\overline{T}_{o3}^{(i)}}\right)\cosh\left(\frac{P\overline{\ell}_{3B}^{(i)}}{2\overline{T}_{o3}^{(i)}}\right) + \cosh\left(\frac{P\overline{\ell}_{3A}^{(i)}}{2\overline{T}_{o3}^{(i)}}\right)\sinh\left(\frac{P\overline{\ell}_{3B}^{(i)}}{2\overline{T}_{o3}^{(i)}}\right) - \frac{P}{2\overline{T}_{o3}^{(i)}}\sqrt{\ell_{w3}^{(i)2} - (h - \overline{z}_{B2}^{(i)})^2} = 0\,, \tag{4.65}$$

$$\ell_{w1}^{(i)} - \frac{\overline{T}_{o1}^{(i)}}{P}\sinh\left(\frac{P\overline{\ell}_1^{(i)}}{\overline{T}_{o1}^{(i)}}\right) - \overline{d}^{(i)} = 0\,, \tag{4.66}$$

$$\ell_{w2}^{(i)} - \frac{\overline{T}_{o2}^{(i)}}{P}\sinh\left(\frac{P\overline{\ell}_{2A}^{(i)}}{\overline{T}_{o2}^{(i)}}\right) - \frac{\overline{T}_{o2}^{(i)}}{P}\sinh\left(\frac{P\overline{\ell}_{2B}^{(i)}}{2\overline{T}_{o2}^{(i)}}\right) = 0\,, \tag{4.67}$$

$$\ell_{w3}^{(i)} - \frac{\overline{T}_{o3}^{(i)}}{P}\sinh\left(\frac{P\overline{\ell}_{3A}^{(i)}}{\overline{T}_{o3}^{(i)}}\right) - \frac{\overline{T}_{o3}^{(i)}}{P}\sinh\left(\frac{P\overline{\ell}_{3B}^{(i)}}{2\overline{T}_{o3}^{(i)}}\right) = 0 \,, \tag{4.68}$$

$$\sqrt{\left(x_m^{(i)} - \overline{x}_{B1}^{(i)}\right)^2 + \left(y_m^{(i)} - \overline{y}_{B1}^{(i)}\right)^2} - \overline{\ell}_1^{(i)} - \overline{d}^{(i)} = 0 \,, \tag{4.69}$$

$$\sqrt{\left(\overline{x}_{B1}^{(i)} - \overline{x}_{B2}^{(i)}\right)^2 + \left(\overline{y}_{B1}^{(i)} - \overline{y}_{B2}^{(i)}\right)^2} - \overline{\ell}_{2A}^{(i)} - \overline{\ell}_{2B}^{(i)} = 0 \,, \tag{4.70}$$

$$\sqrt{\left(\overline{x}_{B2}^{(i)} - \overline{x}_T^{(i)}\right)^2 + \left(\overline{y}_{B2}^{(i)} - \overline{y}_T^{(i)}\right)^2} - \overline{\ell}_{3A}^{(i)} - \overline{\ell}_{3B}^{(i)} = 0 \,, \tag{4.71}$$

for $i = 1, \ldots, n$.

All solutions to equilibrium equations (4.50) - (4.71) produce the system equilibria. The concepts of system pretension, geometry/configuration specifications, nonlinear simulations and stability analysis for this type of systems are a natural extension of the concepts presented in Chapters 2 and 3, and are out of the scope of this report.

4.5. Introduction to Spread Mooring Systems with Multiple Buoys per Line

The results of the previous sections allow us to extend the concept to systems with n_{BL} buoys attached to each mooring line. Letting n be the number of mooring lines in the system, and n_B the total number of buoys, we define n_{BL} as the number of buoys per mooring line as follows:

$$n_{BL} = \frac{n_B}{n} \,. \tag{4.72}$$

Notice that n_{BL} needs not be the same for each mooring line. In this work, for simplicity of representation, we define n_{BL} as a constant number given by equation (4.72).

In brief, the number of equations of motion for the MBSMS is $3(1+n_B)$ and its associated kinematic relations are $3(1+n_B)$, and are extended from the 2-buoy system of the previous section. In the most general form, the equations of motion for the vessel and its kinematics are:

$$(m+m_x)\dot{u} - (m+m_y)rv = X_H + \sum_{i=1}^{n}\left\{T_{O(n_{BL}+1)}^{(i)}\cos\beta^{(i)} - F_{(n_{BL}+1)BDX}^{(i)}\right\} + F_{surge} \,, \tag{4.73}$$

$$(m+m_y)\dot{v}+(m+m_x)ru = Y_H + \sum_{i=1}^{n}\left\{T^{(i)}_{o(n_{BL}+1)}\sin\beta^{(i)} - F^{(i)}_{(n_{BL}+1)BDY}\right\} + F_{sway}\ , \tag{4.74}$$

$$(I_{zz}+J_{zz})\dot{r} = N_H + \sum_{i=1}^{n} x_p^{(i)}\left\{T^{(i)}_{o(n_{BL}+1)}\sin\beta^{(i)} - F^{(i)}_{(n_{BL}+1)BDY}\right\} - \sum_{i=1}^{n} y_p^{(i)}\left\{T^{(i)}_{o(n_{BL}+1)}\cos\beta^{(i)} - F^{(i)}_{(n_{BL}+1)BDX}\right\} + N_{yaw}\ , \tag{4.75}$$

$$\dot{x} = u\cos\psi - v\sin\psi + U_c\cos\alpha\ , \tag{4.76}$$

$$\dot{y} = u\sin\psi + v\cos\psi + U_c\sin\alpha\ , \tag{4.77}$$

$$\dot{\psi} = r\ . \tag{4.78}$$

The $3n_B$ equations of motion for the buoys and their respective kinematics are

$$(m^{(i)}_{B(j)} + A^{(i)}_{11(j)})\dot{u}_{B(j)} = T^{(i)}_{o(j)} + T^{(i)}_{o(j+1)}\cos\beta^{(i)}_{B(j)} - F^{(i)}_{DBX(j)} - F^{(i)}_{A(j)B} - F^{(i)}_{(j+1)ADX}\ , \tag{4.79}$$

$$(m^{(i)}_{B(j)} + A^{(i)}_{22(j)})\dot{v}_{B(j)} = T^{(i)}_{o(j+1)}\cos\beta^{(i)}_{B(j)} - F^{(i)}_{DBY(j)} - F^{(i)}_{L(j)B} - F^{(i)}_{(j+1)ADY}\ , \tag{4.80}$$

$$(m^{(i)}_{B(j)} + A^{(i)}_{33(j)})\dot{w}_{B(j)} = F^{(i)}_{B(j)} - T^{(i)}_{o(j)}\sinh\left(\frac{P\ell^{(i)}_{(j)A}}{T^{(i)}_{o(j)}}\right) - T^{(i)}_{o(j+1)}\sinh\left(\frac{P\ell^{(i)}_{(j+1)A}}{T^{(i)}_{o(j+1)}}\right)\ , \tag{4.81}$$

$$\dot{x}^{(i)}_{B(j)} = u^{(i)}_{B(j)}\cos\gamma^{(i)}_{B(j)} - v^{(i)}_{B(j)}\sin\gamma^{(i)}_{B(j)} + U_c\frac{z^{(i)}_{B(j)}}{h}\cos\alpha\ , \tag{4.82}$$

$$\dot{y}^{(i)}_{B(j)} = u^{(i)}_{B(j)}\sin\gamma^{(i)}_{B(j)} + v^{(i)}_{B(j)}\cos\gamma^{(i)}_{B(j)} + U_c\frac{z^{(i)}_{B(j)}}{h}\sin\alpha\ , \tag{4.83}$$

$$\dot{z}^{(i)}_{B(j)} = w^{(i)}_{B(j)}\ , \tag{4.84}$$

for $i=1, \ldots, n$; $j=1, \ldots, n_{BL}$.

The state space representation of the system (4.73) - (4.84) can be obtained by recasting these equations as a set of first order nonlinear differential equations of the form (3.13). Such state space representation consists of $6+6n_B$ variables as follows: $[u,\ v,\ r,\ x,\ y,\ \psi,\ u^{(i)}_{B(j)},\ v^{(i)}_{B(j)},\ w^{(i)}_{B(j)},\ x^{(i)}_{B(j)},\ y^{(i)}_{B(j)},\ z^{(i)}_{B(j)},\ i=1, \ldots, n;\ j=1, \ldots, n_{BL}]^{\mathrm{T}}$. For the purpose of this work it is important to establish the equilibrium equations of the MBSMS. This is discussed next.

4.6. Equilibrium Equations for SMS with Multiple Buoys per Line

The equilibrium of the nonlinear MBSMS is obtained, as previously mentioned, by recasting equations (4.73) - (4.84) in the form (3.13) and setting such expressions to zero. Additional auxiliary equations for the horizontal tension components and horizontal lengths are needed to solve for the system equilibria. After appropriate elimination of state space variables $\bar{u}$, $\bar{v}$, $\bar{r}$, and $\bar{w}_{Bj}^{(i)}$, ($i=1, \ldots, n$; $j=1, \ldots, n_{BL}$), the number of equilibrium equations N_{EQ} for MBSMS ($n_B = n\, n_{BL}$) derived in Section 4.4 can be written as

$$N_{EQ} = 3(1+n) + 8n_B = 3(1+n) + 8n(n_{BL}) = 3 + n(3 + 8n_{BL}) \ . \tag{4.86}$$

The equilibrium equations that must be solved simultaneously to find the system equilibria are given by equations (4.87) - (4.102) below

$$\bar{X}_H + \sum_{i=1}^{n} \left\{ \bar{T}_{o(n_{BL}+1)}^{(i)} \cos\bar{\beta}^{(i)} - \bar{F}_{(n_{BL}+1)BDX}^{(i)} \right\} + \bar{F}_{surge} = 0 \ , \tag{4.87}$$

$$\bar{Y}_H + \sum_{i=1}^{n} \left\{ \bar{T}_{o(n_{BL}+1)}^{(i)} \sin\bar{\beta}^{(i)} - \bar{F}_{(n_{BL}+1)BDY}^{(i)} \right\} + \bar{F}_{sway} = 0 \ , \tag{4.88}$$

$$\begin{aligned} \bar{N}_H &+ \sum_{i=1}^{n} x_p^{(i)} \left\{ \bar{T}_{o(n_{BL}+1)}^{(i)} \sin\bar{\beta}^{(i)} - \bar{F}_{(n_{BL}+1)BDY}^{(i)} \right\} \\ &- \sum_{i=1}^{n} y_p^{(i)} \left\{ \bar{T}_{o(n_{BL}+1)}^{(i)} \cos\bar{\beta}^{(i)} - \bar{F}_{(n_{BL}+1)BDX}^{(i)} \right\} + \bar{N}_{yaw} = 0 \ , \end{aligned} \tag{4.89}$$

$$\bar{T}_{o(j)}^{(i)} + \bar{T}_{o(j+1)}^{(i)} \cos\bar{\beta}_{B(j)}^{(i)} - \bar{F}_{DBX(j)}^{(i)} - \bar{F}_{A(j)B}^{(i)} - \bar{F}_{(j+1)ADX}^{(i)} = 0 \ , \tag{4.90}$$

$$\bar{T}_{o(j+1)}^{(i)} \sin\bar{\beta}_{B(j)}^{(i)} - \bar{F}_{DBY(j)}^{(i)} - \bar{F}_{L(j)B}^{(i)} - \bar{F}_{(j+1)ADY}^{(i)} = 0 \ , \tag{4.91}$$

$$\bar{F}_{B(j)}^{(i)} - \bar{T}_{o(j)}^{(i)} \sinh\left(\frac{P\bar{\ell}_{(j)A}^{(i)}}{\bar{T}_{o(j)}^{(i)}} \right) - \bar{T}_{o(j+1)}^{(i)} \sinh\left(\frac{\bar{P}\ell_{(j+1)A}^{(i)}}{\bar{T}_{o(j+1)}^{(i)}} \right) = 0 \ , \tag{4.92}$$

$$\bar{u}_{B(j)}^{(i)} \cos\bar{\gamma}_{B(j)}^{(i)} - \bar{v}_{B(j)}^{(i)} \sin\bar{\gamma}_{B(j)}^{(i)} + U_c \frac{\bar{z}_{B(j)}^{(i)}}{h} \cos\alpha = 0 \ , \tag{4.93}$$

$$\bar{u}_{B(j)}^{(i)} \sin\bar{\gamma}_{B(j)}^{(i)} + \bar{v}_{B(j)}^{(i)} \cos\bar{\gamma}_{B(j)}^{(i)} + U_c \frac{\bar{z}_{B(j)}^{(i)}}{h} \sin\alpha = 0 \ , \tag{4.94}$$

for $i=1, \ldots, n$; $j=1, \ldots, n_{BL}$.

For the first line segment ($j=1$):

$$\sinh\left(\frac{P\ell_1^{(i)}}{T_{o1}^{(i)}}\right)-\frac{P}{T_{o1}^{(i)}}\sqrt{z_{B1}^{(i)}\left(z_{B1}^{(i)}+2\frac{T_{o1}^{(i)}}{P}\right)}=0\ , \tag{4.95}$$

for $i=1,\ \ldots.\ ,\ n;\ j=1$.

For line segments $j=2,3,\ldots,\ n_{BL}$:

$$\sinh\left(\frac{P\ell_{(j)A}^{(i)}}{2T_{o(j)}^{(i)}}\right)\cosh\left(\frac{P\ell_{(j)B}^{(i)}}{2T_{o(j)}^{(i)}}\right)+\cosh\left(\frac{P\ell_{(j)A}^{(i)}}{2T_{o(j)}^{(i)}}\right)\sinh\left(\frac{P\ell_{(j)B}^{(i)}}{2T_{o(j)}^{(i)}}\right)$$
$$-\frac{P}{2T_{o(j)}^{(i)}}\sqrt{\ell_{w(j)}^{(i)2}-\left(z_{B(j)}^{(i)}-z_{B(j-1)}^{(i)}\right)^2}=0\ , \tag{4.96}$$

for $i=1,\ \ldots.\ ,\ n;\ j=2,\ \ldots.\ ,\ n_{BL}$.

For line segment $j=n_{BL}+1$:

$$\sinh\left(\frac{P\ell_{(n_{BL}+1)A}^{(i)}}{2T_{o(n_{BL}+1)}^{(i)}}\right)\cosh\left(\frac{P\ell_{(n_{BL}+1)B}^{(i)}}{2T_{o(n_{BL}+1)}^{(i)}}\right)+\cosh\left(\frac{P\ell_{(n_{BL}+1)A}^{(i)}}{2T_{o(n_{BL}+1)}^{(i)}}\right)\sinh\left(\frac{P\ell_{(n_{BL}+1)B}^{(i)}}{2T_{o(n_{BL}+1)}^{(i)}}\right)$$
$$-\frac{P}{2T_{o(n_{BL}+1)}^{(i)}}\sqrt{\ell_{w(n_{BL}+1)}^{(i)2}-\left(h-z_{B(n_{BL}+1)}^{(i)}\right)^2}=0\ , \tag{4.97}$$

for $i=1,\ \ldots.\ ,\ n;\ j=NBL+1$.

For line segment $j=1$:

$$\ell_{w1}^{(i)}-\frac{T_{o1}^{(i)}}{P}\sinh\left(\frac{P\ell_1^{(i)}}{T_{o1}^{(i)}}\right)-d^{(i)}=0\ , \tag{4.98}$$

for $i=1,\ \ldots.\ ,\ n;\ j=1$.

For line segments $j=2,\ldots,\ n_{BL}+1$:

$$\ell_{w(j)}^{(i)} - \frac{T_{o(j)}^{(i)}}{P}\left[\sinh\left(\frac{P\ell_{(j)A}^{(i)}}{T_{o(j)}^{(i)}}\right)+\sinh\left(\frac{P\ell_{(j)B}^{(i)}}{T_{o(j)}^{(i)}}\right)\right]=0\ , \tag{4.99}$$

for $i=1,\ \ldots.\ ,\ n;\ j=2,\ \ldots.\ ,\ n_{BL}+1$.

For line segment $j=1$:

$$\sqrt{\left(x_m^{(i)}-x_{B(j)}^{(i)}\right)^2+\left(y_m^{(i)}-y_{B(j)}^{(i)}\right)^2}-\ell_1^{(i)}-d^{(i)}=0\ , \tag{4.100}$$

for $i=1,\ \ldots.\ ,\ n;\ j=1$.

For line segments $j=2,\ \ldots,\ n_{BL}$:

$$\sqrt{\left(x_{B(j-1)}^{(i)}-x_{B(j)}^{(i)}\right)^2+\left(y_{B(j-1)}^{(i)}-y_{B(j)}^{(i)}\right)^2}-\ell_{(j)A}^{(i)}-\ell_{(j)B}^{(i)}=0\ , \tag{4.101}$$

for $i=1,\ \ldots.\ ,\ n;\ j=2,\ \ldots.\ ,\ n_{BL}$.

For line segment $j=n_{BL}+1$:

$$\sqrt{\left(x_{B(n_{BL})}^{(i)}-x_T^{(i)}\right)^2+\left(y_{B(n_{BL})}^{(i)}-y_T^{(i)}\right)^2}-\ell_{(n_{BL})A}^{(i)}-\ell_{(n_{BL})B}^{(i)}=0\ , \tag{4.102}$$

for $i=1,\ \ldots.\ ,\ n;\ j=n_{BL}+1$.

APPENDICES

APPENDIX 1: FIRST ORDER VARIATION OF ANCHORED CATENARY TENSION WITH RESPECT TO BUOY POSITION

The tension in the anchored segment of the catenary AC depends exclusively on the relative position of the buoy with respect to the mooring point on the sea bed. That is,

$$T_{o1}, T_{v1} = f(x_B, y_B, z_B). \tag{A1.1}$$

In previous work [12], we derived the following relationship between the lengths ℓ_1' and ℓ_1:

$$\frac{\Delta\ell_1}{\Delta\ell_1'} = \frac{d\ell_1}{d\ell_1'} \cong \frac{1}{1-\left[\left(1-\frac{\ell_1}{T_{o1}}\frac{dT_{o1}}{d\ell_1}\right)\cosh\left(\frac{P\ell_1}{T_{o1}}\right)+\frac{1}{P}\frac{dT_{o1}}{d\ell_1}\sinh\left(\frac{P\ell_1}{T_{o1}}\right)\right]}, \tag{A1.2}$$

where we have applied the relation $\lim_{\Delta\ell_1'\to 0}\frac{\Delta\ell_1}{\Delta\ell_1'} = \frac{d\ell_1}{d\ell_1'}$, and [12],

$$\frac{dT_{o1}}{d\ell_1} = \frac{P\sqrt{h_1\left(h_1+2\frac{T_{o1}}{P}\right)}\cosh\left(\frac{P\ell_1}{T_o}\right)}{\sqrt{h_1\left(h_1+2\frac{T_{o1}}{P}\right)}\left[\left(\frac{P\ell_1}{T_{o1}}\right)\cosh\left(\frac{P\ell_1}{T_{o1}}\right)-\sinh\left(\frac{P\ell_1}{T_{o1}}\right)\right]+h_1}. \tag{A1.3}$$

In equation (A1.3), h_1 is the depth of AC, which is approximately equal to z_B, and is taken to be equal to z_B. The first order derivatives of the horizontal tension component T_{o1} with respect to x_B and y_B are given by

$$\frac{dT_{o1}}{dx_B} = \frac{dT_{o1}}{d\ell_1}\frac{d\ell_1}{d\ell_1'}\frac{d\ell_1'}{dx_B}, \tag{A1.4}$$

$$\frac{dT_{o1}}{dy_B} = \frac{dT_{o1}}{d\ell_1}\frac{d\ell_1}{d\ell_1'}\frac{d\ell_1'}{dy_B}, \tag{A1.5}$$

where

$$\frac{d\ell_1'}{dx_B} = -\cos\gamma_B \ , \tag{A1.6}$$

$$\frac{d\ell_1'}{dy_B} = -\sin\gamma_B \ . \tag{A1.7}$$

The first order derivative of T_{o1} with respect to z_B is found directly by taking the derivative of equation (2.18) (where we have replaced h_1 by z_B) with respect to z_B. This yields

$$\frac{dT_{o1}}{dz_B} = \frac{P\left(z_B + \frac{T_{o1}}{P}\right) - P\sqrt{z_B\left(z_B + 2\frac{T_{o1}}{P}\right)}\cosh\left(\frac{P\ell_1}{T_o}\right)\frac{d\ell_1}{dz_B}}{\sqrt{z_B\left(z_B + 2\frac{T_{o1}}{P}\right)}\left[\sinh\left(\frac{P\ell_1}{T_{o1}}\right) - \left(\frac{P\ell_1}{T_{o1}}\right)\cosh\left(\frac{P\ell_1}{T_{o1}}\right)\right] - z_B} \ . \tag{A1.8}$$

Notice that equation (A1.8) contains the unknown term $d\ell_1/dz_B$. To find this term, consider Figure A1.1, which shows how a small displacement in z_B affects ℓ_1.

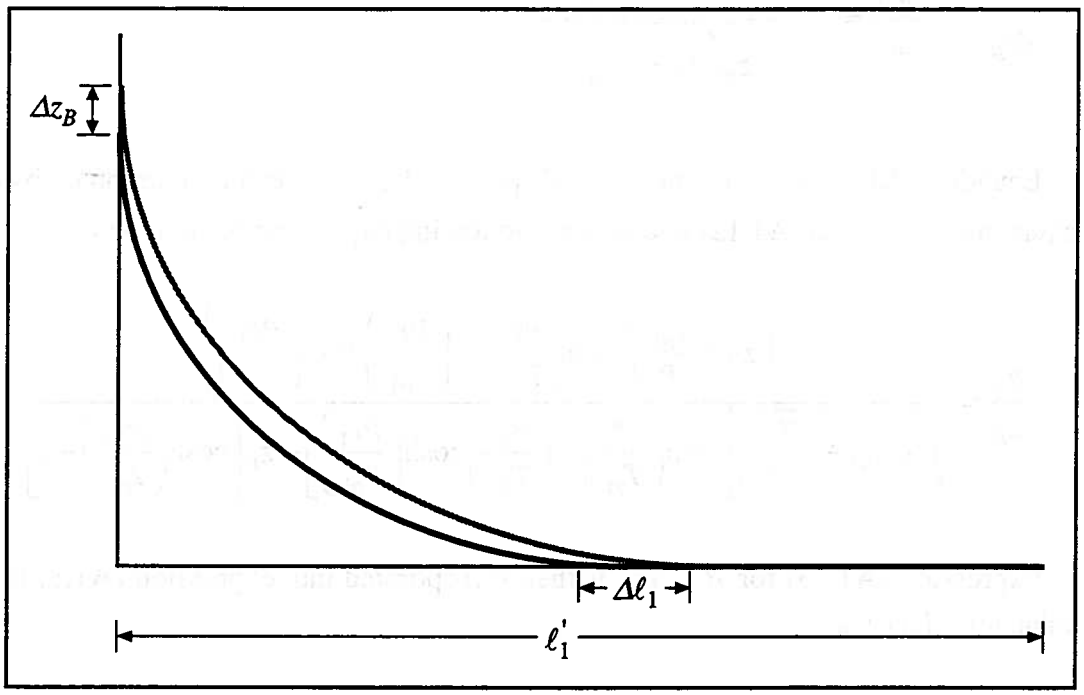

Figure A1.1. AC deformation for a change in z_B

In Figure A1.1, we notice that a change in z_B produces a change in the configuration of catenary segment S1. The length ℓ_1' of the horizontal projection of AC, and the total length ℓ_{w1} of AC, however, remain unchanged, i.e. $\Delta\,\ell_1' = 0$, $\Delta\,\ell_{w1} = 0$.

Noting, from equations (2.1) and (2.8) that

$$\frac{\Delta \ell_1'}{\Delta z_B} = \frac{\Delta \ell_1}{\Delta z_B} + \frac{\Delta d}{\Delta z_B} = 0 \,, \tag{A1.9}$$

$$\frac{\Delta \ell_{w1}}{\Delta z_B} = \frac{\Delta \ell_{eff1}}{\Delta z_B} + \frac{\Delta d}{\Delta z_B} = 0 \,, \tag{A1.10}$$

we can combine the two expressions above to derive the following relation between ℓ_1 and z_B:

$$\frac{\Delta \ell_1}{\Delta z_B} = \frac{\Delta \ell_{eff1}}{\Delta z_B} \,. \tag{A1.11}$$

In the limit, as $\Delta z_B \to 0$, using equation (2.10), we obtain

$$\frac{d\ell_1}{dz_B} = \frac{d\ell_{eff1}}{dz_B} = \frac{z_B + \left(T_{o1}/P\right) + \left(z_B/P\right)\dfrac{T_{o1}}{dz_B}}{\sqrt{z_B\left(z_B + 2\dfrac{T_{o1}}{P}\right)}} \,. \tag{A1.12}$$

Equation (A1.12) has the unknown dT_{o1}/dz_B. This term can be eliminated by combining equations (A1.8) and (A1.12) to obtain the following expression for $d\ell_1/dz_B$:

$$\frac{d\ell_1}{dz_B} = \frac{\left(z_B + \dfrac{T_{o1}}{P}\right)\left[\sinh\left(\dfrac{P\ell_1}{T_{o1}}\right) - \left(\dfrac{P\ell_1}{T_{o1}}\right)\cosh\left(\dfrac{P\ell_1}{T_{o1}}\right)\right]}{\sqrt{z_B\left(z_B + 2\dfrac{T_{o1}}{P}\right)}\left[\sinh\left(\dfrac{P\ell_1}{T_{o1}}\right) - \left(\dfrac{P\ell_1}{T_{o1}}\right)\cosh\left(\dfrac{P\ell_1}{T_{o1}}\right)\right] + z_B\left[\cosh\left(\dfrac{P\ell_1}{T_{o1}}\right) - 1\right]} \,. \tag{A1.13}$$

Expression (A1.13) for $d\ell_1/dz_B$ is then incorporated into expression (A1.8) to obtain the value for dT_{o1}/dz_B.

The first order derivatives of the vertical component of AC tension, namely T_{v1}, with respect to the buoy position vector $(x_B,\ y_B, z_B)$ can be derived as follows:

$$\frac{dT_{v1}}{dx_B} = \frac{dT_{v1}}{d\ell_1}\,\frac{d\ell_1}{d\ell_1'}\,\frac{d\ell_1'}{dx_B} \,, \tag{A1.14}$$

$$\frac{dT_{v1}}{dy_B} = \frac{dT_{v1}}{d\ell_1}\frac{d\ell_1}{d\ell_1'}\frac{d\ell_1'}{dy_B}\,, \tag{A1.15}$$

$$\frac{dT_{v1}}{dz_B} = \frac{dT_{o1}}{dz_B}\left[\sinh\left(\frac{P\ell_1}{T_{o1}}\right) - \left(\frac{P\ell_1}{T_{o1}}\right)\cosh\left(\frac{P\ell_1}{T_{o1}}\right)\right] + P\cosh\left(\frac{P\ell_1}{T_{o1}}\right)\frac{d\ell_1}{dz_B}\,. \tag{A1.16}$$

In expressions (A1.14) and (A1.15), the derivative of the vertical tension component with respect to the horizontal projected length of AC, that is $dT_{v1}/d\ell_1$, is obtained by taking the derivative of equation (2.15) with respect to ℓ_1 as follows

$$\frac{dT_{v1}}{d\ell_1} = P\cosh\left(\frac{P\ell_1}{T_{o1}}\right) + \frac{dT_{o1}}{d\ell_1}\left[\sinh\left(\frac{P\ell_1}{T_{o1}}\right) - \left(\frac{P\ell_1}{T_{o1}}\right)\cosh\left(\frac{P\ell_1}{T_{o1}}\right)\right]\,. \tag{A1.17}$$

The above expressions relate the changes in the horizontal and vertical tension components of ACs as functions of changes in position of the supporting buoy along the mooring line. For mooring lines consisting of several segments connected via buoys, the tension component in AC depends exclusively on the position of the buoy to which AC is connected.

APPENDIX 2: FIRST ORDER VARIATION OF SUSPENDED CATENARY TENSION WITH RESPECT TO VESSEL AND BUOY POSITION

The tension in the suspended segment of the catenary SC depends on the relative position of the buoy with respect to the vessel, and therefore it is a function of the state variables x, y, ψ, x_B, y_B and z_B. That is,

$$T_{o2} = T_{v2} = f(x, y, \psi, x_B, y_B, z_B) \ . \tag{A2.1}$$

An alternative formulation to equation (2.19) is as follows:

$$\sinh\left(\frac{P\ell_2}{2T_{o2}}\right) - \frac{P}{2T_{o2}}\sqrt{\ell_{w2}^2 - (h - h_1)^2} = 0 \ , \tag{A2.2}$$

where h_1 is the depth at which SC is connected to the buoy, and can be approximated by z_B.

The derivative of the horizontal tension component T_{o2} with respect to the length of the total horizontal projection of SC, ℓ_2, is given by (A2.1) as

$$\frac{dT_{o2}}{d\ell_2} = \frac{\left(\frac{P}{2}\right)\cosh\left(\frac{P\ell_2}{2T_{o2}}\right)}{\left(\frac{P\ell_2}{2T_{o2}}\right)\cosh\left(\frac{P\ell_2}{2T_{o2}}\right) - \sinh\left(\frac{P\ell_2}{2T_{o2}}\right)} \ , \tag{A2.3}$$

and thus the derivatives of the horizontal tension component T_{o2} with respect to variables x, y, ψ, x_B and y_B can be obtained readily as:

$$\frac{dT_{o2}}{dx} = \frac{dT_{o2}}{d\ell_2}\frac{d\ell_2}{dx} \ , \tag{A2.4}$$

$$\frac{dT_{o2}}{dy} = \frac{dT_{o2}}{d\ell_2}\frac{d\ell_2}{dy} \ , \tag{A2.5}$$

$$\frac{dT_{o2}}{d\psi} = \frac{dT_{o2}}{d\ell_2}\frac{d\ell_2}{d\psi} , \tag{A2.6}$$

$$\frac{dT_{o2}}{dx_B} = \frac{dT_{o2}}{d\ell_2}\frac{d\ell_2}{dx_B} , \tag{A2.7}$$

$$\frac{dT_{o2}}{dy_B} = \frac{dT_{o2}}{d\ell_2}\frac{d\ell_2}{dy_B} , \tag{A2.8}$$

where

$$\frac{d\ell_2}{dx} = -\cos\gamma , \tag{A2.9}$$

$$\frac{d\ell_2}{dy} = -\sin\gamma , \tag{A2.10}$$

$$\frac{d\ell_2}{d\psi} = \cos\gamma\left(x_p\sin\psi + y_p\cos\psi\right) + \sin\gamma\left(y_p\sin\psi - x_p\cos\psi\right) , \tag{A2.11}$$

$$\frac{d\ell_2}{dx_B} = -\frac{d\ell_2}{dx} = \cos\gamma , \tag{A2.12}$$

$$\frac{d\ell_2}{dy_B} = -\frac{d\ell_2}{dy} = \sin\gamma . \tag{A2.13}$$

Figure A2.1 shows the SC deformation for a small change in z_B. Notice that this change does not produce a change in ℓ_2, but it affects the values of the two horizontal components of SC, namely ℓ_{2A} and ℓ_{2B}.

Noting from Figure A2.1 that

$$\frac{\Delta\ell_2}{\Delta z_B} = 0 , \tag{A2.14}$$

the derivative of the horizontal tension component T_{o2} with respect to $\dot{z}_B$ can be obtained from (A2.2) by approximating h_1 by z_B and taking the derivative directly with respect to z_B.

$$\frac{dT_{o2}}{dz_B} = \frac{P(h-z_B)}{2\sqrt{\ell_{w2}^2-(h-z_B)^2}\left[\sinh\left(\frac{P\ell_2}{2T_{o2}}\right)-\left(\frac{P\ell_2}{2T_{o2}}\right)\cosh\left(\frac{P\ell_2}{2T_{o2}}\right)\right]} . \qquad \text{(A2.15)}$$

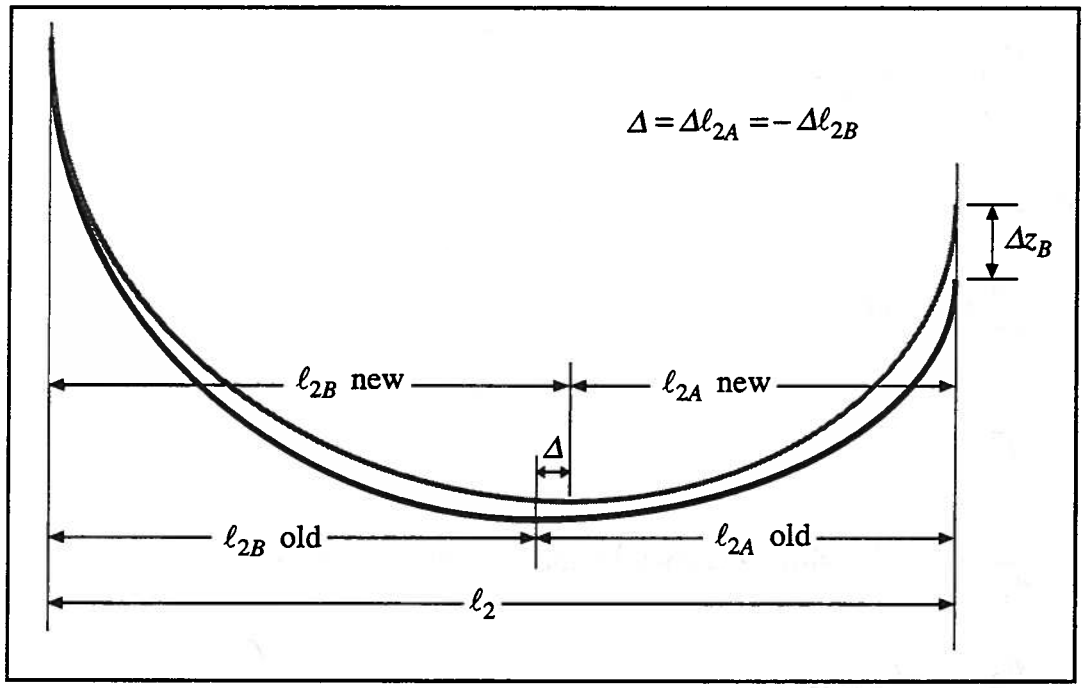

Figure A2.1. SC deformation for a change in z_B

We further need to determine how the changes in the components ℓ_{2A} and ℓ_{2B} relate to a unit change in z_B. This can be achieved by first combining relation (2.22) with (2.16) and (2.17) to obtain

$$P\ell_{w2} - T_{o2}\sinh\left(\frac{P\ell_{2A}}{T_{o2}}\right) - T_{o2}\sinh\left(\frac{P\ell_{2B}}{T_{o2}}\right) = 0 , \qquad \text{(A2.16)}$$

and then by taking the derivative of the above expression with respect to z_B. This yields,

$$\frac{dT_{o2}}{dz_B}\left[\sinh\left(\frac{P\ell_{2A}}{T_{o2}}\right)-\left(\frac{P\ell_{2A}}{T_{o2}}\right)\cosh\left(\frac{P\ell_{2A}}{T_{o2}}\right)+\sinh\left(\frac{P\ell_{2B}}{T_{o2}}\right)-\left(\frac{P\ell_{2B}}{T_{o2}}\right)\cosh\left(\frac{P\ell_{2B}}{T_{o2}}\right)\right]$$
$$+P\left[\cosh\left(\frac{P\ell_{2A}}{T_{o2}}\right)\frac{d\ell_{2A}}{dz_B}+\cosh\left(\frac{P\ell_{2B}}{T_{o2}}\right)\frac{d\ell_{2B}}{dz_B}\right]=0 . \qquad \text{(A2.17)}$$

Noticing that

$$\ell_2 = \ell_{2A} + \ell_{2B} \ , \tag{A2.18}$$

we find that

$$\Delta \ell_2 = \Delta \ell_{2A} + \Delta \ell_{2B} \quad \text{and therefore} \quad \frac{\Delta \ell_2}{\Delta z_B} = \frac{\Delta \ell_{2A}}{\Delta z_B} + \frac{\Delta \ell_{2B}}{\Delta z_B} = 0 \ , \tag{A2.19}$$

In the limit, as $z_B \to 0$,

$$\frac{d\ell_{2A}}{dz_B} = -\frac{d\ell_{2B}}{dz_B} \ . \tag{A2.20}$$

Combining relation (2.20) with equation (A2.17) we obtain the following expression for $d\ell_{2A}/dz_B$:

$$\frac{d\ell_{2A}}{dz_B} = \frac{\dfrac{dT_{o2}}{dz_B}\left[\sinh\left(\dfrac{P\ell_{2A}}{T_{o2}}\right) - \left(\dfrac{P\ell_{2A}}{T_{o2}}\right)\cosh\left(\dfrac{P\ell_{2A}}{T_{o2}}\right)\right]}{P\left[\cosh\left(\dfrac{P\ell_{2B}}{T_{o2}}\right) - \cosh\left(\dfrac{P\ell_{2A}}{T_{o2}}\right)\right]} + \frac{\dfrac{dT_{o2}}{dz_B}\left[\sinh\left(\dfrac{P\ell_{2B}}{T_{o2}}\right) - \left(\dfrac{P\ell_{2B}}{T_{o2}}\right)\cosh\left(\dfrac{P\ell_{2B}}{T_{o2}}\right)\right]}{P\left[\cosh\left(\dfrac{P\ell_{2B}}{T_{o2}}\right) - \cosh\left(\dfrac{P\ell_{2A}}{T_{o2}}\right)\right]} \ . \tag{A2.21}$$

Now we need to find the derivatives of the vertical tension component T_{v2A} which is given by relation (2.16), with respect to the position vector given by $(x, y, \psi, x_B, y_B, z_B)$. To do this, we first need to determine how the changes in the components ℓ_{2A} and ℓ_{2B} are related to a unit change in ℓ_2. A change in ℓ_2 is related to ℓ_{2A} and ℓ_{2B} as follows

$$\frac{\Delta \ell_2}{\Delta \ell_2} = \frac{\Delta \ell_{2A}}{\Delta \ell_2} + \frac{\Delta \ell_{2B}}{\Delta \ell_2} = 1 \ . \tag{A2.22}$$

In the limit, as $\ell_2 \to 0$,

$$\frac{d\ell_{2A}}{d\ell_2}+\frac{d\ell_{2B}}{d\ell_2}=1\ . \tag{A2.23}$$

The first step is to take the derivative of expression (A2.16) with respect to ℓ_2, which yields

$$\frac{dT_{o2}}{d\ell_2}\left[\sinh\left(\frac{P\ell_{2A}}{T_{o2}}\right)-\left(\frac{P\ell_{2A}}{T_{o2}}\right)\cosh\left(\frac{P\ell_{2A}}{T_{o2}}\right)+\sinh\left(\frac{P\ell_{2B}}{T_{o2}}\right)-\left(\frac{P\ell_{2B}}{T_{o2}}\right)\cosh\left(\frac{P\ell_{2B}}{T_{o2}}\right)\right]$$
$$+P\left[\cosh\left(\frac{P\ell_{2A}}{T_{o2}}\right)\frac{d\ell_{2A}}{d\ell_2}+\cosh\left(\frac{P\ell_{2B}}{T_{o2}}\right)\frac{d\ell_{2B}}{d\ell_2}\right]=0\ . \tag{A2.24}$$

Substituting relation (A2.23) into the above equation, and eliminating the dependence of ℓ_{2B} in ℓ_2 we obtain the term $d\ell_{2A}/d\ell_2$ as follows:

$$\frac{d\ell_{2A}}{d\ell_2}=\frac{\dfrac{dT_{o2}}{d\ell_2}\left[\sinh\left(\dfrac{P\ell_{2A}}{T_{o2}}\right)-\left(\dfrac{P\ell_{2A}}{T_{o2}}\right)\cosh\left(\dfrac{P\ell_{2A}}{T_{o2}}\right)\right]}{P\left[\cosh\left(\dfrac{P\ell_{2B}}{T_{o2}}\right)-\cosh\left(\dfrac{P\ell_{2A}}{T_{o2}}\right)\right]}$$
$$+\frac{\dfrac{dT_{o2}}{d\ell_2}\left[\sinh\left(\dfrac{P\ell_{2B}}{T_{o2}}\right)-\left(\dfrac{P\ell_{2B}}{T_{o2}}\right)\cosh\left(\dfrac{P\ell_{2B}}{T_{o2}}\right)\right]}{P\left[\cosh\left(\dfrac{P\ell_{2B}}{T_{o2}}\right)-\cosh\left(\dfrac{P\ell_{2A}}{T_{o2}}\right)\right]}$$
$$+\frac{P\cosh\left(\dfrac{P\ell_{2B}}{T_{o2}}\right)}{P\left[\cosh\left(\dfrac{P\ell_{2B}}{T_{o2}}\right)-\cosh\left(\dfrac{P\ell_{2A}}{T_{o2}}\right)\right]}\ , \tag{A2.25}$$

and the term for $d\ell_{2B}/d\ell_2$ is simply

$$\frac{d\ell_{2B}}{d\ell_2}=1-\frac{d\ell_{2A}}{d\ell_2}\ . \tag{A2.26}$$

Note that as $\ell_{2A}\to\ell_{2B}$, we have

$$\lim_{\ell_{2A}\to\ell_{2B}}\frac{d\ell_{2A}}{d\ell_2}=1-\lim_{\ell_{2A}\to\ell_{2B}}\frac{d\ell_{2B}}{d\ell_2}=0.5\ . \tag{A2.27}$$

The derivatives of tension component T_{v2A} with respect to the position vector variables x, y, ψ, x_B and y_B are given by

$$\frac{dT_{v2A}}{dx} = \frac{dT_{v2A}}{d\ell_2}\frac{d\ell_2}{dx}\,, \tag{A2.28}$$

$$\frac{dT_{v2A}}{dy} = \frac{dT_{v2A}}{d\ell_2}\frac{d\ell_2}{dy}\,, \tag{A2.29}$$

$$\frac{dT_{v2A}}{d\psi} = \frac{dT_{v2A}}{d\ell_2}\frac{d\ell_2}{d\psi}\,, \tag{A2.30}$$

$$\frac{d\ell_2}{dx_B} = \frac{dT_{v2A}}{d\ell_2}\frac{d\ell_2}{dx_B}\,, \tag{A2.31}$$

$$\frac{d\ell_2}{dy_B} = \frac{dT_{v2A}}{d\ell_2}\frac{d\ell_2}{dy_B}\,, \tag{A2.32}$$

where

$$\frac{dT_{v2A}}{d\ell_2} = \frac{dT_{o2}}{d\ell_2}\left[\sinh\left(\frac{P\ell_{2A}}{T_{o2}}\right) - \left(\frac{P\ell_{2A}}{T_{o2}}\right)\cosh\left(\frac{P\ell_{2A}}{T_{o2}}\right)\right] + P\cosh\left(\frac{P\ell_{2A}}{T_{o2}}\right)\frac{d\ell_{2A}}{d\ell_2}\,. \tag{A2.33}$$

Conversely,

$$\frac{dT_{v2A}}{d\ell_2} = \frac{dT_{v2A}}{d\ell_{2A}}\frac{d\ell_{2A}}{d\ell_2}\,, \tag{A2.34}$$

where

$$\frac{dT_{v2A}}{d\ell_{2A}} = \frac{dT_{o2}}{d\ell_{2A}}\left[\sinh\left(\frac{P\ell_{2A}}{T_{o2}}\right) - \left(\frac{P\ell_{2A}}{T_{o2}}\right)\cosh\left(\frac{P\ell_{2A}}{T_{o2}}\right)\right] + P\cosh\left(\frac{P\ell_{2A}}{T_{o2}}\right)\,. \tag{A2.35}$$

The derivative of T_{v2A} with respect to z_B is directly obtained as follows:

$$\frac{dT_{v2A}}{dz_B} = \frac{dT_{o2}}{dz_B}\left[\sinh\left(\frac{P\ell_{2A}}{T_{o2}}\right) - \left(\frac{P\ell_{2A}}{T_{o2}}\right)\cosh\left(\frac{P\ell_{2A}}{T_{o2}}\right)\right] + P\cosh\left(\frac{P\ell_{2A}}{T_{o2}}\right)\frac{d\ell_{2A}}{dz_B} \,. \qquad \text{(A2.36)}$$

The above expressions relate the changes in the horizontal and vertical tension components of a SC as functions of changes in vessel and buoy positions. Notice that the mathematical model for a catenary with one buoy does not require partial derivatives of the tension component term T_{v2B} with respect to the position vector. For mooring lines consisting of several segments of SCs, the tension components will depend on the position vectors of the bodies at the boundaries of such segments. For example, if two buoys are connected at the boundaries of a catenary (see Figure 4.1), the mooring line will consist of two SC segments. The tension components in the lower segment thus depend on the position vectors of both buoys, while the tension components in the upper segment depend on the position vector of the upper buoy and the vessel. In such cases where the partial derivatives must be calculated for equilibrium and/or stability analysis, the required tension-position relations and the associated partial derivatives can be obtained following the procedure shown above.

BIBLIOGRAPHY

BIBLIOGRAPHY

[1] Abkowitz, M.A., "Measurement of Hydrodynamic Characteristics From Ship Maneuvering Trials by System Identification," SNAME Transactions, Vol. 88, 1980, pp. 283-318.

[2] Bernitsas M.M., and Papoulias, F.A., "Nonlinear Stability and Maneuvering Simulation of Single Point Mooring Systems," Proceedings of Offshore Station Keeping Symposium, SNAME, Houston, Texas, February 1-2, 1990, pp. 1-19.

[3] Bernitsas M.M. and Garza-Rios, L.O., "Effect of Mooring Line Arrangement on the Dynamics of Spread Mooring Systems," *Journal of Offshore Mechanics and Arctic Engineering*, Vol. 118, No. 1, February 1996, pp. 7-20.

[4] Bernitsas, M.M. and Garza-Rios, L.O., "Mooring System Design Based on Analytical Expressions of Catastrophes of Slow-Motion Dynamics," *Journal of Offshore Mechanics and Arctic Engineering*, Vol. 119, No. 2, May 1997, pp. 86-95.

[5] Chung, J.S., and Bernitsas, M.M., "Dynamics of Two-Line Ship Towing/Mooring Systems: Bifurcations, Singularities of Stability Boundaries, Chaos," *Journal of Ship Research*, Vol. 36, No. 2, June 1992, pp. 93-105.

[6] Davison, N.J., Thomas, N.T., Nienhus, V. and Pinkster, J.A., "Application of an Alternative Concept in Dynamic Positioning to a Tanker Floating Production System," Proceedings of the 19th Annual Offshore Technology Conference, OTC Paper No. 5444, Houston, April 1987, pp. 207-223.

[7] Fernandes, A.C. and Aratanha, M., "Classical Assessment to the Single Point Mooring and Turret Dynamics Stability Problems," Proceedings of the 15th International Conference on Offshore Mechanics and Arctic Engineering (OMAE), Vol. I-A, Florence, Italy, June 1996, pp. 423-430.

[8] Fernandes, A.C. and Sphaier, S., "Dynamic Analysis of a FPSO System," Proceedings of the Seventh International Offshore and Polar Engineering Conference (ISOPE), Vol. 1, Honolulu, 1997, pp. 330-335.

[9] Fossen, T.I., Guidance and Control of Ocean Vehicles, John Wiley and Sons, Ltd., West Sussex, England, 1994.

[10] Garza-Rios, L.O., "Development of a Design Methodology for Mooring Systems Based on Catastrophe Theory," Doctoral Dissertation, Department of Naval Architecture and Marine Engineering, University of Michigan, Ann Arbor, May 1996.

[11] Garza-Rios, L.O., and Bernitsas, M. M., "Nonlinear Slow Motion Dynamics of Turret Mooring Systems in Deep Water," Proceedings of the 8th International Conference on the Behaviour of Offshore Structures (BOSS), Delft, the Netherlands, July 1997, pp. 177-188.

[12] Garza-Rios, L.O., Bernitsas, M.M. and Nishimoto, K., "Catenary Mooring Lines With Nonlinear Drag and Touchdown," Report to the University of Michigan, Department of Naval Architecture and Marine Engineering, Ann Arbor, Publication No. 333, January 1997.

[13] Garza-Rios, L.O., Bernitsas, M.M. and Nishimoto, K., "Slow Motion Dynamics of DICAS Mooring Systems Under Steady Current, Wind and Steady Drift Excitation," Proceedings of the X International Symposium on Offshore Engineering (Brasil Offshore'97), Rio de Janeiro, Brazil, September 1997, pp. 47-62.

[14] Garza-Rios, L.O., Bernitsas, M.M., Nishimoto, K. and Masetti, I.Q., "Preliminary Design of a DICAS Mooring System for the Brazilian Campos Basin," Proceedings of the ASME 16th International Conference on Offshore Mechanics and Arctic Engineering (OMAE), Vol. I-A, Yokohama, Japan, April 1997, pp. 153-161.

[15] Gottlieb, O., and Kim, S.C.S., "Nonlinear Oscillations, Bifurcations and Chaos in a Multi-Point Mooring System with a Geometric Nonlinearity," *Journal of Applied Ocean Research*, Vol. 14, 1992, pp. 832-839.

[16] Guckenheimer, J., and Holmes, P., Nonlinear Oscillations, Dynamical Systems, and Bifurcations of Vector Fields, Springer-Verlag, New York, Inc., 1983.

[17] Jiang, T., and Schellin, T.E., "Maneuvering Simulation of a Tanker Moored in a Steady Current Including Hydrodynamic Memory Effects and Stability Analysis," Proceedings, RINA International Conference on Ship Maneuverability, London, April 1987, pp. 1-12.

[18] Jiang, T., and Schellin, T.E., "Motion Prediction of a Single Point Moored Tanker Subjected to Current, Wind and Waves," Proceedings, of the ASME 7th International Conference on Offshore Mechanics and Arctic Engineering (OMAE), Vol. II, Houston, Texas, February 1988, pp. 317-326.

[19] Leite, A.J.P., Aranha, J.A.P., Umeda, C. and de Conti, M.B., "Current Forces in Tankers and Bifurcation of Equilibrium of Turret Systems: Hydrodynamic Model and Experiments," *Journal of Applied Ocean Research*, Vol. 20, 1998, pp. 145-156.

[20] Nippon Kaiji Kyokai, Guide to Mooring Systems, N.K.K., Tousei, Tokyo, 1983

[21] Nishimoto, K., Kaster, F., and Aranha, J.A.P., "Full Scale Decay Test of a Moored Tanker, ALAGOAS-DICAS System," Report to Petrobrás, Brazil, February 1996.

[22] Nishimoto, K., Brinati, H.L. and Fucatu, C.H., "Dynamics of Moored Tankers SPM and Turret," Proceedings of the Seventh International Offshore and Polar Engineering Conference (ISOPE), Vol. 1, Honolulu, 1997, pp. 370-378.

[23] Obokata, J., Sasaki, N. and Nagashima, J., "On the Estimation of Current Force Induced on a Ship Hull by Some Model Tests," Kansai Society of Naval Architects of Japan, Vol. 180, 1981, pp. 47-57.

[24] Obokata, J. and Sasaki, N., "On the Horizontal Slow Oscillations and the Dynamic Stability of a Ship Moored to Single Point Moorings," Transactions of the West Japan Society of Naval Architects, Vol. 186, 1982, pp. 87-93.

[25] Papoulias, F.A., "Dynamic Analysis of Mooring Systems," Doctoral Dissertation, Department of Naval Architecture and Marine Engineering, University of Michigan, Ann Arbor, May 1987.

[26] Papoulias, F.A., and Bernitsas, M.M., "MOORLINE: A Program for Static Analysis of MOORing LINEs," Report to the University of Michigan/Sea Grant/Industry Consortium in Offshore Engineering, and Department of Naval Architecture and Marine Engineering, The University of Michigan, Ann Arbor, Publication No. 309, May 1988.

[27] Papoulias, F.A. and Bernitsas, M.M., "Autonomous Oscillations, Bifurcations, and Chaotic Response of Moored Vessels", *Journal of Ship Research*, Vol. 32, No. 3, September 1988, pp. 220-228.

[28] Pinkster, J.A. and Nienhus, V., "Dynamic Positioning of Large Tankers at Sea," Proceedings of 18th Annual Offshore Technology Conference, OTC Paper No. 5208, Houston, May 1986, pp. 459-476.

[29] Press, W.H., Flannery, B.P., Tenkolsky, S.A. and Vetterlug, W.T., Numerical Recipes, The Art of Scientific Computing, Cambridge University Press, New York, 1989.

[30] Sharma, S.D., Jiang, T., and Schellin, T.E., "Dynamic Instability and Chaotic Motions of a Single Point Moored Tanker," Proceedings of the 17th ONR Symposium on Naval Hydrodynamics, The Hague, Holland, August 1988, pp. 543-562.

[31] Takashina, J., "Ship Maneuvering Motion due to Tugboats and its Mathematical Model," *Journal of the Society of Naval Architects of Japan*, Vol. 160, 1986, pp. 93-104.

[32] Tanaka, S., "On the Hydrodynamic Forces Acting on a Ship at Large Drift Angles," *Journal of the West Society of Naval Architects of Japan*, Vol. 91, 1995, pp. 81-94.

[33] Wiggins, S., Introduction to Applied Nonlinear Dynamical Systems and Chaos, Springer-Verlag, New York, Inc., 1990.

University of Michigan
College of Engineering

Department of Naval Architecture and Marine Engineering
NAME Building
2600 Draper Road
Ann Arbor, MI 48109-2145

734-764-6470
734-936-8820 fax
http://www.engin.umich.edu/dept/name/